Title
The Role of Cation/Proton Exchange in Glutamate Transport into Synaptic Vesicles

Author
Goh, Germaine Yen Lin

Publication Date
2009

Peer reviewed|Thesis/dissertation

The Role of Cation/Proton Exchange in Glutamate Transport into Synaptic Vesicles

by

Germaine Yen Lin Goh

A dissertation submitted in partial satisfaction of the

requirements for the degree of

Joint Doctor of Philosophy
with University of California, San Francisco

in

Bioengineering

in the

Graduate Division

of the

University of California, Berkeley

Committee in charge:

Professor Robert H. Edwards, Chair
Professor Terry E. Machen
Professor Yang Dan

Fall 2009

The Role of Cation/Proton Exchange in Glutamate Transport into Synaptic Vesicles

by Germaine Yen Lin Goh

Abstract

The Role of Cation/Proton Exchange in Glutamate Transport into Synaptic Vesicles

by

Germaine Yen Lin Goh

Joint Doctor of Philosophy in Bioengineering with

University of California, San Francisco

University of California, Berkeley

Professor Robert H. Edwards, Chair

Chemical synaptic transmission is the primary mode of communication between neurons, and involves release of neurotransmitter from synaptic vesicles in the presynaptic cell, which then activates receptors on the postsynaptic cell. The amount of neurotransmitter stored in a synaptic vesicle can determine the size of the postsynaptic response, but the factors regulating vesicle filling remain poorly understood. A proton electrochemical gradient ($\Delta\mu_{H+}$) generated by the vacuolar H^+-ATPase drives accumulation of classical transmitters into synaptic vesicles. The chemical component of $\Delta\mu_{H+}$ (ΔpH) has received particular attention for its role in the vesicular transport of cationic transmitters, as well as protein sorting and degradation. Thus, considerable work has addressed the factors that promote ΔpH. Although the electrical component of $\Delta\mu_{H+}$ ($\Delta\psi$) drives uptake of the principal excitatory transmitter glutamate into synaptic vesicles, the mechanisms that promote $\Delta\psi$ remain poorly understood.

We thus employed biochemical methods on isolated synaptic vesicles to better understand the fluxes that occur across vesicle membranes. We used fluorescent dyes to measure ΔpH and $\Delta\psi$ dynamics across synaptic vesicles and their dependence on cations, and radioisotopes to measure uptake of glutamate and sodium into synaptic vesicles. To assess the physiological relevance of our in vitro data, we then tested the findings using electrophysiological recordings at a central synapse. We also performed immunofluorescence studies on transfected primary hippocampal cultures to test the synaptic localization of some candidate proteins. We find that synaptic vesicles exhibit a cation/H^+ exchange activity that converts ΔpH into $\Delta\psi$, thus promoting synaptic vesicle filling with glutamate. Manipulating presynaptic K^+ concentration at a glutamatergic synapse influences quantal size, demonstrating that K^+ regulates glutamate release and synaptic transmission. Some proteins tested display synaptic localization and are thus potential molecular candidates for the phenomenon we report.

Acknowledgments

I would like to thank the many people who have, in diverse ways, enriched my graduate career and my life.

Firstly, I thank my PI Robert Edwards for his support, guidance, and unwavering enthusiasm throughout my time in the lab, and without whom the project would not have been initiated in the first place. He has been a very approachable advisor, always open to listen to my ideas. I am thankful to my thesis committee members Alan Verkman, Terry Machen, David Copenhagen, and Yang Dan for their support and kind encouragement, especially Alan, who always provided most input during meetings, and Terry, for his incisive comments on this dissertation. I am also grateful to my qualifying exam committee members Sanjay Kumar and Diane Barber for helping to ensure that I got a good start on the project.

I would like to express my sincere thanks to all past and present members of the Edwards lab who have defined much of my life in graduate school. Lars Borre, with whom I worked closely for two years and who should be personally experienced rather than heard about, was rather like the big brother one loves to hate - variably annoying, endearing, worth learning from, and giving (sometimes unwanted) advice, but always worth fighting with. I hope our interactions in lab were entertaining to all who had the (mis)fortune to witness. Magda Santos, with whom I worked when I first joined the lab, always gave me patient and careful guidance, along with Haiyan Li who never failed to provide friendly advice and kind words. Susan Voglmaier was characteristically generous in helping me decapitate rats in my early days, and has always been an admirable role model to me. Ken Nakamura took the time to give me feedback after almost every lab meeting, something I truly appreciate. Becky Seal, Zhaolin Hua, and Bibiana Onoa have been awesome baymates. Zhaolin and Bibiana are great to chat with about anything under the sun, including science and life, and have dispensed tons of helpful advice to me. Zhaolin has also been an informal scientific mentor, sharing much of her knowledge and thoughts, bench and otherwise, with me. Becky, in her honest assessments of me, assured me early on that I could trust whatever she said, and has offered me much encouragement, support and friendship. I have much to learn from these wonderful women. I thank everyone else in the Edwards lab for the helpful discussions, advice, and camaraderie - Akanksha Bapna, Cedric Asensio, Dan Sirkis, Tom Hnasko, Shila Manandhar, Jim Maas, Venu Nemani, Erika Wallender, Tomomi Someya, Taslim Saiyed, Pedro Cano, Todd Logan, Sang Myun Park, Sarah Foss, Alice Zhang, Bipasha Mukherjee, and Malcolm Anthony, who are all treasured labmates I'm glad to have gotten to know.

I would also like to acknowledge Janet Yau, who has unfailingly offered excellent administrative support to the lab, and Rebecca Pauling, who has been a consistently helpful administrator for Bioengineering graduate students at Berkeley.

I am grateful to my friends, near and far, for sticking around, for being ready to reconnect even after long periods, and for all the good times. I am especially indebted to

Alice Tay, for whom I worked only three months in my last year of teenagehood, and who nevertheless remained in contact over the past eight years, periodically sending me delightful parcels of little gifts. I am blessed to have the honor of her friendship.

I would like to express my appreciation for my dear family. I thank my dad, John, for his optimistic personality and for challenging me to get out of my comfort zone, and my mom, Patricia, for her compassion towards everyone, and for always caring. Despite all my years away, we may actually have grown closer, and I am glad to find myself becoming like her in some ways. I am so fortunate to have grown up with my lovely sisters, Dawn and Gerri, who really are just wonderful people and best friends to me. Again, despite my time away and my incompetence at keeping frequent contact, nothing binds people together like sisterhood. I look forward to growing up (and old) with them. I am also very appreciative of my aunts, Luan King and Celeste, for always sending me back to the US with priceless home-made food after my visits home, and my other aunts, Rosalind and Catherine, for always keeping me in their thoughts.

Finally, I thank Davis Beekman for being my best friend and companion. You mean the world to me and I am ever so glad that we can share anything with each other. You, more than anything else, have made me feel that I have really lived.

Table of Contents

List of Figures

Chapter 1

Chapter 2

Chapter 3

List of Tables

Chapter 3

Chapter 1. Introduction

1.1 MEMBRANE TRANSPORT PROTEINS IN CELLS

Eukaryotic cells contain a complex organization of functionally diverse, internal membrane-bound structures, collectively referred to as the endomembrane system. Each compartment has a unique solute composition appropriate for its specialized functions. For example, specific pH values in different organelles are required for the optimal function of enzymatic reactions such as protein and lipid degradation, as well as for the dissociation of endocytosed receptors from their ligands and their subsequent degradation or targeting to another location. The cell and its internal organelles are enclosed by lipid bilayer membranes that delimit the various compartments. The hydrophobic membrane interior acts as an effective barrier to the movement of polar molecules, creating the distinct environments necessary for the suite of processes that occur in the cell.

Communication and exchange between compartments, however, are essential for the cell to respond dynamically to internal and external changes. Each lipid bilayer membrane thus contains an assortment of proteins, integral to or associated with the membrane, that are indispensable for the proper functioning of the cell. Indeed, proteins typically account for about 50% of the mass of the plasma membrane (Alberts 2002). Some proteins serve as a mode of communication between the interior and exterior of the cell, altering their conformations upon sensing a change on one side and effecting responses on the other side. Examples are the cell surface receptors such as the epidermal growth factor receptor (EGFR), tropomyosin-receptor kinase (Trk) receptor and the G-protein coupled receptors (GPCRs). Some proteins function as scaffolds, interacting with and localizing other proteins; an example is PSD95, located at the post-synaptic density of neuronal dendritic spines and interacting with proteins such as glutamate receptors and potassium channels. Other proteins serve as marker proteins that distinguish one organelle from another, thus directing protein and lipid traffic in a specific manner, such as the Rab family of proteins.

Mechanisms of Membrane Transport Proteins

Another important group of proteins are the membrane transport proteins that define the internal and external milieus of the compartments and allow for the movement of ions and small molecules across the otherwise relatively impermeable membrane. Membrane transport proteins make up 15 to 30% of the membrane proteins in all cells (Alberts 2002), attesting to their importance in cellular physiology. The transport functions performed by these proteins are essential for a variety of processes such as the cellular uptake of nutrients from the extracellular space as well as the removal of cellular metabolic waste products, the concentrative uptake of molecules from the cytoplasm into secretory vesicles for subsequent secretion, and the generation of particular ion gradients across membranes, required for other transport activities including those just mentioned. These transport proteins are integral membrane proteins, spanning the entire length of the

bilayer, and mediate transport via facilitated diffusion or active transport, often with a high degree of specificity for their substrate, or a group of like substrates (**Fig. 1-1**).

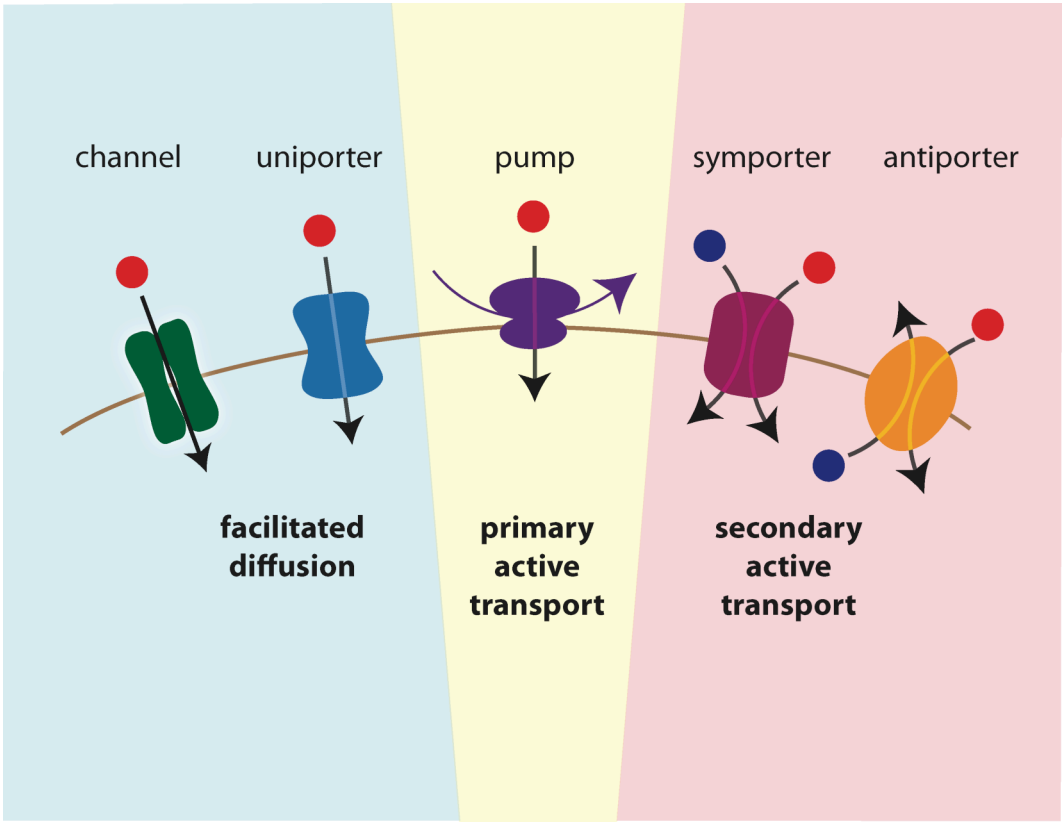

Figure 1-1. Types of membrane transport proteins
Facilitated diffusion can occur through a channel (green), or a uniporter (blue) lacking a pore, and involves the downhill movement of substrate (red circle) down its electrochemical gradient. Primary active transport by a pump (purple) requires the direct input of energy in the form of ATP or photons (purple arrow) in order to move the substrate across the membrane. Secondary active transport can take the form of symport (burgundy) or antiport (orange), where movement of the substrate molecule up its electrochemical gradient is driven by movement of another molecule (navy circle) down its electrochemical gradient).

Facilitated diffusion, as its name suggests, involves no input of chemical energy since the membrane protein simply provides a lower-resistance pathway through which the hydrophilic substrate molecule may pass. Since this is a diffusive process, the substrates can only move down their concentration or electrical potential gradients, never against. The membrane protein can either be a pore-containing channel that is often gated so that it can open or close in response to stimuli, or a carrier protein that lacks a pore but assumes multiple reversible inward- and outward-facing conformations so that it can effectively bind substrate on one side and release it on the other (**Fig. 1-1**). Examples of pore-containing channels are the voltage-gated and ligand-gated ion channels critical in neurotransmission, each of which has a characteristic selectivity for particular cations or

anions, while pore-lacking carrier proteins include certain glucose and amino acid transporters important for the cellular uptake of nutrients.

Active transport, on the other hand, involves the expense of energy to drive solute transport across the membrane. This energy can be provided directly in the form of ATP or light, or indirectly in the form of pre-existing ion gradients (**Fig. 1-1**). In the former, sometimes referred to as primary active transport, the input of energy through ATP hydrolysis or photon absorption is coupled to conformational changes of the transporter that result in translocation of the substrate from one side of the membrane to the other. In the latter, also known as secondary active transport, the movement of one ion down its electrochemical gradient is coupled to the movement of another ion or solute against its electrochemical gradient. Secondary active transport can take the form of symport, where the coupled ion or solute is transported in the same direction as the driving ion, or antiport, where the coupled ion or solute is transported in the opposite direction from the driving ion. Henceforth, all carrier proteins that lack pores will be referred to as *transporters*, distinct from pore-carrying channels. Both active transport carriers and non-pore facilitated diffusion carriers resemble enzymes in that each transporter has a maximal rate at which it can transport substrate (V_{max}), achieved when all binding sites are saturated with substrate, and a specific affinity for its substrate indicated by K_m, the concentration of substrate at which the rate of transport is half-maximal. Like enzymes, the function of transporters can also be blocked by competitive or non-competitive inhibitors. Unlike enzymes, however, the substrates are not covalently modified by the transporters, but conveyed from one side of the membrane to the other unaltered.

Channels and transporters, owing to their different modes of operation, thus have some divergent properties: (i) Classically, channels are thought to provide a continuous aqueous passageway through which ions flow undisrupted, though they are often gated such that they can be closed or open under different conditions. Transporters, in contrast, must ensure that they never allow access to both sides of the membrane at once, but instead alternate access of the substrate between the two sides. (ii) Channels hence conduct ions much faster than transporters, achieving conduction rates of up to 10^7 - 10^8 ions per second, since ions diffuse through an aqueous passageway through the relatively-static channel. A transporter, however, has to undergo rather major conformational changes, making sure that each substrate-binding site is exposed to only one side of the membrane at any time, and thus achieves rates of transport typically 10^5 slower (Alberts 2002). (iii) Channels basically allow simple diffusion of ions, so the ions can only move down their electrochemical gradients, whereas transporters are structurally able to move substrates against their electrochemical gradient by coupling the process to an input of energy. A transporter is thus able to generate a gradient of its substrate rather than diminishing it.

Cellular Functions of Membrane Transport Proteins

Together, transport proteins are thus indispensable for the unique compositions of cells and their compartments. Firstly, they are essential for generating ion gradients

across membranes – the resting cytoplasmic potassium (K^+) concentration in most cells is several-fold larger than the extracellular potassium concentration, while the opposite is true of sodium (Na^+), calcium (Ca^{2+}) and chloride (Cl^-). The Na^+,K^+-ATPase is primarily responsible for the resting K^+ and Na^+ concentrations, harnessing the energy derived from ATP hydrolysis to power the pumping of K^+ and Na^+ into and out of the cell, respectively, against their electrochemical gradients. At rest, the predominant channels that are open are K^+ channels, and the outflow of a small fraction of K^+ through these channels results in a more negative interior of the cell relative to the outside. This is primarily responsible for the negative electrical membrane potential of most cells at steady-state – the plasma membrane functions as a capacitor, with cations and anions drawn to it on either side by electrostatic attraction to each other, forming the basis for the electrical potential across membranes. The intracellular concentration of Cl^- is largely determined by the activities of the cation chloride cotransporters of the *SLC12* gene family, namely the NKCCs that mediate coupled influx of Na^+, K^+ and 2 Cl^-, and the KCCs that mediate coupled efflux of K^+ and Cl^- (Gamba & Bobadilla 2004; Payne et al 2003). Ca^{2+}, like Na^+ and K^+, is kept low in the cytoplasm by the plasma membrane and endoplasmic reticulum (ER) Ca^{2+}-ATPases that pump Ca^{2+} out of the cytoplasm against its electrochemical gradient, using energy released from ATP hydrolysis. A Na^+/Ca^{2+} exchanger (antiporter) on the plasma membrane also pumps Ca^{2+} out of the cell, using the inwardly-directed Na^+ gradient as driving force. Finally, the acidic lumen of vesicles in the secretory and endocytic pathways (as low as pH 4.5 in lysosomes) is maintained by the vacuolar H^+-translocating ATPase (V-ATPase) that pumps protons against their electrochemical gradient. Net acidification, however, does not occur without the movement of counterions – the pumping of H^+ rapidly creates a positive membrane potential in the interior of the vesicle relative to the exterior, which counters further proton influx. The entry of anions or the exit of cations is therefore necessary for dissipation of the electrical potential build-up, to allow net influx of protons (and hence acidification). Chloride channels in a number of organelles are responsible for this counter-conductance, by allowing chloride entry parallel to proton influx. Therefore, a cell at steady-state continuously maintains gradients of ions by means of these and other transporters.

These steady-state ion gradients, in turn, are vital for myriad other processes. As introduced above in the example of the Na^+/Ca^{2+} exchanger, the Na^+ gradient is important for driving other secondary active transport systems. These include the Na^+-driven glucose and amino acid transporters that use the inwardly-directed Na^+ gradient to drive glucose or amino acid symport into the cell, processes critical for the cell's nutrient uptake. The proton electrochemical gradient (also termed "proton-motive force", or "pmf") across the bacterial and mitochondrial inner membranes and eukaryotic vesicular membranes is another important driving force for the transport of other solutes. For example, the pH gradient across the mitochondrial inner membrane is used to drive symport of pyruvate and inorganic phosphate from the intermembrane space into the matrix, while the electrical gradient (voltage difference) across the membrane is

important for ADP/ATP exchange, since each transport cycle involves the net movement of one negative charge out of the matrix (Klingenberg & Rottenberg 1977; Kramer & Klingenberg 1980). Importantly, the proton gradient is also used to drive the formation of ATP in the inner mitochondrial membrane of eukaryotic cells as well as in the bacterial plasma membrane. This pmf across bacterial and mitochondrial inner membranes is formed during electron transport, when the free energy released by the oxidation of NADH or $FADH_2$ is coupled to the uphill pumping of protons. In eukaryotic vesicular membranes, the pmf is generated by the vacuolar H^+-pumping ATPase (V-ATPase). Another important function of the proton electrochemical gradient, fundamental to the work described in this dissertation and which will be discussed further, is its role in driving the transport of small-molecule neurotransmitters including glutamate, γ-aminobutyric acid (GABA), acetylcholine, and monoamines into secretory and synaptic vesicles. All cells thus rely critically on the generation and dissipation of ion gradients for many processes.

1.2 CHEMICAL SYNAPTIC TRANSMISSION AND QUANTAL SIZE

Neurons are cells that depend heavily on membrane transport proteins and ion gradients for their main, specialized functions, using up to 25 percent of the ATP produced by the cell for ion transport (Lodish 2000). The central and peripheral nervous systems together are responsible for all of our conscious behavior as well as many autonomous bodily functions, and mediate our relationship with our external environments in terms of sensing and responding to external stimuli. The human brain itself is an inconceivably complex information processing, storage and transmission system, in which neuronal communication between its estimated 10^{10} neurons via 10^{14} synapses is necessarily a key feature (Lodish 2000). Communication involves both electrical and chemical signaling within intricately organized and highly interconnected circuits. Because information has to be conveyed across relatively large distances, such as from a sensory nerve ending in the foot to a cell in the spinal cord, neurons have evolved specialized elongated shapes and structures to optimize their signal-carrying function, being able to transmit a nerve impulse at rates of 100 meters per second (Alberts 2002).

The Neuronal Action Potential and Neurotransmitter Release

This internal signal transmission within the neuron takes the form of electrical conductance mediated, expectedly, by ion channels. The temporal and spatial summation of external signals received by the neuron's dendrites causes a change in membrane potential at a part of its cell body, the axon hillock, the site of origin of the axon that contains a dense array of ion channels poised to fire action potentials. An action potential is generated when a depolarized (less negative) threshold membrane potential is reached, leading to the opening of voltage-gated Na^+ channels, the influx of Na^+ down its electrochemical gradient into the cell (both its concentration gradient and the inside-negative membrane potential favor Na^+ entry), a further depolarization of the neighboring axonal membrane, activation of neighboring Na^+ channels, and so on. Voltage-gated K^+

channels are also present and are responsible for repolarizing the membrane quickly to allow for higher frequencies of successive impulse propagation. Certain types of axons are enwrapped along their length by consecutive segments of myelin sheaths, each composed of a stack of specialized cell membrane which forms an insulating layer around the plasma membrane and enhances the conductivity of the axonal cytoplasm, thus aiding more rapid action potential transmission. In this manner, action potentials (i.e., electrical nerve impulses characterized by a sharp waveform of depolarization followed by repolarization) are conducted without attenuation down the length of an axon, towards its terminal, or bouton.

Chemical Synaptic Transmission

At the bouton, chemical synaptic transmission – chemical communication between an axon and a dendrite of two separate neurons across a narrow extracellular space, the synaptic cleft – is thus initiated (**Fig. 1-2**).

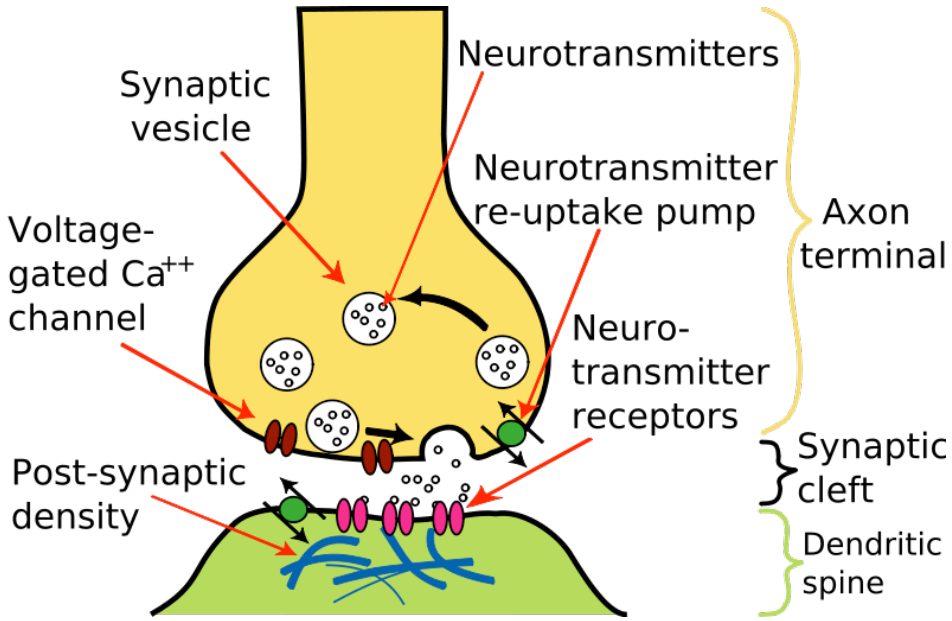

Figure 1-2. Chemical synaptic transmission
Chemical synaptic transmission involves the following events: (1) An action potential arrives at the bouton (axon terminal); (2) Voltage-sensitive calcium channels open upon sensing the change in membrane potential, causing local calcium concentrations to rise; (3) Calcium-sensing proteins on the synaptic vesicles trigger fusion with the plasma membrane, resulting in the release of neurotransmitter stored in the vesicles; (4) Neurotransmitter diffuses across the synaptic cleft, binding to and activating their cognate receptors on the postsynaptic dendrite; (5) Free neurotransmitter is recycled into the axon terminal by plasma membrane transporters ("re-uptake pump"). Figure from http://en.wikipedia.org/wiki/File:Synapse_Illustration2_tweaked.svg, assessed November 11, 2009.

Depolarization of the bouton opens voltage-gated Ca^{2+} channels which allow Ca^{2+} entry into the terminal, triggering the fusion of specialized neurotransmitter-containing synaptic vesicles with the plasma membrane (exocytosis) and the consequent release of neurotransmitter into the synaptic cleft. The free extracellular neurotransmitter then diffuses across the cleft and binds to its cognate receptor on the dendrite of the post-synaptic cell, resulting again in opening of ion channels and a perturbation of its membrane potential. It is these changes in membrane potential, received by the numerous dendrites of each neuron from multiple axon terminals, which are temporally and spatially summated across the cell to determine the familiar all-or-none response at the neuron's axon hillock – either the generation of an action potential upon reaching a threshold membrane potential, or no generation of action potential. Chemical synaptic transmission is therefore the critical point of intercellular communication between neurons, and is instrumental in forms of plasticity such as long-term potentiation (LTP) and long-term depression (LTD) that underlie aspects of synaptic development, learning and memory.

In the central nervous system, the postsynaptic site receiving chemical signals from the presynaptic axon terminal is usually a dendrite or the cell body or even another axon of a neuron. The signal is terminated by diffusion of the neurotransmitter out of the synaptic cleft, re-uptake of neurotransmitter into the presynaptic cell and glial cells by specific plasma membrane transporters, and/or degradation by extracellular enzymes. The overall excitability of the brain hinges on the balance between excitatory and inhibitory transmission (postsynaptic depolarization and hyperpolarization, respectively). The strength of signaling between neurons is thus clearly a key factor determining the function of neural circuits. The presynaptic and postsynaptic components of the synapse determine the extent of neurotransmitter released and the response to it, respectively.

Presynaptic versus Postsynaptic Determinants of Quantal Size

The postsynaptic response to release of neurotransmitter from a single synaptic vesicle (quantal size) is considered to be the elementary unit in synaptic transmission. The quantal size has traditionally been regarded as invariant (Katz 1971), and the amplitude of the postsynaptic response an integral multiple of the quantal size, but it is now appreciated that quantal size is actually variable at many synapses, in both peak amplitude and kinetics (Bekkers et al 1990; Ropert et al 1990). Much attention has been paid to the role of postsynaptic factors in quantal size modulation (Nusser et al 1998), and the regulation of receptors for the principal excitatory transmitter glutamate as a mechanism for LTP has been intensively studied (Bredt & Nicoll 2003; Kerchner & Nicoll 2008).

However, glutamate and $GABA_A$ receptors are not saturated at many synapses in response to single quantum of transmitter. Loose-patch recordings of single spontaneously-released glutamatergic quanta at individual hippocampal synapses found a variation of 30% in receptor conductance that cannot be attributed to random opening of receptor channels, suggesting that these receptors are not a limiting factor in quantal

response (Forti et al 1997). In cultured retinal amacrine cells where pre- and postsynaptic cells sample the same transmitter quantum, simultaneous pre- and postsynaptic measurements of mini amplitudes (amplitudes of miniature postsynaptic currents, i.e. quantal size) show strong correlation which accounts for more than half of the observed quantal size variation. Further, treatment with diazepam which enhances GABA binding to its receptor increases mini amplitude, implying that the transmitter concentration is not saturating (Frerking et al 1995). At single excitatory synapses in cultured hippocampal neurons, quantal excitatory postsynaptic currents (EPSCs) display much more variation than currents evoked by focal application of glutamate (Liu et al 1999; McAllister & Stevens 2000), with the median EPSC being less than half that of the maximal current evocable by focal application (Forti et al 1997; Frerking et al 1995; Liu et al 1999), leading to the conclusion that glutamate receptors are far from saturation during quantal transmission.

Even high-affinity NMDA receptors display non-saturation by a quantum of glutamate. Measuring NMDA receptor activation by imaging calcium transients at single dendritic spines of hippocampal CA1 pyramidal neurons shows that a second release event evoked 10 ms after the first one results in 80% more receptor activation. Because glutamate unbinds from the NMDA receptor slowly, receptors activated in the first event cannot respond to the second event, indicating that the first single release event does not saturate the receptors (Mainen et al 1999). Dissociation of the AMPA and NMDA receptor components of mEPSCs at single cultured hippocampal synapses reveals that both responses are highly variable and strongly correlated, further arguing for non-saturation of the receptors (Mainen et al 1999; McAllister & Stevens 2000).

The above observations of non-saturation of postsynaptic receptors render presynaptic mechanisms a potential source of quantal size variability. Variation in the concentration of transmitter in the synaptic cleft has indeed been determined as a contributing factor in quantal size variability (Barberis et al 2004; Frerking et al 1995; Liu et al 1999; Nusser et al 2001). Analysis of miniature inhibitory postsynaptic currents (mIPSCs) triggered by GABA release under various pharmacological manipulations including receptor antagonists and allosteric binding enhancers determined that the peak cleft concentration of GABA is an important source of variability (Barberis et al 2004). Nonstationary noise analysis and modeling techniques applied to mIPSCs measured in a variety of cell types demonstrates that the large variability has to be due in part to a significant variability in cleft GABA transient (Nusser et al 2001). The amount of neurotransmitter released by the presynaptic cell defines the temporal and spatial profile of transmitter in the synaptic cleft, which in turn affects the extent of activation of postsynaptic receptors. For example, the number of AMPA receptor subunits bound to glutamate determines the conductance of the channel (Rosenmund et al 1998; Smith & Howe 2000), while glutamate spillover to neighboring postsynaptic sites can activate extra-synaptic receptors. In retinal ganglion cells, analysis of EPSCs evoked by electrical stimulation of presynaptic bipolar cells and mEPSCs resulting from spontaneous vesicle release reveals that NMDA receptors encounter less glutamate than AMPA receptors, and that manipulation of cleft glutamate concentration preferentially affects the NMDA response, indicating that NMDA receptors are located extrasynaptically and are activated

as a result of spillover of glutamate from the cleft (Chen & Diamond 2002; DiGregorio et al 2002). At cerebellar mossy fiber-granule cell synapses, single AMPA receptor EPSCs are composed of two components, direct glutamate release with fast-rising kinetics and rapid glutamate diffusion from neighboring synapses with slow-rising kinetics, a phenomenon also attributed to extrasynaptic spillover of glutamate (DiGregorio et al 2002).

Vesicular Release Modes

The variation in transmitter cleft profile is often attributed to variation in vesicle release probability (Ahmed & Siegelbaum 2009; Behrends & ten Bruggencate 1998; Fourcaudot et al 2009), which can increase the frequency of multivesicular release (Ahmed & Siegelbaum 2009; Bender et al 2009; Kirischuk et al 1999; Singer 2007). Interestingly, compound vesicle fusion has recently been suggested as an alternative explanation to multivesicular release at conventional synapses (He et al 2009); it involves the fusion of synaptic vesicles with each other before fusion with plasma membrane, and was initially observed at ribbon synapses of the visual system (Li et al 2009; Matthews & Sterling 2008). Even without considering multiple vesicles, quantal size can be influenced by regulation of a single vesicle – modulation of the diameter of the fusion pore (the aqueous passage between the vesicle lumen and the extracellular fluid when a vesicle is partially fused with the plasma membrane) is another potential way to vary transmitter release, with larger pore diameter or longer open-pore duration allowing for greater release (Choi et al 2003; Fernandez-Peruchena et al 2005; Sorensen 2009). For example, single-cell amperometric measurements of secretory granule release from adrenal chromaffin cells expressing a mutant of Munc-18, a protein involved in a late-step of exocytosis, reveal marked changes in spike characteristics, with a significant correlation between total charge and half-width of spikes, suggesting that the decrease in catecholamine release is due to a shorter time course of release (Fisher et al 2001). Many other studies of exocytotic proteins, especially SNAREs and synaptotagmins, have found effects on the properties of the fusion pore. Short variations in the molecular length of synaptobrevin 2 affect the quantal kinetics of chromaffin granule exocytosis by slowing the rate of fusion pore expansion (Kesavan et al 2007). Expression of mutant synaptotagmin 1 with defects in calcium-dependent SNARE binding in PC12 cells results in reduced fusion pore open probabilities and fusion pore expansion (Lynch et al 2008). Amperometric recordings of catecholamine efflux through individual fusion pores in PC12 cells shows that different mutants of synaptotagmin 1 and 4 determine the choice between kiss-and-run and full vesicle fusion (Wang et al 2003).

Biosynthesis and Metabolism of Neurotransmitters

Evidently, there is substantial contribution of the presynapse to regulation of quantal size. Apart from the mode and frequency of vesicular release, could the extent of vesicular filling itself be another source of quantal size variation? Vesicle filling depends partly on the cytoplasmic concentration of transmitter, which in turn depends on the

biosynthetic and metabolic enzymes present, as well as transmitter recycling from the synaptic cleft. Recycling can occur directly via specific transporters on the presynaptic plasma membrane, indirectly via recycling of the metabolic products, or indirectly via uptake by glial cells. Acetylcholine is metabolized by acetylcholinesterase in the synaptic cleft into acetate and choline, the latter of which is recycled from the cleft via choline transporters to be reused for synthesis of acetylcholine. The case of glutamate is more complex, since it is taken up after release primarily by glial cells (Rothstein et al 1996; Takayasu et al 2005; Tanaka et al 1997). It is thought to be recycled back into neurons in the form of glutamine synthesized in and released from glia, because most of the glutamate released as transmitter derives from its precursor glutamine (Hamberger et al 1979; Laake et al 1995; Pow & Crook 1996) through the action of phosphate-activated glutaminase (Conti & Minelli 1994), and inhibition of glutamine synthetase (GS) in glial cells inhibits neuronal glutamate release (Pow & Robinson 1994; Rothstein & Tabakoff 1984). However, experiments with GS and glutamate transporter inhibition in the isolated rat retina suggest that uptake of released glutamate into photoreceptors plays a more important role in transmitter recycling than does uptake of glutamate into Muller cells and its subsequent conversion to glutamine (Winkler et al 1999). Further, although the release of glutamine from glia and its uptake into neurons are thought to be mediated by system N (Chaudhry et al 1999) and system A (Armano et al 2002), respectively, the localization of system A to excitatory axon terminals is controversial (Chaudhry et al 2002; Mackenzie et al 2003), and a study of the effects of exogenous and extracellular glutamine and of pharmacological inhibitors of GS or system A concludes that neurons can store or produce glutamate for long periods independently of glia and the glutamate-glutamine cycle (Kam & Nicoll 2007).

Further evidence for the importance of transmitter recycling is found in the knockout of the glycine transporter GlyT2 (a plasma membrane glycine transporter that recycles glycine from the extracellular space), which exhibits a reduction in glycinergic quantal size (Gomeza et al 2003). Administration of L-3,4-dihydroxyphenylalanine (L-DOPA), a precursor of dopamine made by tyrosine hydroxylase (TH), increases vesicular catecholamine content in pheochromocytoma (PC12) cells (Colliver et al 2000), while inhibition of TH reduces quantal size, a phenomenon reversible by L-DOPA (Pothos et al 1998). TH is itself subjected to feedback inhibition by L-DOPA and dopamine (Fujisawa & Okuno 2005; Kumer & Vrana 1996). Additionally, there is much evidence for the regulation of TH by neuronal activity, both through phosphorylation, transcriptional and post-transcriptional control (Fitzpatrick 2000; Zigmond et al 1989). Indeed, direct evidence that cytosolic transmitter concentration impacts quantal size is that quantal size at the calyx of Held scales with the concentration of glutamate dialyzed into the presynaptic terminal (Ishikawa et al 2002).

Vesicular Size

The size of a synaptic vesicle can affect the amount of neurotransmitter it can contain. Although it is generally thought that membranes are relatively inelastic and hence constant in dimensions, there is evidence for variation in synaptic vesicle size. For

example, treatment of PC12 cells with reserpine, an inhibitor of the vesicular monoamine transporter (VMAT), decreases catecholamine content together with vesicle size, while treatment with L-DOPA increases catecholamine content and vesicle size, with the concentration within the vesicles remaining relatively constant (Colliver et al 2000; Gong et al 2003). Interestingly, overexpression of adaptor protein 3, involved in cargo sorting into budding vesicles, decreases quantal and vesicle size in mouse chromaffin cells while its deletion increases quantal and vesicle size (Grabner et al 2006), providing further evidence for the link between vesicle size and transmitter content. However, since the biogenesis of dense core vesicles from the Golgi contrasts with that of synaptic vesicles, which are recycled by endocytosis from the synaptic plasma membrane, the determinants of vesicle size may differ too. Yet there is also evidence that increasing expression of the *Drosophila* vesicular glutamate transporter (DVGLUT) in *Drosophila* motoneurons increases quantal size, which is accompanied by an increase in synaptic vesicle volume (Daniels et al 2004). On the other hand, mutants with reduced levels of DVGLUT demonstrate a dose-dependent reduction in the frequency of spontaneous quantal release with no reduction in quantal size, leading to the intriguing conclusion that a single DVGLUT is necessary and sufficient to fill a synaptic vesicle. Further, vesicles in *dvglut* mutants are smaller than those in wildtype (Daniels et al 2006). However, a study at the calyx of Held determining vesicle volume by measuring the capacitance jump evoked by single vesicle fusion concluded that the vesicular glutamate concentration, not vesicle volume, is the main source of quantal size variation (Wu et al 2007).

Vesicular Neurotransmitter Transporter Expression

Transport of neurotransmitter into synaptic vesicles occurs via specific vesicular transporters, hence variation in the transporter levels can have an impact on the extent of vesicle filling with transmitter, as mentioned above with the DVGLUT mutants. This phenomenon is well demonstrated in VMAT2 knockout mice, whose monoamine release is eliminated and total monoamine levels are reduced despite normal numbers and recycling of synaptic vesicles (Fon et al 1997; Wang et al 1997), in VGLUT1 knockout mice whose quantal size and excitatory synaptic transmission are also reduced with no defects in vesicle recycling (Wojcik et al 2004), and in VGLUT2 knockout mice whose quantal size is reduced (Moechars et al 2006; Wallen-Mackenzie et al 2006). In mice genetically engineered to have reduced levels of vesicular acetylcholine transporter (VAChT), quantal size is also reduced in parallel with protein reduction, and this is accompanied by neuromuscular and cognitive behavioral defects (Prado et al 2006). Mice with VAChT completely knocked out display lethality soon after birth (de Castro et al 2009), as do the other vesicular transporter knockout mice mentioned, attesting to their importance in synaptic and organismal physiology. On the other hand, overexpression of VAChT (Song et al 1997) or VGLUT (Wilson et al 2005) both increase quantal size.

The vesicular neurotransmitter transporters have also been demonstrated to be sensitive to regulation by heterotrimeric G proteins. $G\alpha o_2$ was first found to inhibit catecholamine uptake by VMAT1 in PC12 cells (Ahnert-Hilger et al 1998), and then to also inhibit VMAT2 in neurons (Holtje et al 2000). It has also been reported to alter the

chloride sensitivity of VGLUT, shifting the maximal activation by chloride to lower concentrations (Winter et al 2005). Further, VMAT2 is subject to feedback regulation – vesicle filling initiates $G\alpha_q$ inhibition of VMAT2 (Holtje et al 2003), and this seems to be mediated by the first lumenal domain of VMAT (Brunk et al 2006).

Driving Force for Neurotransmitter Transport

Under less drastic manipulations as altering vesicular neurotransmitter transporter (VNT) expression, what other factors determine transporter activity? The VNTs are secondary active transporters, having no direct input of energy such as ATP or light. They are thus energetically driven only by chemical and/or electrical gradients. As introduced above, the V-ATPase provides the primary driving force for neurotransmitter uptake into synaptic vesicles by generating a proton electrochemical gradient ($\Delta\mu_{H+}$; acidic-inside and positive-inside) across the vesicular membrane. Clearly, inhibition of the V-ATPase would be predicted to inhibit vesicle filling, and this has indeed been demonstrated in rat hippocampal neurons treated with V-ATPase inhibitor Bafilomycin A1, which produce miniature excitatory and inhibitory postsynaptic currents (mEPSCs and mIPSCs, respectively) with reduced amplitudes (Zhou et al 2000).

The dependence of VNTs on the $\Delta\mu_{H+}$ is dictated by the stoichiometry of the transporter. While the stoichiometry of transport has only been determined for VMAT and VAChT to be 2 H^+:1 protonated neurotransmitter (Johnson et al 1981; Knoth et al 1981a; Knoth et al 1981b), the other transporters VGLUT and VGAT (vesicular GABA transporter; alternatively termed VIAAT, or vesicular inhibitory amino acid transporter, because it also transports glycine) are also believed to operate via proton/neurotransmitter exchange due to their dependence on the V-ATPase (**Fig. 1-3**). For VMAT and VAChT, each transport cycle involves the exit of 2 protons but only 1 positive charge from the vesicle, and hence the transporter depends more on ΔpH, the chemical component of $\Delta\mu_{H+}$, than on the electrical component Δψ. In the presence of constant pumping by the V-ATPase, the dissipation of ΔpH by substrate uptake tips the energetic balance toward accumulation of Δψ (Blackmore et al 2001; Johnson & Scarpa 1979), which hence limits vesicle filling. However, the entry of Cl^- through carriers of the ClC family is important for the formation of ΔpH – the V-ATPase generates a large Δψ but only a small ΔpH in the absence of Cl^-. Cl^- entry decreases Δψ, allowing the enhancement of ΔpH (Johnson et al 1979; Maycox et al 1988; Tabb et al 1992; Van Dyke 1988) and thereby stimulating the transport of monoamines into secretory vesicles.

The formation and maintenance of a driving force is clearly an important determinant of vesicular filling with neurotransmitter. Although the precise stoichiometry of ionic coupling by the VGLUTs remains unknown, these carriers are commonly considered to be H^+/glutamate exchangers (Liu & Edwards 1997; Schuldiner et al 1995; Shioi & Ueda 1990) with a stoichiometry of *n*:1 (H^+:glu^-), with net outward movement of *n* + 1 charge per cycle of *n* protons leaving (**Fig. 1-3**). The VGLUTs thus rely more on

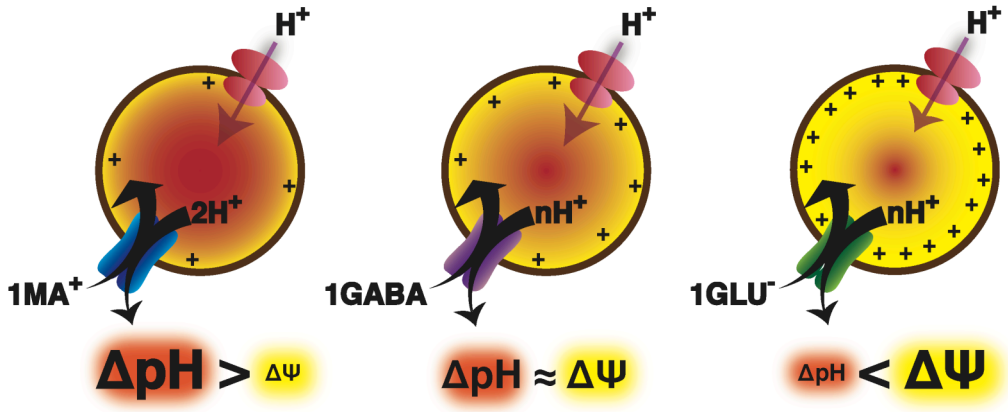

Figure 1-3. Vesicular neurotransmitter transporters
The dependence of the vesicular neurotransmitter transporters on the proton electrochemical gradient generated by the vacuolar H^+-ATPase (red) depends on the stoichiometry of the transporter. The vesicular monoamine transporter (VMAT; blue) depends more on ΔpH than Δψ, the vesicular GABA transporter (VGAT, also known as VIAAT; purple) depends equally on ΔpH and Δψ, and the vesicular glutamate transporter (VGLUT; green) depends more on Δψ than ΔpH. The relative proportions of ΔpH and Δψ are depicted by red and yellow, respectively.

Δψ than ΔpH (Maycox et al 1988; Tabb et al 1992), which predicts the dissipation of Δψ and accumulation of ΔpH during vesicular glutamate uptake.

Indeed, glutamate entry does acidify synaptic vesicles (Cidon & Sihra 1989; Hartinger & Jahn 1993; Maycox et al 1988), limiting the ability of the H^+ pump to maintain Δψ and drive glutamate transport. Despite the primary role of glutamate in excitatory transmission and the importance of Δψ for vesicular glutamate transport, little is known about the role of Δψ in most organelles, or the mechanisms that promote its formation. In this dissertation, we thus explore the mechanisms governing the transport of glutamate into synaptic vesicles, an old yet unresolved subject of fundamental importance to neurotransmission, as well as a model for Δψ-driven transport processes.

1.3 OVERVIEW OF DISSERTATION

The overall goal of this dissertation is to gain a better understanding of the factors underlying glutamate transport into synaptic vesicles and that hence regulate quantal size. Specifically, we sought to determine if there are factors that actively promote glutamate transport by promoting formation of its driving force, Δψ. We employed largely biochemical methods involving *in vitro* assays on isolated rodent brain synaptic vesicles, as well as some *in vivo* characterization in brain slice preparations and in dissociated neuronal cultures.

Chapter 2 begins with an overview of the current understanding of vesicular glutamate transport and introduces our hypothesis regarding facilitation of glutamate

transport as well as our experimental strategies and goals. It then describes our experimental results: the electroneutral cation/H^+ exchange activity we demonstrate on synaptic vesicles that serves to increase membrane potential, the effect of cations on glutamate transport and quantal size, and the use of pharmacology to identify the family of proteins responsible for the cation/H^+ exchange.

Chapter 3 describes our efforts towards determining the molecular identity of the protein catalyzing cation/H^+ exchange by co-transfection and immunocytochemistry.

Finally, Chapter 4 summarizes the findings presented in this thesis and offers some perspectives of the results, followed by future directions based on this work.

1.4 REFERENCES

Ahmed MS, Siegelbaum SA. 2009. Recruitment of N-Type Ca(2+) channels during LTP enhances low release efficacy of hippocampal CA1 perforant path synapses. *Neuron* 63:372-85

Ahnert-Hilger G, Nurnberg B, Exner T, Schafer T, Jahn R. 1998. The heterotrimeric G protein Go2 regulates catecholamine uptake by secretory vesicles. *EMBO J* 17:406-13

Alberts B. 2002. *Molecular biology of the cell*. New York: Garland Science. xxxiv, [1548] p. pp.

Armano S, Coco S, Bacci A, Pravettoni E, Schenk U, et al. 2002. Localization and functional relevance of system a neutral amino acid transporters in cultured hippocampal neurons. *J Biol Chem* 277:10467-73

Barberis A, Petrini EM, Cherubini E. 2004. Presynaptic source of quantal size variability at GABAergic synapses in rat hippocampal neurons in culture. *Eur J Neurosci* 20:1803-10

Behrends JC, ten Bruggencate G. 1998. Changes in quantal size distributions upon experimental variations in the probability of release at striatal inhibitory synapses. *J Neurophysiol* 79:2999-3011

Bekkers JM, Richerson GB, Stevens CF. 1990. Origin of variability in quantal size in cultured hippocampal neurons and hippocampal slices. *Proc Natl Acad Sci U S A* 87:5359-62

Bender VA, Pugh JR, Jahr CE. 2009. Presynaptically expressed long-term potentiation increases multivesicular release at parallel fiber synapses. *J Neurosci* 29:10974-8

Blackmore CG, Varro A, Dimaline R, Bishop L, Gallacher DV, Dockray GJ. 2001. Measurement of secretory vesicle pH reveals intravesicular alkalinization by vesicular monoamine transporter type 2 resulting in inhibition of prohormone cleavage. *J Physiol* 531:605-17

Bredt DS, Nicoll RA. 2003. AMPA receptor trafficking at excitatory synapses. *Neuron* 40:361-79

Brunk I, Blex C, Rachakonda S, Holtje M, Winter S, et al. 2006. The first luminal domain of vesicular monoamine transporters mediates G-protein-dependent regulation of transmitter uptake. *J Biol Chem* 281:33373-85

Chaudhry FA, Reimer RJ, Krizaj D, Barber D, Storm-Mathisen J, et al. 1999. Molecular analysis of system N suggests novel physiological roles in nitrogen metabolism and synaptic transmission. *Cell* 99:769-80

Chaudhry FA, Schmitz D, Reimer RJ, Larsson P, Gray AT, et al. 2002. Glutamine uptake by neurons: interaction of protons with system a transporters. *J Neurosci* 22:62-72

Chen S, Diamond JS. 2002. Synaptically released glutamate activates extrasynaptic NMDA receptors on cells in the ganglion cell layer of rat retina. *J Neurosci* 22:2165-73

Choi S, Klingauf J, Tsien RW. 2003. Fusion pore modulation as a presynaptic mechanism contributing to expression of long-term potentiation. *Philos Trans R Soc Lond B Biol Sci* 358:695-705

Cidon S, Sihra TS. 1989. Characterization of a H+-ATPase in rat brain synaptic vesicles. Coupling to L-glutamate transport. *J Biol Chem* 264:8281-8

Colliver TL, Pyott SJ, Achalabun M, Ewing AG. 2000. VMAT-Mediated changes in quantal size and vesicular volume. *J Neurosci* 20:5276-82

Conti F, Minelli A. 1994. Glutamate immunoreactivity in rat cerebral cortex is reversibly abolished by 6-diazo-5-oxo-L-norleucine (DON), an inhibitor of phosphate-activated glutaminase. *J Histochem Cytochem* 42:717-26

Daniels RW, Collins CA, Chen K, Gelfand MV, Featherstone DE, DiAntonio A. 2006. A single vesicular glutamate transporter is sufficient to fill a synaptic vesicle. *Neuron* 49:11-6

Daniels RW, Collins CA, Gelfand MV, Dant J, Brooks ES, et al. 2004. Increased expression of the Drosophila vesicular glutamate transporter leads to excess glutamate release and a compensatory decrease in quantal content. *J Neurosci* 24:10466-74

de Castro BM, De Jaeger X, Martins-Silva C, Lima RD, Amaral E, et al. 2009. The vesicular acetylcholine transporter is required for neuromuscular development and function. *Mol Cell Biol* 29:5238-50

DiGregorio DA, Nusser Z, Silver RA. 2002. Spillover of glutamate onto synaptic AMPA receptors enhances fast transmission at a cerebellar synapse. *Neuron* 35:521-33

Fernandez-Peruchena C, Navas S, Montes MA, Alvarez de Toledo G. 2005. Fusion pore regulation of transmitter release. *Brain Res Brain Res Rev* 49:406-15

Fisher RJ, Pevsner J, Burgoyne RD. 2001. Control of fusion pore dynamics during exocytosis by Munc18. *Science* 291:875-8

Fitzpatrick PF. 2000. The aromatic amino acid hydroxylases. *Adv Enzymol Relat Areas Mol Biol* 74:235-94

Fon EA, Pothos EN, Sun BC, Killeen N, Sulzer D, Edwards RH. 1997. Vesicular transport regulates monoamine storage and release but is not essential for amphetamine action. *Neuron* 19:1271-83

Forti L, Bossi M, Bergamaschi A, Villa A, Malgaroli A. 1997. Loose-patch recordings of single quanta at individual hippocampal synapses. *Nature* 388:874-8

Fourcaudot E, Gambino F, Casassus G, Poulain B, Humeau Y, Luthi A. 2009. L-type voltage-dependent Ca(2+) channels mediate expression of presynaptic LTP in amygdala. *Nat Neurosci* 12:1093-5

Frerking M, Borges S, Wilson M. 1995. Variation in GABA mini amplitude is the consequence of variation in transmitter concentration. *Neuron* 15:885-95

Fujisawa H, Okuno S. 2005. Regulatory mechanism of tyrosine hydroxylase activity. *Biochem Biophys Res Commun* 338:271-6
Gamba G, Bobadilla NA. 2004. Molecular physiology of the renal Na(+)-Cl- and Na(+)-K(+)-2Cl- cotransporters. *Adv Exp Med Biol* 559:55-65
Gomeza J, Ohno K, Hulsmann S, Armsen W, Eulenburg V, et al. 2003. Deletion of the mouse glycine transporter 2 results in a hyperekplexia phenotype and postnatal lethality. *Neuron* 40:797-806
Gong LW, Hafez I, Alvarez de Toledo G, Lindau M. 2003. Secretory vesicles membrane area is regulated in tandem with quantal size in chromaffin cells. *J Neurosci* 23:7917-21
Grabner CP, Price SD, Lysakowski A, Cahill AL, Fox AP. 2006. Regulation of large dense-core vesicle volume and neurotransmitter content mediated by adaptor protein 3. *Proc Natl Acad Sci U S A* 103:10035-40
Hamberger A, Chiang GH, Sandoval E, Cotman CW. 1979. Glutamate as a CNS transmitter. II. Regulation of synthesis in the releasable pool. *Brain Res* 168:531-41
Hartinger J, Jahn R. 1993. An anion binding site that regulates the glutamate transporter of synaptic vesicles. *J Biol Chem* 268:23122-7
He L, Xue L, Xu J, McNeil BD, Bai L, et al. 2009. Compound vesicle fusion increases quantal size and potentiates synaptic transmission. *Nature* 459:93-7
Holtje M, von Jagow B, Pahner I, Lautenschlager M, Hortnagl H, et al. 2000. The neuronal monoamine transporter VMAT2 is regulated by the trimeric GTPase Go(2). *J Neurosci* 20:2131-41
Holtje M, Winter S, Walther D, Pahner I, Hortnagl H, et al. 2003. The vesicular monoamine content regulates VMAT2 activity through Galphaq in mouse platelets. Evidence for autoregulation of vesicular transmitter uptake. *J Biol Chem* 278:15850-8
Ishikawa T, Sahara Y, Takahashi T. 2002. A single packet of transmitter does not saturate postsynaptic glutamate receptors. *Neuron* 34:613-21
Johnson RG, Carty SE, Scarpa A. 1981. Proton: substrate stoichiometries during active transport of biogenic amines in chromaffin ghosts. *J Biol Chem* 256:5773-80
Johnson RG, Pfister D, Carty SE, Scarpa A. 1979. Biological amine transport in chromaffin ghosts. Coupling to the transmembrane proton and potential gradients. *J Biol Chem* 254:10963-72
Johnson RG, Scarpa A. 1979. Protonmotive force and catecholamine transport in isolated chromaffin granules. *J Biol Chem* 254:3750-60
Kam K, Nicoll R. 2007. Excitatory synaptic transmission persists independently of the glutamate-glutamine cycle. *J Neurosci* 27:9192-200
Katz B. 1971. Quantal mechanism of neural transmitter release. *Science* 173:123-6
Kerchner GA, Nicoll RA. 2008. Silent synapses and the emergence of a postsynaptic mechanism for LTP. *Nat Rev Neurosci* 9:813-25
Kesavan J, Borisovska M, Bruns D. 2007. v-SNARE actions during Ca(2+)-triggered exocytosis. *Cell* 131:351-63
Kirischuk S, Veselovsky N, Grantyn R. 1999. Relationship between presynaptic calcium transients and postsynaptic currents at single gamma-aminobutyric acid (GABA)ergic boutons. *Proc Natl Acad Sci U S A* 96:7520-5

Klingenberg M, Rottenberg H. 1977. Relation between the gradient of the ATP/ADP ratio and the membrane potential across the mitochondrial membrane. *Eur J Biochem* 73:125-30

Knoth J, Isaacs JM, Njus D. 1981a. Amine transport in chromaffin granule ghosts. pH dependence implies cationic form is translocated. *J Biol Chem* 256:6541-3

Knoth J, Zallakian M, Njus D. 1981b. Stoichiometry of H+-linked dopamine transport in chromaffin granule ghosts. *Biochemistry* 20:6625-9

Kramer R, Klingenberg M. 1980. Modulation of the reconstituted adenine nucleotide exchange by membrane potential. *Biochemistry* 19:556-60

Kumer SC, Vrana KE. 1996. Intricate regulation of tyrosine hydroxylase activity and gene expression. *J Neurochem* 67:443-62

Laake JH, Slyngstad TA, Haug FM, Ottersen OP. 1995. Glutamine from glial cells is essential for the maintenance of the nerve terminal pool of glutamate: immunogold evidence from hippocampal slice cultures. *J Neurochem* 65:871-81

Li GL, Keen E, Andor-Ardo D, Hudspeth AJ, von Gersdorff H. 2009. The unitary event underlying multiquantal EPSCs at a hair cell's ribbon synapse. *J Neurosci* 29:7558-68

Liu G, Choi S, Tsien RW. 1999. Variability of neurotransmitter concentration and nonsaturation of postsynaptic AMPA receptors at synapses in hippocampal cultures and slices. *Neuron* 22:395-409

Liu Y, Edwards RH. 1997. The role of vesicular transport proteins in synaptic transmission and neural degeneration. *Annu Rev Neurosci* 20:125-56

Lodish HF. 2000. *Molecular cell biology*. New York: W.H. Freeman. xxxvi, 1084, G-17, I-36 p. pp.

Lynch KL, Gerona RR, Kielar DM, Martens S, McMahon HT, Martin TF. 2008. Synaptotagmin-1 utilizes membrane bending and SNARE binding to drive fusion pore expansion. *Mol Biol Cell* 19:5093-103

Mackenzie B, Schafer MK, Erickson JD, Hediger MA, Weihe E, Varoqui H. 2003. Functional properties and cellular distribution of the system A glutamine transporter SNAT1 support specialized roles in central neurons. *J Biol Chem* 278:23720-30

Mainen ZF, Malinow R, Svoboda K. 1999. Synaptic calcium transients in single spines indicate that NMDA receptors are not saturated. *Nature* 399:151-5

Matthews G, Sterling P. 2008. Evidence that vesicles undergo compound fusion on the synaptic ribbon. *J Neurosci* 28:5403-11

Maycox PR, Deckwerth T, Hell JW, Jahn R. 1988. Glutamate uptake by brain synaptic vesicles. Energy dependence of transport and functional reconstitution in proteoliposomes. *J Biol Chem* 263:15423-8

McAllister AK, Stevens CF. 2000. Nonsaturation of AMPA and NMDA receptors at hippocampal synapses. *Proc Natl Acad Sci U S A* 97:6173-8

Moechars D, Weston MC, Leo S, Callaerts-Vegh Z, Goris I, et al. 2006. Vesicular glutamate transporter VGLUT2 expression levels control quantal size and neuropathic pain. *J Neurosci* 26:12055-66

Nusser Z, Hajos N, Somogyi P, Mody I. 1998. Increased number of synaptic GABA(A) receptors underlies potentiation at hippocampal inhibitory synapses. *Nature* 395:172-7

Nusser Z, Naylor D, Mody I. 2001. Synapse-specific contribution of the variation of transmitter concentration to the decay of inhibitory postsynaptic currents. *Biophys J* 80:1251-61

Payne JA, Rivera C, Voipio J, Kaila K. 2003. Cation-chloride co-transporters in neuronal communication, development and trauma. *Trends Neurosci* 26:199-206

Pothos EN, Przedborski S, Davila V, Schmitz Y, Sulzer D. 1998. D2-Like dopamine autoreceptor activation reduces quantal size in PC12 cells. *J Neurosci* 18:5575-85

Pow DV, Crook DK. 1996. Direct immunocytochemical evidence for the transfer of glutamine from glial cells to neurons: use of specific antibodies directed against the d-stereoisomers of glutamate and glutamine. *Neuroscience* 70:295-302

Pow DV, Robinson SR. 1994. Glutamate in some retinal neurons is derived solely from glia. *Neuroscience* 60:355-66

Prado VF, Martins-Silva C, de Castro BM, Lima RF, Barros DM, et al. 2006. Mice deficient for the vesicular acetylcholine transporter are myasthenic and have deficits in object and social recognition. *Neuron* 51:601-12

Ropert N, Miles R, Korn H. 1990. Characteristics of miniature inhibitory postsynaptic currents in CA1 pyramidal neurones of rat hippocampus. *J Physiol* 428:707-22

Rosenmund C, Stern-Bach Y, Stevens CF. 1998. The tetrameric structure of a glutamate receptor channel. *Science* 280:1596-9

Rothstein JD, Dykes-Hoberg M, Pardo CA, Bristol LA, Jin L, et al. 1996. Knockout of glutamate transporters reveals a major role for astroglial transport in excitotoxicity and clearance of glutamate. *Neuron* 16:675-86

Rothstein JD, Tabakoff B. 1984. Alteration of striatal glutamate release after glutamine synthetase inhibition. *J Neurochem* 43:1438-46

Schuldiner S, Shirvan A, Linial M. 1995. Vesicular neurotransmitter transporters: from bacteria to humans. *Physiol Rev* 75:369-92

Shioi J, Ueda T. 1990. Artificially imposed electrical potentials drive L-glutamate uptake into synaptic vesicles of bovine cerebral cortex. *Biochem J* 267:63-8

Singer JH. 2007. Multivesicular release and saturation of glutamatergic signalling at retinal ribbon synapses. *J Physiol* 580:23-9

Smith TC, Howe JR. 2000. Concentration-dependent substate behavior of native AMPA receptors. *Nat Neurosci* 3:992-7

Song H, Ming G, Fon E, Bellocchio E, Edwards RH, Poo M. 1997. Expression of a putative vesicular acetylcholine transporter facilitates quantal transmitter packaging. *Neuron* 18:815-26

Sorensen JB. 2009. Conflicting views on the membrane fusion machinery and the fusion pore. *Annu Rev Cell Dev Biol* 25:513-37

Tabb JS, Kish PE, Van Dyke R, Ueda T. 1992. Glutamate transport into synaptic vesicles. Roles of membrane potential, pH gradient, and intravesicular pH. *J Biol Chem* 267:15412-8

Takayasu Y, Iino M, Kakegawa W, Maeno H, Watase K, et al. 2005. Differential roles of glial and neuronal glutamate transporters in Purkinje cell synapses. *J Neurosci* 25:8788-93

Tanaka K, Watase K, Manabe T, Yamada K, Watanabe M, et al. 1997. Epilepsy and exacerbation of brain injury in mice lacking the glutamate transporter GLT-1. *Science* 276:1699-702

Van Dyke RW. 1988. Proton pump-generated electrochemical gradients in rat liver multivesicular bodies. Quantitation and effects of chloride. *J Biol Chem* 263:2603-11

Wallen-Mackenzie A, Gezelius H, Thoby-Brisson M, Nygard A, Enjin A, et al. 2006. Vesicular glutamate transporter 2 is required for central respiratory rhythm generation but not for locomotor central pattern generation. *J Neurosci* 26:12294-307

Wang CT, Lu JC, Bai J, Chang PY, Martin TF, et al. 2003. Different domains of synaptotagmin control the choice between kiss-and-run and full fusion. *Nature* 424:943-7

Wang YM, Gainetdinov RR, Fumagalli F, Xu F, Jones SR, et al. 1997. Knockout of the vesicular monoamine transporter 2 gene results in neonatal death and supersensitivity to cocaine and amphetamine. *Neuron* 19:1285-96

Wilson NR, Kang J, Hueske EV, Leung T, Varoqui H, et al. 2005. Presynaptic regulation of quantal size by the vesicular glutamate transporter VGLUT1. *J Neurosci* 25:6221-34

Winkler BS, Kapousta-Bruneau N, Arnold MJ, Green DG. 1999. Effects of inhibiting glutamine synthetase and blocking glutamate uptake on b-wave generation in the isolated rat retina. *Vis Neurosci* 16:345-53

Winter S, Brunk I, Walther DJ, Holtje M, Jiang M, et al. 2005. Galphao2 regulates vesicular glutamate transporter activity by changing its chloride dependence. *J Neurosci* 25:4672-80

Wojcik SM, Rhee JS, Herzog E, Sigler A, Jahn R, et al. 2004. An essential role for vesicular glutamate transporter 1 (VGLUT1) in postnatal development and control of quantal size. *Proc Natl Acad Sci U S A* 101:7158-63

Wu XS, Xue L, Mohan R, Paradiso K, Gillis KD, Wu LG. 2007. The origin of quantal size variation: vesicular glutamate concentration plays a significant role. *J Neurosci* 27:3046-56

Zhou Q, Petersen CC, Nicoll RA. 2000. Effects of reduced vesicular filling on synaptic transmission in rat hippocampal neurones. *J Physiol* 525 Pt 1:195-206

Zigmond RE, Schwarzschild MA, Rittenhouse AR. 1989. Acute regulation of tyrosine hydroxylase by nerve activity and by neurotransmitters via phosphorylation. *Annu Rev Neurosci* 12:415-61

Chapter 2. Monovalent Cation/H^+ Exchange on Synaptic Vesicles Stimulates Glutamate Transport by Increasing Membrane Potential

2.1 INTRODUCTION

Glutamate is the primary excitatory neurotransmitter in the brain, thus the transport of glutamate into synaptic vesicles has been of interest for many years. Because synaptic vesicles are small and relatively homogeneous in size, they are readily purified and amenable to study (Craige et al 2004; Nagy et al 1976). Out of these numerous studies in a variety of systems including bovine and rat synaptic vesicles, as well as synaptic vesicle proteins reconstituted in proteoliposomes, has emerged a number of salient features characteristic of synaptic vesicle glutamate uptake.

Characteristics of Vesicular Glutamate Transport

Unlike the plasma membrane glutamate transporters, the vesicular glutamate transporters have a high specificity for glutamate and do not transport aspartate (Bellocchio et al 2000; Carlson et al 1989; Juge et al 2006; Maycox et al 1988; Moriyama et al 1990). They also have a lower substrate affinity than the plasma membrane transporters, with a K_m for glutamate of 1-2 mM (Bellocchio et al 2000; Carlson et al 1989; Maycox et al 1988; Wolosker et al 1996). Further, they are Na^+-independent, in contrast to the plasma membrane glutamate transporters which are Na^+-driven.

The primary driving force for the VGLUTs that concentrate glutamate into synaptic vesicles is the proton electrochemical gradient generated by the V-ATPase. The $\Delta\psi$ component is generally accepted to be critical in driving uptake, with some studies concluding that uptake is driven solely by $\Delta\psi$ (Cidon & Sihra 1989; Hell et al 1990; Maycox et al 1988; Moriyama et al 1990), while other studies show that ΔpH can also drive uptake (Shioi & Ueda 1990; Tabb et al 1992). Most of these conclusions were based on the chloride sensitivity of uptake and the effects of ionophores that change the ΔpH and $\Delta\psi$ components of the proton electrochemical gradient.

The VGLUTs have a biphasic sensitivity to chloride concentration – low millimolar concentrations of chloride stimulate transport 3- to 6-fold compared to the absence of chloride, but further increases of chloride beyond 4-10 mM become inversely correlated with glutamate uptake (Bellocchio et al 2000; Carlson et al 1989; Juge et al 2006; Tabb et al 1992; Wolosker et al 1996). This inhibition of uptake by high chloride, together with observations that NH_4^+ and, in some cases, nigericin (both of which essentially convert ΔpH to $\Delta\psi$) stimulate glutamate uptake, led to the conclusion that high ΔpH is detrimental for glutamate transport and hence that glutamate transport depends only on $\Delta\psi$ rather than ΔpH. On the other hand, other observations led to the

conclusion that ΔpH may also play a role, albeit smaller than Δψ, in driving glutamate transport: (i) Low concentrations of chloride, at which there is formation of some ΔpH, stimulate glutamate uptake; (ii) A23187, a divalent cation/H^+-exchanging ionophore that essentially converts ΔpH into Δψ, in the presence of high chloride decreases rather than increases uptake (Wolosker et al 1996); and (iii) there is residual uptake in the presence of valinomycin, which is abolished in the additional presence of nigericin or FCCP (Bellocchio et al 2000; Cidon & Sihra 1989; Juge et al 2006). However, treatment of native vesicles with valinomycin in the presence of an actively pumping V-ATPase may not fully dissipate Δψ (depending on the relative K^+ concentrations inside and outside the vesicle), hence the residual uptake in the presence of valinomycin may well be still driven by Δψ.

The stimulation of glutamate transport by low millimolar chloride concentrations has been attributed to a direct interaction of chloride with a binding site on the transporter, separate from the glutamate binding site. This is drawn from observations that 4,4-diisothiocyanatostilbenedisulphonic acid (DIDS) inhibition of glutamate transport as well as efflux is preventable by high chloride concentrations but not by glutamate (Hartinger & Jahn 1993; Moriyama & Yamamoto 1995), and that the inhibition of glutamate uptake by α-keto acids is also relieved by high chloride (Reis et al 2000). Further, a detailed study of the dependence of glutamate uptake on chloride determined that (i) at high glutamate concentrations, chloride alters the initial rate but not maximal filling at steady-state, and (ii) in the absence of ΔpH, increasing chloride increasingly stimulates glutamate efflux, with half-maximal effect attained at 30 mM (Wolosker et al 1996). These observations support the idea that chloride directly interacts with the transporter and is responsible for its stimulation at low millimolar concentrations.

Potential Mechanisms to Increase Glutamate Transport

The progressive buildup of ΔpH during glutamate transport would be predicted to be detrimental to continued glutamate uptake by dissipating Δψ. Furthermore, if protons were the counterion to the glutamate stored in synaptic vesicles, a conservative estimate of 1 mM of glutamic acid in the vesicles would correspond to an intravesicular pH of about 3.7, inconsistent with current knowledge about vesicular pH (Miesenbock et al 1998). Also, an increase in the uncharged, protonated species of glutamate may increase its non-specific leakage across the vesicle membrane. Maycox et al. suggested the possibility of an intravesicular buffer system that modulates pH in the vesicles, and proposed that intravesicular protons could exchange for extravesicular cations by an antiporter (Maycox et al 1988). This idea was supported by their observations that glutamate-induced acidification stopped before glutamate uptake did, a phenomenon also observed in our data, and that kinetic analysis of glutamate uptake suggested that uptake saturated at higher concentrations than did glutamate-dependent acidification. VMAT-containing vesicles possess a chloride conductance which promotes formation of ΔpH

(Johnson et al 1982; Johnson & Scarpa 1979), so we wondered if VGLUT-containing vesicles also possess a mechanism to promote $\Delta\psi$, by decreasing ΔpH.

A number of possible mechanisms might serve to dissipate the ΔpH accumulated during vesicular glutamate transport, and so increase the production of $\Delta\psi$ by the V-ATPase. First, a H^+ leak conductance might simply allow the efflux of protons down their electrochemical gradient, but this would reduce $\Delta\psi$ to a much greater extent than ΔpH, since the movement of only a few protons would quickly dissipate $\Delta\psi$ while having little effect on ΔpH. Furthermore, the presence of a H^+ leak in direct opposition to the action of the V-ATPase would be difficult to justify in terms of energy efficiency. Second, the efflux of anions from synaptic vesicles might directly create positive internal $\Delta\psi$, inhibiting net H^+-pumping and thus formation of ΔpH by the V-ATPase. This would, however, require the pre-existence of an outwardly directed anion gradient. Recent work using VGLUT1 reconstituted into artificial membranes has indeed shown that chloride efflux can promote vesicular glutamate transport, possibly by increasing $\Delta\psi$ (Schenck et al 2009). Nevertheless, the physiological role of this mechanism in transmitter release using more native preparations has not been demonstrated. Alternatively, the influx of cytoplasmic cation might increase $\Delta\psi$ either by permeation through an ion channel, or through a mechanism of stoichiometrically coupled cation/H^+ exchange, a possibility originally raised many years ago (Maycox et al 1988). Coupled cation/H^+ exchange has the additional advantage that it uses ΔpH to drive cation uptake and, if electroneutral, does not itself dissipate $\Delta\psi$, allowing the V-ATPase to increase $\Delta\psi$ at the expense of the ΔpH that accumulates during vesicular glutamate transport.

Na^+/H^+ exchangers (NHEs)

The family of mammalian Na^+/H^+ exchangers (NHEs) catalyzes the electroneutral exchange of Na^+ for H^+ (1 : 1). Mammalian NHEs are integral membrane proteins with 12 predicted transmembrane domains and a hydrophilic C terminus that diverges among members of the family and is the site of interaction with other proteins (Orlowski & Grinstein 2004). NHE1-5 reside mainly on the plasma membrane, where extensive work has demonstrated important roles in the regulation of cytoplasmic pH and salt absorption (Orlowski & Grinstein 2007; Zachos et al 2005). In contrast, the intracellular isoforms NHE6-9 remain poorly understood. NHE6 and NHE9 have been localized to early and late recycling endosomes, respectively, and NHE7 and NHE8 to the trans- and mid-Golgi, respectively, though the localizations are not discrete but rather overlapping (Nakamura et al 2005), characteristic of the highly dynamic endomembrane system. NHE3 and NHE5 have been observed to recycle between endosomes and the plasma membrane via clathrin-mediated pathways (Chow et al 1999; Szaszi et al 2002). NHE5, 6, 7 and 9 interact with the receptor for activated C kinase 1 (RACK1) which regulates their cycling to the plasma membrane (Ohgaki et al 2008; Onishi et al 2007). Secretory carrier membrane proteins (SCAMPs) interact with NHE5 and 7, modulating their trafficking to recycling endosomes from the plasma membrane and trans-Golgi network (TGN), respectively (Diering et al 2009; Lin et al 2005). NHE5 surface expression is also

modulated by interactions with β-arrestins (Szabo et al 2005), while NHE7 also interacts with caveolin and recycles through both clathrin-dependent and clathrin-independent pathways (Lin et al 2007).

Despite the scarcity of knowledge regarding the functional roles of the intracellular NHEs, organellar pH regulation is likely. Their plasma membrane counterparts undoubtedly regulate cytoplasmic pH and, consistent with a functional role in endomembranes, intracellular isoforms, unlike most of the plasma membrane isoforms, recognize K^+ (Hill et al 2006; Nakamura et al 2005; Numata & Orlowski 2001). Indeed, overexpression of NHE8 and NHE9 in COS7 cells raises Golgi and recycling endosomal pH, respectively (Nakamura et al 2005). Furthermore, double-knockdown of NHE6 and NHE9 in HeLa cells by RNA interference (RNAi) causes enhanced acidification of early endosomes, while single knockdown of either isoform alone had no effect, supporting the view that localization of the NHEs are overlapping and dynamic (Roxrud et al 2009). NHE6 and NHE9 have also been implicated in the regulation of cytoplasmic pH in vestibular hair cells which are surrounded by K^+-rich endolymph, where they appear to traffic to the plasma membrane to fulfill that role (Hill et al 2006). It is conceivable, then, that an NHE resides on and modulates the pH of synaptic vesicles, which recycle via clathrin-mediated endocytosis and can be considered as specialized endosomes.

Experimental Strategies and Goals

The purification of synaptic vesicles is a well-established procedure, and myriad biochemical studies have been performed with this system. With isolated synaptic vesicles, biochemical assays can be performed with finely manipulated conditions to probe the function of proteins and/or lipids on the vesicles. The advantage of using native vesicles is that all molecular species present are endogenous, and at their physiological abundances and ratios. Thus experimental results, when carefully interpreted, generally reflect the physiological relevance of the question at hand.

We thus used the same system to address our questions regarding the ion conductances across the synaptic vesicle membrane. Specifically, we employed pH- and membrane potential-sensitive fluorescent dyes to measure ΔpH and $\Delta\psi$ dynamically over time, in response to various manipulations. We also used radiolabeled compounds to directly monitor transport of glutamate and Na^+, again under different conditions. Our goals were to determine the ion fluxes that occur across the vesicle membrane, and how these may affect glutamate uptake. Further, we performed electrophysiological recordings at a large central synapse, the calyx of Held, to confirm the *in vivo* physiological relevance of our *in vitro* biochemical results.

2.2 MATERIALS AND METHODS

2.2.1 Materials

Bafilomycin A1 was obtained from EMD Biosciences, Oxonol VI from Invitrogen, and all other chemicals from Sigma. ^{22}NaCl and [^{3}H]L-glutamate were obtained from Perkin-Elmer, and HT-200 Tuffryn filters and Supor 200 filters from Pall. Stock solutions of choline gluconate (2 M) were made by titration of choline bicarbonate with gluconic acid to pH 7.4; stock solutions of choline glutamate (1 M) and choline aspartate (1 M) by titration of choline base with glutamic or aspartic acid, respectively.

2.2.2 Synaptic Vesicle Preparation

Synaptic vesicles were isolated by differential centrifugation from rat brain synaptosomes lysed in hypotonic buffer, as previously described (Hell & Jahn 1994). Briefly, the brains of 16 Sprague-Dawley rats, at least four weeks old, were homogenized in 320 mM sucrose, 4 mM HEPES-Tris, pH 7.4, 1 mM $MgCl_2$, 1 mM EGTA (homogenization buffer) containing 1 μg/ml pepstatin A and 200 μM PMSF using nine strokes of a Kontes #22 glass-Teflon homogenizer at 900 rpm. After sedimentation at 1,000 g_{max} for 10 min, the supernatant (S1) was collected, recentrifuged at 12,000 g_{max} for 15 min, and the resulting supernatant (S2) as well as the dark brown middle part of the pellet discarded. The remaining pellet (P2) was washed by resuspension in 6 ml homogenization buffer per brain, sedimenting at 13,000 g_{max} for 15 min and again discarding the supernatant (S2') and dark brown part of the pellet. The pellet (P2') was then resuspended in 0.6 ml homogenization buffer per brain, and 9 volumes of ice-cold water added along with 1 M HEPES-Tris, pH 7.4 to a final concentration of 8 mM. After incubation on ice for 30 min, the suspension was homogenized using five strokes at 3,000 rpm, and centrifuged at 33,000 g_{max} for 20 min. The supernatant (lysate supernatant, or LS1) was immediately collected and centrifuged at 260,000 g_{max} for 2 h. The pellet (lysate pellet, or LP2) was resuspended in 400-500 μl 150 mM choline gluconate (or 150 mM Na gluconate for the experiments described in Fig. 1) containing 10 mM HEPES-Tris, pH 7.4 by pipetting through progressively narrower 200-μl micropipette tips, and finally by 3 passes through a 25-gauge needle. LP2 was frozen in liquid N_2 for storage at -80°C, and thawed on ice before use. Protein concentration was determined by Bradford assay using bovine serum albumin as standard.

2.2.3 Oxonol and Acridine Orange Fluorescence Spectroscopy

ΔpH and $\Delta\psi$ were measured by acridine orange and oxonol VI fluorescence, respectively. 150-200 μg LP2 was added to 1.5 ml 150 mM choline gluconate (unless otherwise indicated), 10 mM HEPES-Tris, pH 7.4 and either 5 μM acridine orange or 100 nM oxonol VI, and the reaction stirred constantly at 30ºC. A decrease in the fluorescence of acridine orange reflects generation of an inside-acidic ΔpH; an increase in the fluorescence ratio of oxonol VI reflects generation of an inside-positive $\Delta\psi$. In the experiments using LP2 loaded with high Na^+ (which did not involve MgATP), 4 mM $MgSO_4$ and 0.5 μM bafilomycin A1 were included in the external solution. Acridine orange fluorescence was excited at 492 nm and emission detected at 530 nm; oxonol VI

was excited at 560 nm and emission detected at 640 and 615 nm using a Hitachi F-4500 fluorescence spectrophotometer.

2.2.4 ^{3}H-Glutamate and ^{22}Na Uptake

The standard assay buffer for glutamate uptake contained (in mM): 148 choline or K gluconate, 2 choline or KCl, 4 MgATP, 10 HEPES-Tris, pH 7.4, 1 choline glutamate (unless otherwise indicated), and 40 μCi/ml [^{3}H]L-glutamate. When specified, Na gluconate and Li gluconate were used at 150 mM and ammonium tartrate at 10 mM. Transport was initiated by the addition of 100 μg LP2 protein to 200 μl reaction buffer (pre-warmed to 30°C), the reaction incubated at 30°C for 10 min (unless otherwise indicated) and terminated by rapid filtration followed by four washes each with 2 ml cold 150 mM HEPES-Tris, pH 7.4. Radioactivity was detected by liquid scintillation, and background transport measured in the presence of 100 μM Evans Blue subtracted from the data unless otherwise specified.

The standard assay buffer for $^{22}Na^{+}$ transport contained (in mM): 148 choline gluconate, 2 choline chloride, 10 choline glutamate, 4 MgATP, 10 HEPES-Tris, pH 7.4, 0.1 ouabain, 0.1 bumetanide and 175 nM ^{22}NaCl (5 μCi/ml). Transport was initiated by adding 100 μg LP2 to 200 μl reaction buffer (pre-warmed to 30°C). The mixture was incubated at 30°C for 10 min (unless otherwise indicated) and the reaction terminated by rapid filtration followed by four washes each with 1.5 ml cold 150 mM HEPES-Tris, pH 7.4. Radioactivity was detected by liquid scintillation, and non-specific background at 0 min incubation subtracted from all the data presented.

Within each ^{3}H-glutamate or ^{22}Na transport experiment, each condition was assayed in triplicate, and at least three independent experiments were performed using at least two different synaptic vesicle preparations.

2.2.5 Calyx of Held Electrophysiological Recordings

Slice preparation: 200 μm thick coronal slices containing the medial nucleus of the trapezoid body (MNTB) were prepared from P9-P12 Wistar rats as previously described (Borst et al 1995). Slices were cut in cold artificial cerebrospinal fluid (ACSF) (composition, in mM: NaCl 125, KCl 2.5, glucose 25, $NaHCO_3$ 25, NaH_2PO_4 1.25, ascorbic acid 0.4, 3-myo-inositol 3, Na pyruvate 2, $MgCl_2$ 3, $CaCl_2$ 0.1), incubated for 30-60 minutes at 37°C in a chamber with ACSF and thereafter at room temperature. For several experiments, slices were also cut using 250 mM sucrose instead of 125 mM KCl.

Recordings: Slices were transferred to a recording chamber, perfused with recording ACSF that contains (in mM) NaCl 125, KCl 2.5, $CaCl_2$ 2, $MgCl_2$ 1, NaH_2PO_4 1.25, ascorbic acid 0.4, myo-Inositol 3, Na Pyruvate 2, $NaHCO_3$ 25, glucose 25, and bubbled with 5% CO_2/95% O_2. To record mEPSCs, the ACSF contained 0.5 μM

strychnine and 10 μM SR95531, with or without 0.5 μM TTX. Slices were viewed using IR-DIC or Dodt contrast optics and a 63x water immersion lens. Recordings were made using an Axon Multiclamp 700B amplifier (Molecular Devices). For paired recordings, the solution in the postsynaptic electrode was (in mM): KCl 75, K gluconate 75, Na_2Phosphocreatine 10, HEPES 10, EGTA 5, MgATP 2. The K-based solution in the presynaptic electrode contained (in mM): K-gluconate 113, $MgCl_2$ 4.5, Na_2ATP 4, TrisGTP 0.3, Tris-phosphocreatine 14, EGTA 0.1, HEPES 9, adjusted to pH 7.25 with KOH. The low-K presynaptic solution contained (in mM): NMDG-Gluconate 113, $MgCl_2$ 4.5, Na_2ATP 4, TrisGTP 0.3, Tris-P-creatine 14, EGTA 0.1, HEPES 9, adjusted to pH 7.25 with NMDG-OH. Both solutions also contained 1 mM glutamate and 20 μM Alexa-594. Calyces were clamped at -70 mV (not corrected for junction potential) during mEPSC recording. Two tests were used to confirm recording from a calyx: first, the fluorescent dye fill of the calyx was visualized at the end of each recording; second, a single voltage pulse to 0 mV was injected into the calyx and a large postsynaptic response was measured. Miniature excitatory postsynaptic currents (mEPSCs) were recorded with extracellular TTX (0.5 μM), strychnine (2 μM) and GABAzine (10 μM) in the ACSF. Signals were filtered at 5 kHz, sampled at 20kHz, and mEPSCs detected using a sliding template algorithm. For each recording, a mEPSC was selected visually as a template. The fit was adjusted so that, when judged visually, 10-20% of the events detected were deemed spurious and rejected, and no obvious mEPSCs went undetected.

Data Analysis: Data were analyzed using Clampfit 9.2 (Molecular Devices), Axograph 1.0 (AxographX) and Igor 6.0 (Wavemetrics).

2.2.6 Statistical Analysis

All mean data were obtained from at least three measurements from at least two different synaptic vesicle preparations. Error bars represent the standard error of the mean (s.e.m). Statistical significance was assessed by two-tailed paired t-tests, unless otherwise indicated. Significance levels used are *$p < 0.05$, **$p < 0.01$, ***$p < 0.0001$. "NS" denotes differences that are not statistically significant ($p > 0.05$).

2.3 RESULTS

2.3.1 Synaptic Vesicles Express an Electroneutral Cation/H^+ Exchange Activity

As introduced above, we hypothesized that coupled cation/H^+ exchange might be a solution to the problem of ΔpH buildup and consequent $\Delta\psi$ deficiency. By electroneutrally removing protons from the vesicle lumen, cation/H^+ exchange would decrease ΔpH without itself affecting $\Delta\psi$, thus allowing the V-ATPase to increase proton pumping and tip the balance towards $\Delta\psi$. The additional cations in the vesicle would also themselves contribute to greater $\Delta\psi$.

The mechanism of cation/H^+ exchange predicts that a cation gradient can drive the formation of ΔpH in the absence of the V-ATPase. To test this hypothesis in synaptic vesicles, we determined if a pre-existing outwardly-directed cation gradient (high inside, low outside) could drive vesicle acidification. We monitored vesicle ΔpH by measuring the fluorescence of acridine orange, a fluorescent amine which is freely permeable to membranes in its uncharged form but not when protonated (Cools & Janssen 1986; Schuldiner et al 1972). Thus when it enters acidic compartments, it gets protonated, trapped and concentrated, resulting in quenching of total fluorescence. We pre-loaded synaptic vesicles (LP2; see Methods) with high Na^+ at pH 7.4, inhibited the H^+ pump with bafilomycin A1 and diluted the vesicles into pH 7.4 buffer lacking Na^+. **Figure 2-1a** shows that the resulting outwardly directed Na^+ gradient suffices to acidify synaptic vesicles in the absence of V-ATPase activity, whereas dilution into buffer with Na^+ eliminates this effect, demonstrating its dependence on a Na^+ gradient.

Although consistent with coupled cation/H^+ exchange, cation-driven H^+ translocation might reflect the development of negative Δψ due to the efflux of Na^+ through a channel, followed by H^+ influx down this negative membrane potential through another, distinct channel. If driven by Δψ, this H^+ flux should increase in the presence of the H^+ ionophore carbonyl cyanide chlorophenylhydrazone (CCCP). However, CCCP has no effect on the observed acidification (**Fig. 2-1b**), implying that Na^+ is not a charge-dissipating counterion for H^+ flux through CCCP, and thus likely excluding a role for Δψ in this phenomenon. Na^+ efflux and H^+ influx thus do not appear to occur through distinct channels, but rather through stoichiometrically coupled exchange by an electroneutral transporter. It should be noted that, in the case of two separate channels, the conductance of the cation channel could be limiting compared to the proton channel, thus the addition of CCCP does not change the acidification rate. However, this would suggest that cation flux is small and insignificant compared to proton flux, which would not help to increase positive Δψ in the vesicles. In contrast, addition of 15μM 5-(N-ethyl-N-isopropyl)amiloride (EIPA, an NHE inhibitor) blocks the Na^+-induced acidification (**Fig. 2-1c**), providing support that the phenomenon is due to coupled Na^+/H^+ exchange.

After the formation of stable ΔpH, addition of external Na^+ alkalinizes the vesicles, demonstrating flux reversal. We took advantage of this phenomenon to compare the effects of the monovalent cations Na^+, K^+ and Li^+. At all concentrations tested (5, 20 and 150 mM), Na^+ and Li^+ demonstrate greater and faster alkalinization than K^+ (**Fig. 2-2**).

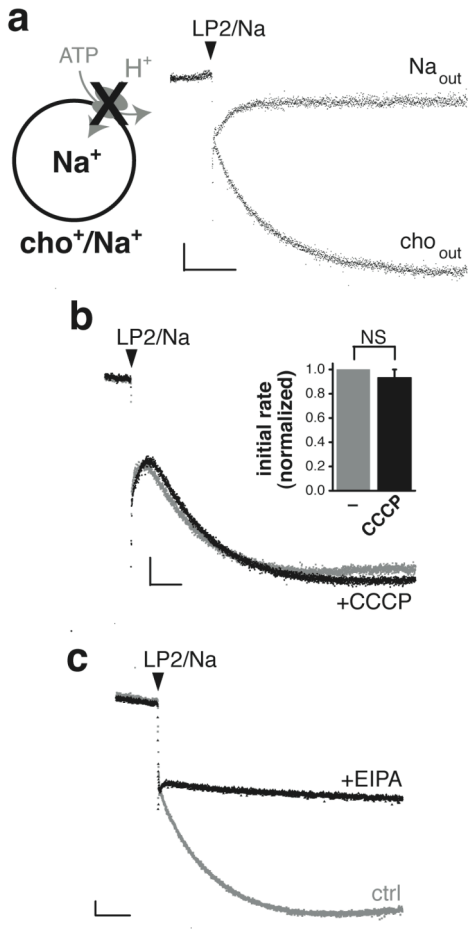

Figure 2-1. Synaptic vesicles express a Na^+/H^+ exchange activity.
Measurement of ΔpH across synaptic vesicles using acridine orange fluorescence. Quenching of fluorescence reflects generation of an inside-acidic pH. Synaptic vesicles preloaded with Na^+ (LP2/Na) and pretreated with bafilomycin to inhibit the V-ATPase were diluted into buffer with either (a) 150 mM Na gluconate (Na_{out}) or 150 mM choline gluconate (cho_{out}), or (b) into 150 mM choline gluconate buffer with or without CCCP. The bar graph (inset) indicates the mean initial rate of acidification with and without 5 μM CCCP (n = 3) (NS indicates p = 0.42, by two-tailed paired t-test). CCCP does not affect the rate or extent of acidification, indicating that the outwardly directed Na^+ gradient does not drive H^+ flux through changes in membrane potential. (c) The acidification of synaptic vesicles by an outwardly directed Na^+ gradient is inhibited by the amiloride analogue 5-(N-ethyl-N-isopropyl)amiloride (EIPA, 15 μM). Horizontal scale bars indicate 30 s, vertical scale bars indicate 10 arbitrary fluorescence units.

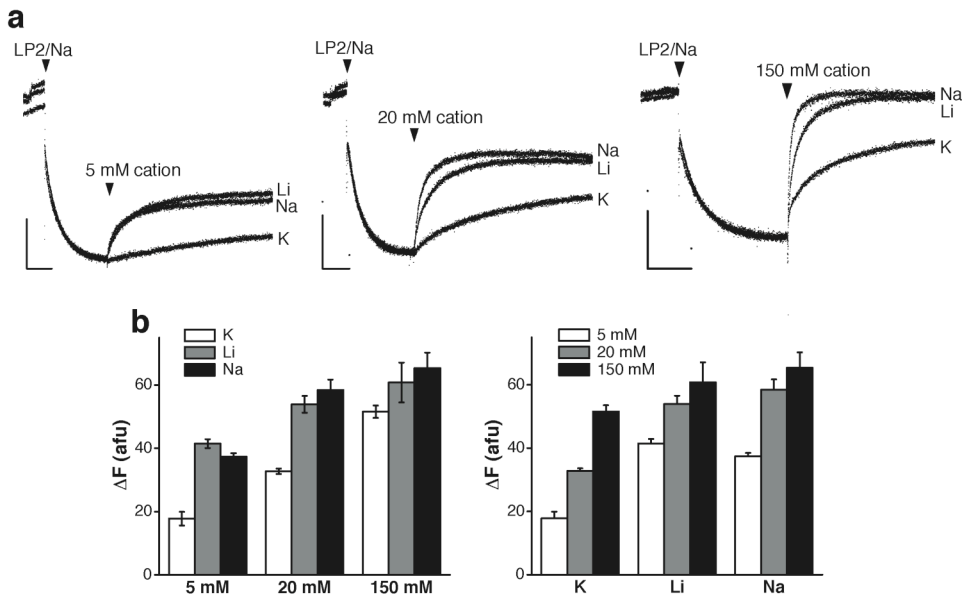

Figure 2-2. The Na^+/H^+ exchange activity also recognizes K^+ and Li^+.
Measurement of ΔpH across synaptic vesicles using acridine orange fluorescence. (a) The monovalent cations Na^+, Li^+ and K^+ (5, 20, 150 mM) were added to synaptic vesicles acidified by an outwardly directed Na^+ gradient, as in Figure 2-1. (b) The extent of alkalinization evoked by each cation is quantified as the increase in arbitrary fluorescence units, ΔF (n = 3). Horizontal scale bars indicate 60 s, vertical scale bars indicate 30 arbitrary fluorescence units.

A dose-response analysis shows that the EC_{50} for alkalinization by Na^+ is approximately ten-fold lower than that for K^+ (1.69 ± 0.19 mM for Na^+ vs. 17.8 ± 2.2 mM for K^+), while analysis of initial rate yields a K_m of 4.10 ± 2.35 mM for Na^+ and 140 ± 118 mM for K^+ (Hill coefficient = 1.04 ± 0.10 and 1.18 ± 0.30, respectively) (**Fig. 2-3**). The low K_m for K^+ observed here is consistent with the low K_m for K^+ demonstrated by NHE8 in reconstituted liposomes (Nakamura et al 2005).

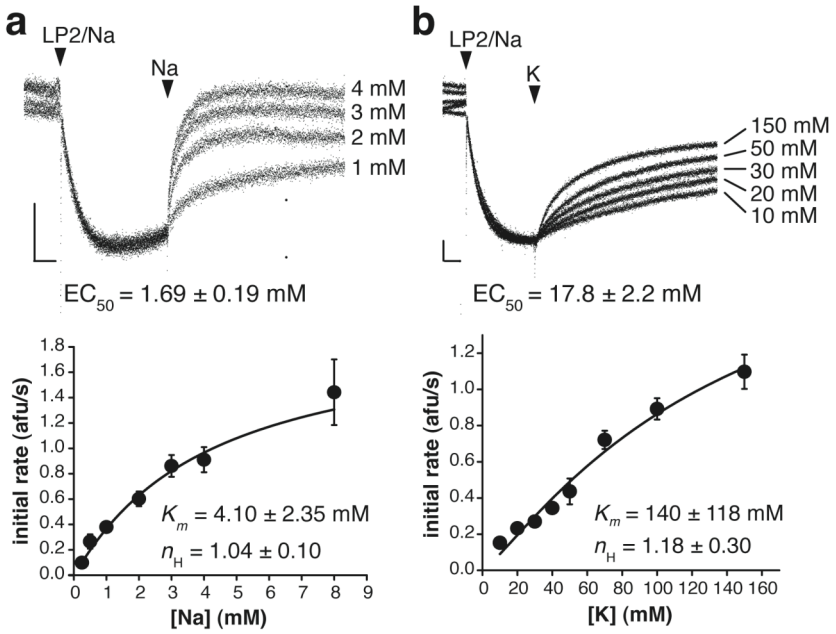

Figure 2-3. Dose response of the Na^+/H^+ exchange activity to Na^+ and K^+.
Measurement of ΔpH across synaptic vesicles using acridine orange fluorescence. Synaptic vesicles were acidified by an outwardly directed Na^+ gradient, as in Figure 2-1. After acidification as above by an outwardly directed Na^+ gradient, synaptic vesicles alkalinize in a dose-dependent manner to Na^+ (a) and K^+ (b). The EC_{50} indicates the concentration of cation required for half-maximal alkalinization (mean ± SEM of 3 independent dose-response experiments). The mean initial rates of alkalinization also vary as a function of cation concentration (bottom, n=3), with K_m and Hill coefficient (n_H) obtained by fitting to the Hill equation. Horizontal scale bars indicate 30 s, vertical scale bars indicate 10 arbitrary fluorescence units.

To evaluate further the possibility that cation flux through a channel drives H^+ translocation, we tested for the presence of an endogenous cation conductance on synaptic vesicles. An artificial ΔpH was created by loading the vesicles with ammonium tartrate (100 mM), inhibiting the V-ATPase with bafilomycin and diluting the membranes into 150 mM choline gluconate or potassium gluconate buffer, both lacking NH_4^+. The efflux of NH_3 due to dilution rapidly produces ΔpH (**Fig. 2-4**). Addition of the H^+ ionophore CCCP to the choline gluconate buffer does not dissipate the ΔpH formed by dilution, presumably because the initial efflux of H^+ rapidly creates negative Δψ that opposes further net efflux. Further, the inability of CCCP to dissipate ΔpH even in K gluconate indicates that synaptic vesicles lack an endogenous K^+ channel which would shunt the developing Δψ. As control, the addition of K^+ ionophore valinomycin to K gluconate dilution buffer immediately triggers H^+ efflux which increases in the presence of CCCP. Valinomycin does not have this effect in buffer lacking K^+ (**Fig. 2-4**). The inability to dissipate Δψ in the absence of valinomycin thus likely excludes a role for endogenous channels in the observed cation-driven H^+ flux by synaptic vesicles. Again,

as with the Na^+-driven acidification, there exists the formal possibility that a cation conductance exists which is limiting compared to the proton conductance.

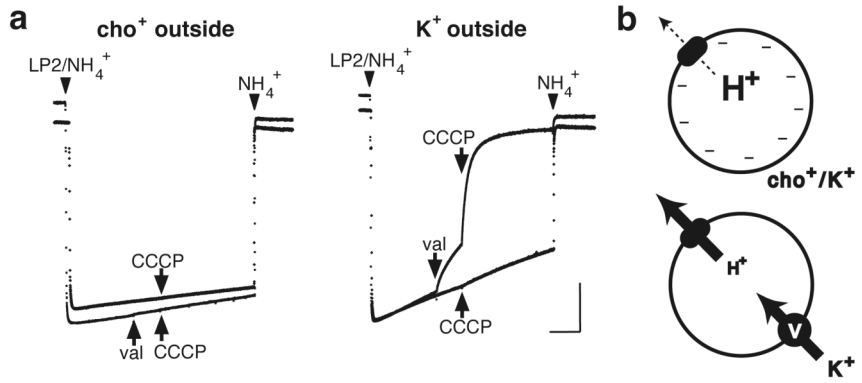

Figure 2-4. Synaptic vesicles lack a detectable K^+ channel conductance.
Measurement of ΔpH across synaptic vesicles using acridine orange fluorescence. (a) Synaptic vesicles were acidified by preloading with 200 mM NH_4^+ ($LP2/NH_4^+$) and dilution into NH_4^+-free buffer containing no K^+ (cho^+ outside) or 150 mM K^+ (K^+ outside). In each panel, arrows in the same direction indicate addition to one trace, and arrows in the opposite direction indicate addition to the other trace. CCCP (5 μM) has no effect in the absence of K^+, with or without the addition of 50 nM valinomycin (val). CCCP alone also has no effect in the presence of K^+, indicating the absence of a significant K^+ conductance. However, the prior addition of valinomycin enables CCCP to alkalinize the vesicles rapidly, indicating that CCCP would have produced alkalinization in the presence of an endogenous K^+ conductance. Addition of 100 mM NH_4^+ to the external medium immediately reverses the acidification. (b) Diagram of the conditions described in (a). The top panel depicts synaptic vesicles with or without external K^+. In the absence of a K^+ conductance to shunt the accumulating negative membrane potential that results from H^+ efflux, pH remains quite stable, even in the presence of the H^+ ionophore CCCP (rounded rectangle). The addition of K^+ ionophore valinomycin (v) in the presence of external K^+ rapidly dissipates ΔpH, indicating that an endogenous K^+ channel, if present, would also have dissipated ΔpH by allowing proton efflux from the apparent proton leak present endogenously. Horizontal scale bars indicate 60 s, vertical scale bars indicate 40 arbitrary fluorescence units.

2.3.2 Cation/H^+ Exchange Increases Synaptic Vesicle Membrane Potential

The results suggest that synaptic vesicles express a cation/H^+ exchange activity, but do not indicate its physiological role in the presence of an active V-ATPase. In addition, the use of synaptic vesicles from whole brain does not specifically address the properties of the subset that stores glutamate. We thus used ATP and glutamate (rather than chloride) to acidify synaptic vesicles. In the presence of 1 mM MgATP and a low concentration of chloride (2mM; to serve as an allosteric activator of the VGLUTs), 1 mM glutamate produces substantial acidification (**Fig. 2-5**). Under the same conditions, the closely related aspartate (which is not recognized by VGLUTs) causes no

acidification, confirming that the ΔpH produced by glutamate depends specifically on vesicular glutamate transport. The subsequent addition of 50 mM Na^+ produces a substantial alkalinization in the presence of glutamate, but much less in the presence of aspartate. The alkalinization induced by Na^+ in the presence of aspartate likely reflects reversal of the acidification produced by chloride (**Fig. 2-5**). To compare Na^+, K^+ and Li^+, we quantified the initial rate of alkalinization by these cations (50 mM) again in vesicles acidified with 1 mM glutamate and found that, consistent with the results in the absence of a functioning V-ATPase (**Fig. 2-2**), Na^+ and Li^+ have more pronounced effects than K^+ ($Li^+ \sim Na^+ >> K^+$; **Fig. 2-6**). Thus, cation/H^+ exchange can modulate the ΔpH of glutamatergic synaptic vesicles even in the presence of an active V-ATPase.

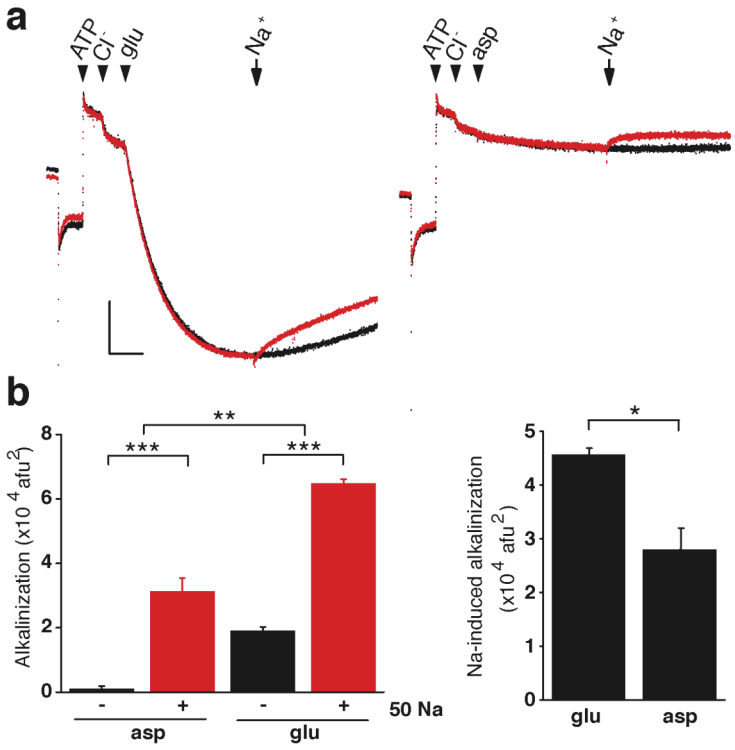

Figure 2-5. Na^+/H^+ exchange activity is present on glutamatergic synaptic vesicles.
(a) Using acridine orange to assess the acidification of synaptic vesicles, the sample traces show progressive acidification of 150 μg LP2 protein by 1 mM MgATP, 2 mM choline Cl, and either 1 mM choline glutamate (left) or choline aspartate (right). After acidification, 50 mM Na gluconate was applied at the arrows only in red traces. (b) The extent of alkalinization was determined by summing the increase in fluorescence over the 225s after the time of Na^+ addition (using the fluorescence immediately before Na^+ addition as baseline), and shows that Na^+ has a greater effect on vesicles acidified with glutamate than aspartate (n = 3) (**p < 0.01, ***p < 0.0001, two-way ANOVA). The Na-induced alkalinization was determined by calculating the area between the control and Na curves after the time of Na^+ addition, and also shows that Na^+ has a greater effect on vesicles acidified with glutamate than aspartate (n=3) (*p<0.05, two-tailed paired t test). Horizontal scale bars indicate 60 s, vertical scale bars indicate 40 arbitrary fluorescence units.

By selectively dissipating ΔpH, cation/H^+ exchange should increase Δψ generated by the V-ATPase. To measure Δψ, we used the potential-sensitive, ratiometric fluorescent dye oxonol VI, focusing on the effects of K^+ due to its physiological relevance as the most abundant cytoplasmic cation. Activation of the V-ATPase with ATP increases the fluorescence ratio of oxonol VI, indicating formation of a positive membrane potential, and K^+ causes a further increase of ~40% (**Fig. 2-7**), confirming that it does increase Δψ. As a proof of principle to demonstrate that dissipation of ΔpH results in secondary activation of the V-ATPase to increase Δψ, we used ammonia. Ammonia added to the extravesicular buffer enters the acidic vesicles as a weak, permeant base and dissipates ΔpH by binding protons, and it indeed causes an increase in Δψ as measured by oxonol VI (**Fig. 2-7**).

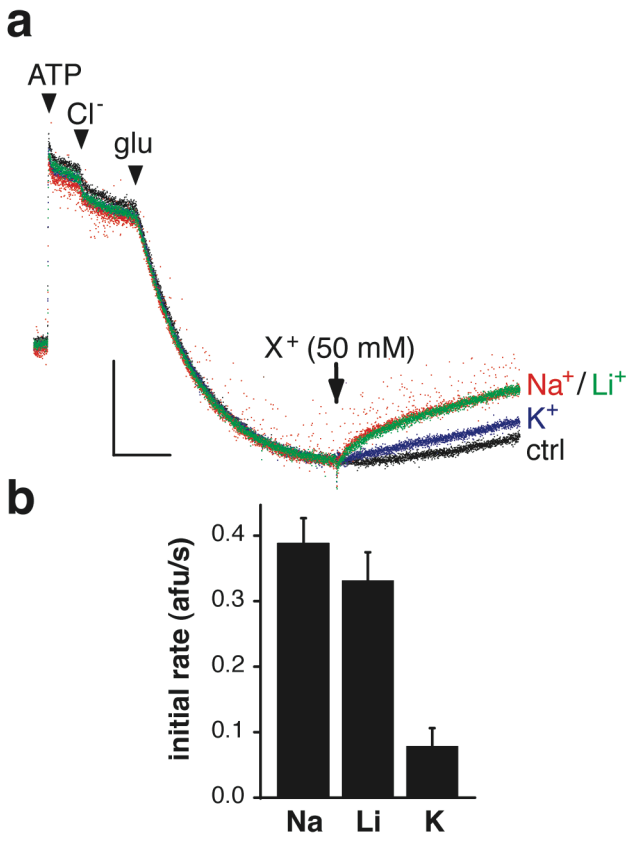

Figure 2-6. The Na^+/H^+ exchange activity on glutamatergic synaptic vesicles also recognizes K^+ and Li^+.
(a) The sample traces show acridine orange fluorescence after sequential addition to 150 μg LP2 of 1 mM MgATP, 2 mM choline Cl, and 1 mM choline glutamate. After acidification by glutamate, 50 mM of the indicated cation was added as a gluconate salt at the arrow. (b) Mean initial rate of alkalinization triggered by each cation (n = 3). Error bars indicate the SEM. Horizontal scale bars indicate 60 s, vertical scale bars indicate 40 arbitrary fluorescence units.

In addition, the presence of ammonia reduces the effect of K^+ and vice versa, indicating that both act through a common mechanism that requires ΔpH. Taken together with the previous observations of K^+/H^+ exchange and the probable absence of a substantial K^+ conductance, this result indicates that K^+/H^+ exchange across synaptic vesicle membranes dissipates ΔpH to increase Δψ.

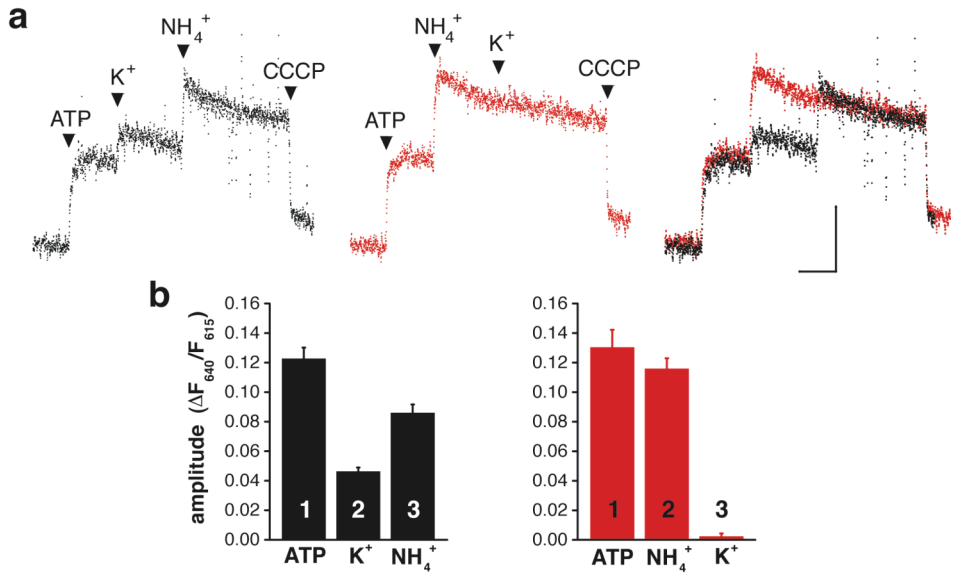

Figure 2-7. Cation/H^+ exchange activity on synaptic vesicles increases Δψ.
Synaptic vesicle membrane potential was measured using the ratiometric fluorescence of oxonol VI. An increase in the ratio reflects greater inside-positive potential across the membrane. (a) Sample traces with the arrowheads indicating sequential addition of 1 mM MgATP, 50 mM K gluconate, 10 mM $(NH_4)_2$ tartrate and 5 μM CCCP (black). The order of K^+ and NH_4^+ addition is reversed in the red trace, and the two traces are superimposed on the right. (b) Mean amplitude of fluorescence ratio change, with the order of addition indicated by numbers on or above the bars (n = 9, 4 for black and red panels, respectively). Analysis by two-tailed unpaired t-test shows $p < 0.05$ for the effect of NH_4^+ after versus before K^+, and $p < 0.0001$ for the effect of K^+ before and after NH_4^+. Horizontal scale bars indicate 60 s, vertical scale bars indicate a ratio change of 0.10.

2.3.3 Monovalent Cations Increase Glutamate Uptake into Synaptic Vesicles

The ability of cation/H^+ exchange to increase Δψ suggests that cations should stimulate glutamate transport into synaptic vesicles by increasing its primary driving force. To test this hypothesis, we compared the effects of K gluconate and choline gluconate on ^{3}H-glutamate uptake by synaptic vesicles, using either 2 mM KCl or choline Cl to provide allosteric activation of the VGLUTs. We used K^+ rather than Na^+ to minimize the activity of any contaminating plasma membrane excitatory amino acid transporters, which rely on an inwardly directed Na^+ gradient to drive glutamate co-transport. As shown in **Figure 2-8**, external K^+ stimulates glutamate uptake into synaptic

vesicles by ~50%, and the uptake as well as the stimulation by K^+ are blocked by Evans Blue, an inhibitor of the VGLUTs (Chaudhry et al 2008).

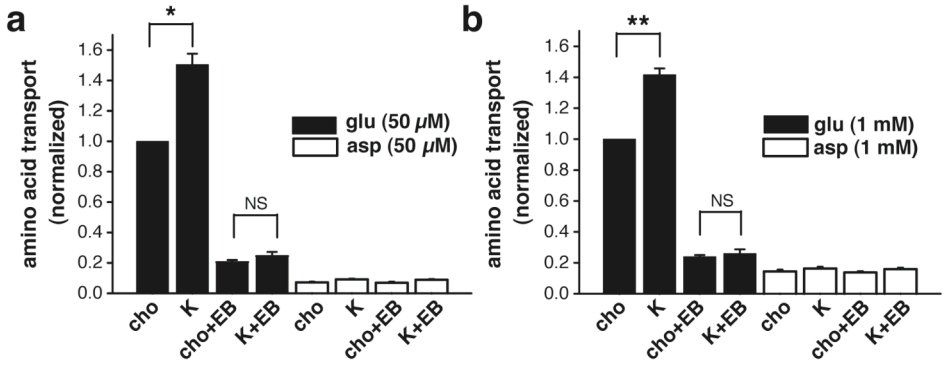

Figure 2-8. Potassium increases glutamate transport into synaptic vesicles.
The uptake of ^{3}H-glutamate (filled bars) or -aspartate (open bars) by rat brain synaptic vesicles was measured after incubation for 10 minutes at 30ºC in assay buffer containing either 2 mM choline Cl and 148 mM choline gluconate (cho) or 2 mM KCl and 148 mM K gluconate (K), in the presence of either (a) 50 μM or (b) 1 mM amino acid, with or without the VGLUT inhibitor Evans Blue (EB) (at 10 and 100 μM for (a) and (b), respectively). Uptake was normalized to that observed with choline in the absence of Evans Blue. Data were analyzed by two-tailed paired t tests (* $p < 0.05$, ** $p < 0.01$, NS indicates $p = 0.11$ for left panel and 0.40 for right, $n = 3$).

We also observed no specific uptake of ^{3}H-aspartate, which is recognized by the plasma membrane glutamate transporters but not by the VGLUTs, confirming the specificity of the assay for vesicular glutamate transport.

To characterize the effect of K^+ on glutamate uptake, we examined the time course and found that the stimulation by K^+ increases over time, with less effect at 1-2 minutes than at later times, when it approaches 100% after background subtraction (**Fig. 2-9a**). Consistent with this, a kinetic analysis measuring uptake over 1 minute demonstrates only a small effect of K^+ on the K_m of vesicular glutamate transport and no effect on the V_{max} (**Fig. 2-9b**), whereas an analysis of dose-response to K^+ shows a linear relationship up to 150 mM (**Fig. 2-10a**), supporting an effect on thermodynamic equilibrium rather than kinetics. To assess the effects of Na^+ and Li^+ in this assay, we replaced K^+ with Na^+ or Li^+ (all at 150 mM), inhibiting any contaminating plasma membrane glutamate transporters with 1 mM DL-*threo*-β-benzyloxyaspartic acid (TBOA). Consistent with the acridine orange experiments, we find that Na^+ and Li^+ also stimulate vesicular glutamate uptake (**Fig. 2-10b**).

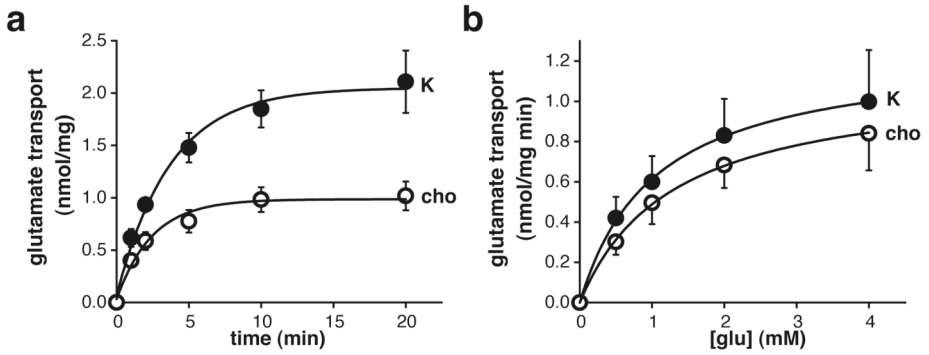

Figure 2-9. The effect of K^+ on glutamate transport increases over time.
(a) Time course and (b) kinetics of glutamate uptake in either 150 mM choline (open circles) or 150 mM K^+ (filled circles). The time course was performed using 1 mM glutamate, and the kinetic analysis at 1 minute. Michaelis-Menten fits to individual experiments yielded mean K_m values of 1.02 ± 0.08 mM for K and 1.27 ± 0.04 mM for cho ($p < 0.05$), and mean V_{max} values of 1.26 ± 0.33 nmol/mg and 1.12 ± 0.24 nmol/mg for K and cho, respectively ($p = 0.31$). Two-tailed paired t tests were used ($n = 3$).

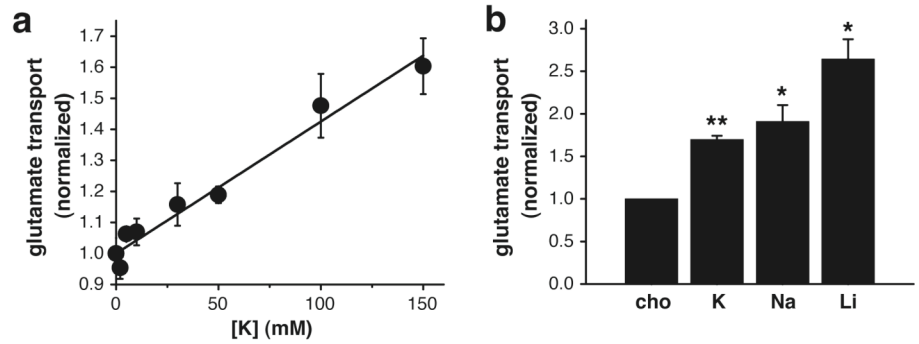

Figure 2-10. Comparison of the effects of monovalent cations on glutamate transport.
(a) Dose response of glutamate uptake to increasing potassium concentrations under standard assay conditions, where choline and K gluconate were varied to maintain a total of 150 mM. Uptake was normalized to that in 0 mM potassium. (b) Uptake of 1 mM ^{3}H-glutamate for 10 minutes in the presence of 150 mM K, Na or Li gluconate, normalized to that in 150 mM choline. * indicates $p < 0.05$ and ** $p < 0.01$ relative to cho, using two-tailed paired t tests ($n = 3$). Values represent the mean and error bars the SEM.

The more similar effects of the three cations ($Li^+ > Na^+ \sim K^+$) on glutamate uptake contrasts with the variation in their effect on ΔpH ($Li^+ \sim Na^+ >> K^+$), but this likely reflects differences in the two assays. Our radiotracer flux assay, measured after 10 minutes with 150 mM cation, better reflects steady-state conditions, with equilibriums more dependent on the stoichiometry of coupling for the different cations than on their kinetics, whereas the real-time measurements of fluorescence (performed with 20-50 mM cation) better distinguishes differences in kinetics.

The stimulation of glutamate uptake into synaptic vesicles by monovalent cations could result from an allosteric effect on VGLUT activity, or an increase in the driving force for transport. Direct allosteric regulation should influence the kinetics of transport or exhibit saturation, but K^+ does not have much effect on the observed kinetics (**Fig. 2-9b**), and the dose-response to K^+ also shows no evidence of saturation (**Fig. 2-10a**). To determine whether K^+ stimulates glutamate uptake by influencing $\Delta\mu_{H+}$, we again used ammonia to convert ΔpH into Δψ. By itself, 20 mM NH_4^+ stimulates glutamate uptake, consistent with the primary dependence of the VGLUTs on Δψ rather than ΔpH (**Fig. 2-11**).

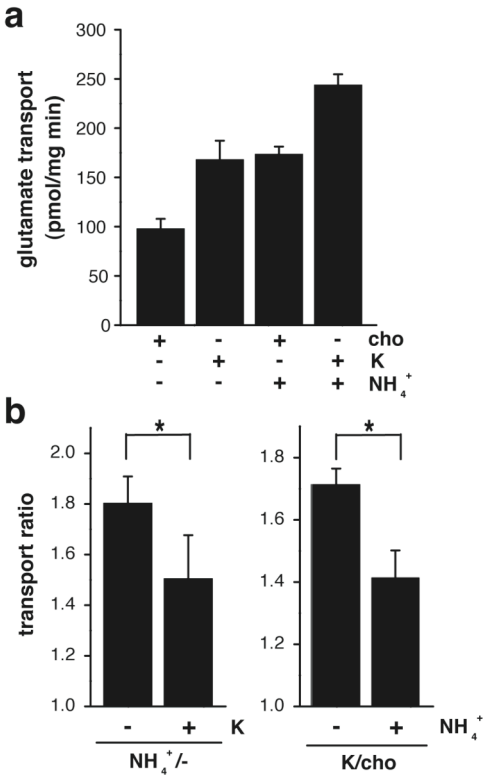

Figure 2-11. Cation/H^+ exchange stimulates glutamate uptake by increasing Δψ.
(a) Synaptic vesicle uptake of 1 mM ^{3}H-glutamate was measured in either 150 mM choline or 150 mM K^+, in the presence or absence of 10 mM $(NH_4)_2$tartrate (left). (b) The fold-stimulation of transport by NH_4^+ in the presence or absence of K^+ (middle), or by K^+ in the presence or absence of NH_4^+ (right) was derived by dividing the appropriate uptake measurements. * indicates $p < 0.05$, using two-tailed paired t tests (n = 4).

The extent of stimulation resembles that produced by 150 mM K^+. We then tested whether K^+ can stimulate glutamate transport in the presence of ammonia and found that, although not eliminated, the stimulation by K^+ is significantly reduced by ammonia. Conversely, the stimulation by ammonia is reduced by K^+, corroborating the studies with

oxonol VI which suggest that potassium and ammonia act through a common mechanism (**Fig. 2-11**). Since ammonia dissipates ΔpH, the results suggest that ΔpH is required for the full effect of K^+, so that H^+ efflux partly drives K^+ entry through the K^+/H^+ exchange mechanism we demonstrate in the acridine orange assays. The residual stimulation of glutamate uptake by K^+ in the presence of NH_4^+ (**Fig. 2-11**) can be attributed to the same exchange mechanism driven solely by a K^+ gradient rather than by both ΔpH and a K^+ gradient.

To test whether a cation channel even has the potential to influence vesicular glutamate transport, we measured glutamate uptake in the presence of the K^+ ionophore valinomycin and 15 mM K^+, a concentration that has little effect on uptake by itself (**Fig. 2-10a**) and therefore minimizes the role of endogenous K^+ carriers and conductances. Valinomycin has no effect on vesicular glutamate transport under these conditions (**Fig. 2-12**) as well as at physiological concentrations of K^+, indicating that even if a cation channel were present, it would not promote vesicle filling with glutamate. This result seems inconsistent with the observations in **Figure 2-4**, where the addition of valinomycin demonstrates a clear proton conductance. This proton conductance might be expected to similarly dissipate the ΔpH upon valinomycin addition in the glutamate uptake assay, in which case valinomycin should stimulate uptake. However, in the glutamate uptake assay, the V-ATPase is active and maintaining a positive interior. The lack of effect of valinomycin thus suggests that the proton leak, if activated, likely allows efflux of the same small amount of charge as that due to K^+ influx, resulting in no net change in ΔpH or Δψ. In contrast, the electroneutral K^+/H^+-exchanging ionophore nigericin markedly increases glutamate uptake even with 15 mM K^+ (**Fig. 2-12**), confirming that K^+/H^+ exchange potently stimulates vesicular glutamate transport.

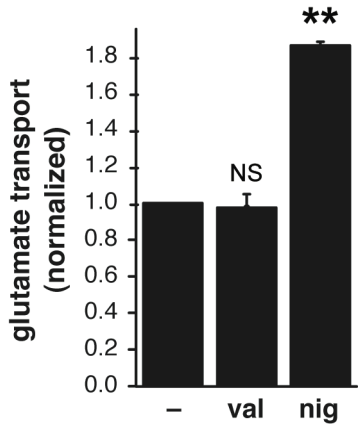

Figure 2-12. An exchanger, rather than a channel, stimulates glutamate uptake.
The uptake of ^{3}H-glutamate (1 mM) by synaptic vesicles was measured in standard assay buffer, except with 15 mM K gluconate/135 mM choline gluconate instead of 150 mM of either, with or without either 50 nM nigericin or 50 nM valinomycin. ** indicates $p < 0.01$ and NS $p = 0.76$ by two-tailed paired t-tests ($n = 3$). Values indicate mean ± SEM.

2.3.4 Presynaptic K^+ Increases Quantal Size at the Calyx of Held

Since cations increase the glutamate content of synaptic vesicles *in vitro*, presynaptic K^+ may also influence quantal size, defined as the postsynaptic response to release of a single vesicle's contents. We thus performed paired recordings at the calyx of Held, a giant glutamatergic terminal in the brainstem auditory pathway where it is possible to dialyze cytosolic contents by whole-cell patch clamp, and simultaneously measure the postsynaptic response. Since glutamate receptors at this synapse are not saturated by a single quantum of transmitter (Ishikawa et al 2002; Wu et al 2007), it should be possible to detect changes in miniature excitatory postsynaptic current (mEPSC) amplitude due to changes in the amount of transmitter released per vesicle. Indeed, we find that terminals dialyzed with high K^+ produce mEPSCs with larger amplitudes than those dialyzed with the organic cation $NMDG^+$ (**Fig. 2-13a**). Cumulative probability histograms show a shift in the distribution of mEPSC amplitudes during dialysis, supporting that high presynaptic K^+ results in greater vesicle filling and thus larger mEPSCs (**Fig. 2-13b**). Further, the averaged data (**Fig. 2-13c**) show remarkable quantitative agreement with the extent of stimulation by K^+ observed *in vitro*. Taken together, the results indicate that synaptic vesicle cation/H^+ exchange modulates quantal size through the regulation of vesicular glutamate transport.

2.3.5 EIPA Inhibits Synaptic Vesicle Cation/H^+ Exchange and Cation-Stimulated Glutamate Transport

Stoichiometric cation/H^+ exchange predicts that, just as a cation gradient can drive H^+ flux, a H^+ gradient should also drive the accumulation of cations. We thus measured the uptake of $^{22}Na^+$ by synaptic vesicles acidified with ATP and glutamate to functionally isolate the glutamatergic population. Na^+ was chosen instead of K^+ because our carrier of interest has greater affinity for Na^+, and most studies of mammalian NHEs have utilized Na^+ to characterize transport. We observe more $^{22}Na^+$ uptake in the presence of glutamate than in aspartate as control (**Fig. 2-14a**), suggesting that vesicle acidification mediated by the VGLUTs drives $^{22}Na^+$ influx.

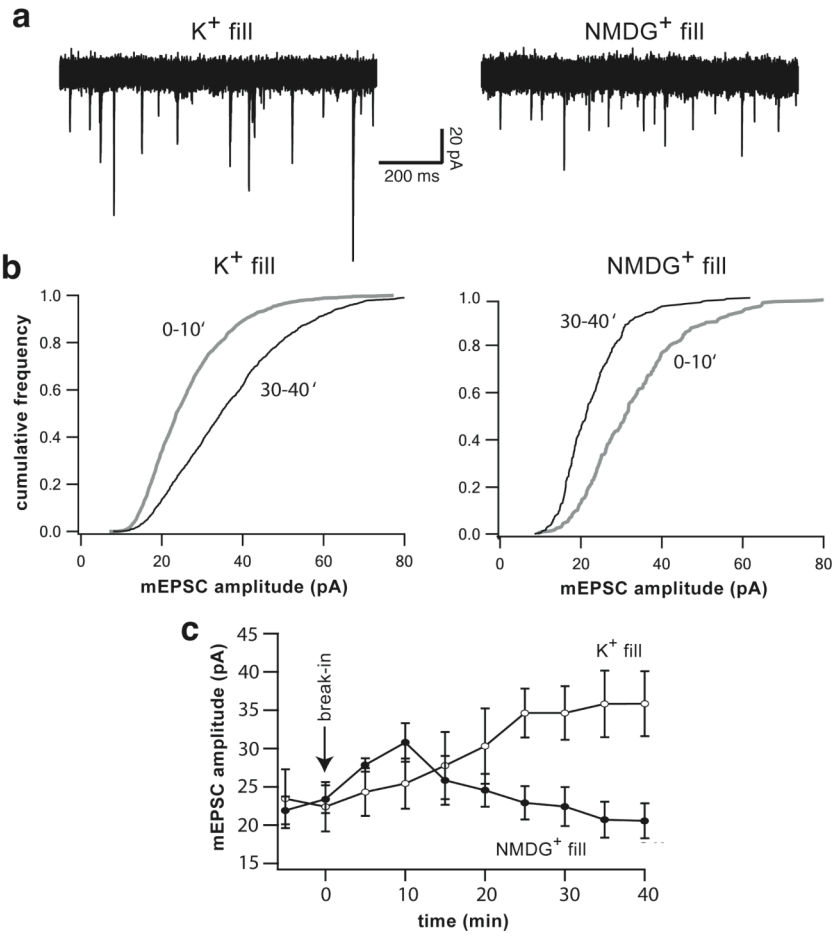

Figure 2-13. Presynaptic K^+ regulates mEPSC amplitude at the calyx of Held.
(a) Paired recordings were performed from both pre- and postsynaptic elements at the calyx of Held. Miniature excitatory postsynaptic currents (mEPSCs) were recorded postsynaptically before and for 40 minutes after break-in to the presynaptic terminal with a pipette containing either high K^+ (left) or low K^+ ($NMDG^+$; right) solution. Ten superimposed sweeps illustrate mEPSCs after 30-40 minutes of intra-terminal dialysis. (b) Cumulative probability histograms of mEPSC amplitude early and late during dialysis are shown below the corresponding sweeps. Each panel derives from an individual paired recording. Mean mEPSC amplitudes at 30-40 min differ significantly from those at 0-10 min. ($p < 0.01$ for K^+ and $p < 0.05$ for $NMDG^+$). (c) Time course of the average data from 5 paired recordings for each condition, plotted from before rupture of the presynaptic patch to 40 minutes after. Each point represents the mean and SEM of the previous 5 minutes of recording. In both ionic conditions, mEPSC amplitude began to rise following rupture (t=0). With $NMDG^+$ pipettes, however, this trend reversed soon after break-in whereas mEPSC amplitude continued to rise with K^+ pipettes.

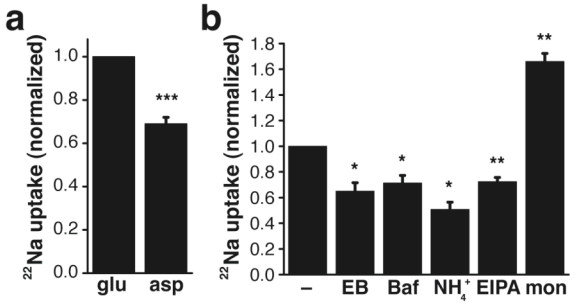

Figure 2-14. Glutamate-acidified synaptic vesicles demonstrate pH-driven $^{22}Na^+$ uptake. Synaptic vesicle uptake of $^{22}Na^+$ was measured for 10 minutes in the presence of ATP and either 10 mM choline glutamate or 10 mM choline aspartate (a), and the results normalized to uptake in glutamate (n = 25). (b) $^{22}Na^+$ uptake was measured in the presence of ATP, glutamate and the following compounds: EIPA (15 μM), Bafilomycin A1 (Baf) (0.5 μM), Evans Blue (EB) (100 μM), $(NH_4)_2$ tartrate (NH_4^+) (10 mM), and the Na^+ ionophore monensin (mon) (5 μM) as positive control (n = 3-5). Inhibition by NH_4^+ indicates the dependence of Na^+ uptake on pH, and inhibition by Evans Blue indicates the dependence on acidification by glutamate. Inhibition by bafilomycin further excludes the role for a channel, since bafilomycin should increase Na^+ entry through a channel by reducing the inwardly positive membrane potential. * indicates $p < 0.05$, ** indicates $p < 0.01$, and *** indicates $p < 0.0001$ by two-tailed paired t tests.

Indeed, the VGLUT inhibitor Evans Blue blocks the stimulation by glutamate (**Fig. 2-14b**). Although the effect of glutamate appears modest, the ionophore monensin, which directly exchanges H^+ for Na^+, only increases uptake by ~70%, indicating that the endogenous activity is substantial. The V-ATPase inhibitor bafilomycin also blocks glutamate-stimulated $^{22}Na^+$ uptake (**Fig. 2-14b**), confirming that the uptake depends on a $\Delta\mu_{H+}$ generated by the V-ATPase, and arguing against the role for a channel since cation uptake by a channel should increase (rather than decrease) in the absence of a positive $\Delta\psi$ produced by the V-ATPase. Further, the dissipation of ΔpH by ammonia blocks the stimulation of $^{22}Na^+$ uptake by glutamate (**Fig. 2-14b**), consistent with its dependence on ΔpH.

To characterize the proteins responsible for synaptic vesicle cation/H^+ exchange, we took advantage of the available pharmacology. In particular, we compared the effects of glutamate and aspartate on $^{22}Na^+$ uptake in the presence of different inhibitors. The K^+ channel inhibitor tetraethylammonium (TEA) and Na^+ channel inhibitor tetrodotoxin (TTX), as well as TRP channel inhibitors ruthenium red (RuR) and 2-aminoethoxydiphenyl borate (2-APB) all have no effect on glutamate-induced $^{22}Na^+$ uptake (**Fig. 2-15**), consistent with the evidence against a cation channel.

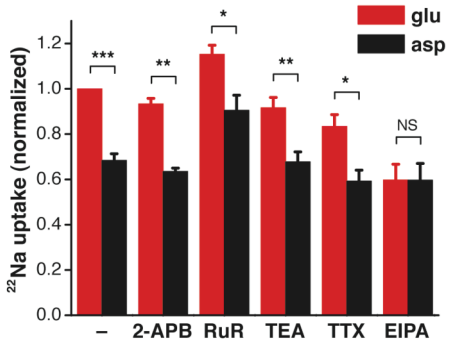

Figure 2-15. $^{22}Na^{+}$ uptake into glutamatergic vesicles is not likely via a channel.
Uptake of $^{22}Na^{+}$ in 10 mM choline glutamate or aspartate as described in Figure 2-14, with and without the following compounds: 2-aminoethoxydiphenylborate (2-APB) (50 μM), ruthenium red (RuR) (100 μM), tetraethylammonium (TEA) (5 mM), tetrodotoxin (TTX) (0.5 μM) and EIPA (50 μM) (n = 3-5). * indicates $p < 0.05$, ** indicates $p < 0.01$, *** indicates $p < 0.0001$, and NS indicates $p = 0.99$ by two-tailed paired t tests.

Coupled cation/H^{+} exchange suggests the involvement of Na^{+}/H^{+} exchangers (NHEs). In general, the NHEs show sensitivity to inhibition by the amiloride analogue 5-(N-ethyl-N-isopropyl)amiloride (EIPA) (Masereel et al 2003; Orlowski & Grinstein 2004). However, most studies of NHE pharmacology have examined the uptake of trace $^{22}Na^{+}$, requiring only low micromolar or submicromolar concentrations of competitive inhibitors such as EIPA to block Na^{+} uptake (Chambrey et al 1997; Orlowski 1993; Szabo et al 2000; Yu et al 1993). Physiological levels of Na^{+} or K^{+} would require much higher concentrations of EIPA, at which nonspecific effects may arise. We thus used $^{22}Na^{+}$ to assess the EIPA sensitivity of cation uptake by synaptic vesicles. Dose-response analysis shows that EIPA inhibits glutamate-activated $^{22}Na^{+}$ uptake in the very low micromolar range, with no effect of much higher concentrations on $^{22}Na^{+}$ uptake in the presence of aspartate (**Fig. 2-16a**), indicating that the EIPA-inhibitable uptake resides specifically on glutamatergic vesicles. EIPA also inhibits $^{22}Na^{+}$ uptake more potently than amiloride (**Fig. 2-16b**), a feature characteristic of the NHEs (Chambrey et al 1997; Orlowski 1993; Szabo et al 2000; Yu et al 1993).

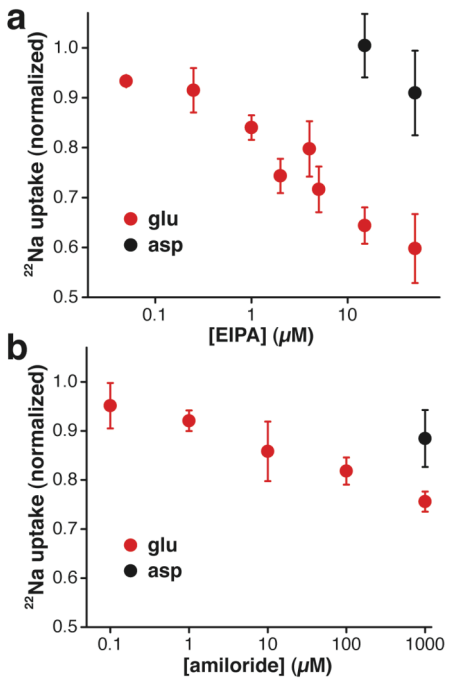

Figure 2-16. pH-driven $^{22}Na^+$ uptake into glutamatergic vesicles is EIPA-sensitive.
(a) EIPA inhibits $^{22}Na^+$ uptake more potently in vesicles acidified with glutamate (n = 3-6). (b) Amiloride also inhibits, but less potently than EIPA (n = 5-6).

Having obtained inhibition of glutamate-dependent $^{22}Na^+$ transport at low micromolar concentrations of EIPA, we decided to test if we could observe a similar inhibition of Na^+-stimulated glutamate uptake by EIPA. We compared glutamate uptake in 20 and 0 mM Na gluconate (balanced to 150 mM total cation using choline gluconate), in the presence or absence of varying concentrations of EIPA. Because EIPA is a competitive inhibitor, we used larger concentrations than those in the $^{22}Na^+$ assay and observed that increasing amounts of EIPA do indeed increasingly inhibit Na^+-stimulated glutamate uptake (**Fig. 2-17**), in support of our hypothesis that cation/H^+ exchange is responsible for the stimulation of glutamate uptake.

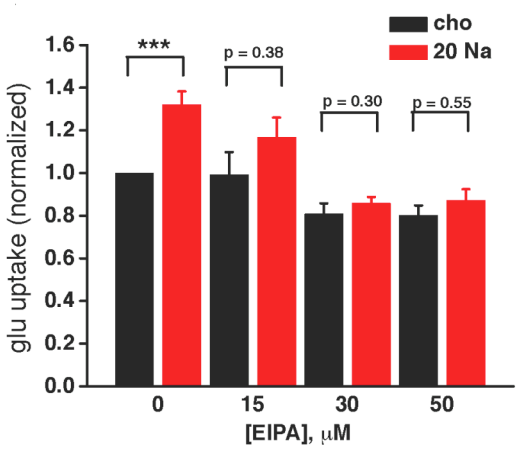

Figure 2-17. Cation stimulation of glutamate uptake is EIPA-sensitive.
Synaptic vesicle uptake of 1 mM ^{3}H-glutamate was measured in either 150 mM choline or 20 mM Na^+ (and 130 mM choline), in the presence or absence of the indicated concentrations of EIPA. The stimulation by Na^+ is eliminated by increasing amounts of EIPA, suggesting that the stimulation is due to an NHE. *** indicates $p < 0.0001$, using two-tailed paired t tests (n = 9, 4, 4, 3 from left to right).

In summary, EIPA inhibits the Na^+ gradient-driven flux of H^+ observed in the acridine orange assay (**Fig. 2-1c**), glutamate-dependent $^{22}Na^+$ uptake (**Fig. 2-14b, 2-16**), as well as Na^+-dependent stimulation of glutamate uptake (**Fig. 2-17**). NHEs are thus the likely molecular candidates responsible for mediating the stimulation of vesicular glutamate transport by cation/H^+ exchange.

2.4 DISCUSSION

The results presented here describe a novel, presynaptic mechanism for the regulation of quantal size (**Fig. 2-18**). During vesicular glutamate transport, ΔpH increases, opposing the activity of the H^+ pump and hence limiting the storage of glutamate. Cation/H^+ exchange dissipates ΔpH but, due to its electroneutrality, spares $\Delta\psi$. As a result, $\Delta\psi$ is selectively increased with continuing activity of the V-ATPase. The exchange mechanism thus effectively converts ΔpH into $\Delta\psi$, similar to the action of NH_3. Since vesicular glutamate transport depends primarily on $\Delta\psi$, electroneutral cation/H^+ exchange thus increases vesicle filling with glutamate.

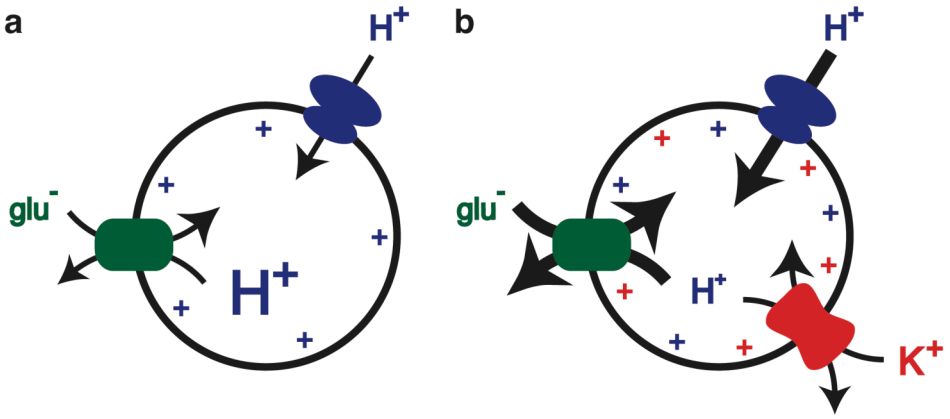

Figure 2-18. Model for stimulation of vesicular glutamate transport by K^+/H^+ exchange. (a) Vesicular glutamate transport (green) driven by the vacuolar H^+-ATPase (blue) increases ΔpH at the expense of Δψ. (b) Electroneutral K^+/H^+ exchange (red) selectively decreases ΔpH, enabling the accumulation of larger Δψ. As a result, K^+/H^+ exchange effectively converts ΔpH into Δψ, increasing the driving force for glutamate filling.

Electroneutral cation/H^+ exchange stimulates glutamate uptake

Several observations support that synaptic vesicles express an electroneutral cation/H^+ exchange activity. First, the efflux of preloaded cation down a concentration gradient drives H^+ entry, suggesting that cation flux is directly coupled to H^+ exchange. This might reflect the production of negative Δψ by cation efflux through a channel, followed by the Δψ-driven influx of H^+ through a distinct channel. If driven by Δψ, H^+ entry should be accelerated by the H^+ ionophore CCCP, but CCCP affects neither the rate nor extent of acidification. The inability of CCCP to affect acidification may reflect the presence of a large H^+ leak that occludes the effect of CCCP, and we do find that synaptic vesicles can exhibit a H^+ leak (**Fig. 2-4**). However, CCCP greatly increases H^+ flux when driven by Δψ (**Fig. 2-4**), indicating that CCCP should also have stimulated cation-driven H^+ entry if it were dependent on Δψ. The lack of CCCP effect thus supports a mechanism of direct cation/H^+ coupling that is independent of membrane potential.

Second, we do not detect a cation conductance on synaptic vesicles (**Fig. 2-4**). In the absence of extravesicular permeant cations, CCCP does not dissipate ΔpH produced by the efflux of NH_3 because the development of negative Δψ opposes net H^+ efflux. This is true even in the presence of extravesicular K^+, indicating that the developing Δψ is not shunted by cation entry through endogenous channels. Only the addition of K^+ ionophore valinomycin in the presence of external K^+ allows significant H^+ efflux, demonstrating that we would have detected an endogenous cation channel if one were present. Although we cannot exclude the presence of any cation channel on synaptic vesicles, the results suggest that the conductance, if present at all, must be miniscule.

Third, inhibition of the V-ATPase with bafilomycin reduces $^{22}Na^+$ uptake. Since V-ATPase activity makes $\Delta\psi$ more positive, cation uptake through a channel should increase if the V-ATPase is inhibited. The reduction in $^{22}Na^+$ uptake by bafilomycin thus indicates that $\Delta\psi$ does not drive flux. Rather, the decrease in $^{22}Na^+$ uptake produced by ammonia supports a selective role for ΔpH, consistent with cation/H^+ exchange. Although electroneutral, cation/H^+ exchange and the resulting dissipation of ΔpH shifts the expression of $\Delta\mu_{H+}$ generated by the V-ATPase from ΔpH to $\Delta\psi$. Indeed, oxonol VI fluorescence demonstrates the effect of K^+ on $\Delta\psi$ and the occlusion of this effect by ammonia suggests that K^+, like NH_4^+, increases $\Delta\psi$ by decreasing ΔpH. Taken together, the results indicate that in the presence of an active V-ATPase, a stoichiometrically coupled, electroneutral cation/H^+ exchange mechanism increases $\Delta\psi$. By acidifying synaptic vesicles with glutamate, we further demonstrate that cation/H^+ exchange occurs on the glutamatergic population.

Assuming for a moment that a cation (K^+, Na^+) channel is present and responsible for our results, we may consider the implications of each of our observations: (1) The acridine orange assay described in **Figure 2-4** indicates that the channel must be inactivated at negative potentials (relative to the vesicle exterior) and not activated by ΔpH alone, since external K^+ in the presence of CCCP is unable to shunt the interior-negative potential to allow net H^+ efflux; (2) The abolishment of $^{22}Na^+$ uptake by NH_4^+ (**Fig. 2-14b**) indicates that the channel must be activated by ΔpH and/or inactivated at positive potentials since NH_4^+ converts ΔpH into positive $\Delta\psi$. For a channel to be consistent with both observations, the channel in question must thus be activated by both ΔpH and a positive potential together, a condition unlikely to be conducive for cation influx.

Cation/H^+ exchange provides a mechanism to convert the ΔpH produced by glutamate accumulation back into $\Delta\psi$ that drives vesicular glutamate transport. Indeed, we find that K^+ increases the uptake of glutamate into synaptic vesicles in a manner consistent with thermodynamic effects on the driving force. The time course shows greater stimulation by K^+ at later time points, during which depletion of the driving force is expected to be more severe. Further, the dose-response to K^+ does not saturate, consistent with an effect on driving force rather than kinetics. In addition, K^+ has no effect on V_{max}, although it does reduce K_m slightly. Although a kinetic parameter, the K_m of vesicular glutamate transport has previously been suggested to depend on $\Delta\psi$: the divalent cation/H^+ exchanger A23187 both increases $\Delta\psi$ and decreases K_m at low chloride concentrations, while high chloride concentrations, which decrease $\Delta\psi$, increase K_m (Wolosker et al 1996). The effect of K^+ on K_m may thus similarly reflect a change in $\Delta\psi$.

To further test whether the stimulation of VGLUT activity by K^+ involves the observed increase in $\Delta\psi$, we again used ammonia. Like K^+, ammonia stimulates

glutamate uptake, and the two effects partially occlude each other, suggesting that dissipation of ΔpH accounts for the stimulation by K^+, consistent with cation/H^+ exchange. An alternative interpretation is that K^+ influx through a channel could increase Δψ and reduce ΔpH by inhibiting the H^+ pump. Indeed, recent work has suggested that the cation channel TRPM7 found on cholinergic synaptic vesicles has a role in the regulation of acetylcholine release, but this was attributed to protein-protein interactions and changes in vesicle fusion rather than filling (Brauchi et al 2008; Krapivinsky et al 2006). Furthermore, acetylcholine is a positively charged substrate whose uptake depends more on ΔpH than Δψ, indicating a distinct mechanism of action from our results. As described above, we find no functional evidence for a cation channel on synaptic vesicles. Further, valinomycin does not enable K^+ to stimulate vesicular glutamate transport, indicating that a channel would not increase vesicle filling even if one were present. Rather, nigericin strongly augments glutamate uptake, demonstrating the potency of an electroneutral K^+/H^+ exchange mechanism.

A presynaptic role for NHE in transmitter release

The effect of presynaptic K^+ on glutamatergic transmission at the calyx of Held indicates a physiological role for K^+ flux in vesicle filling and glutamate release. Dialysis of the presynaptic terminal with a solution containing K^+ rather than $NMDG^+$ increases quantal size measured postsynaptically. In contrast, considerable work *in vitro* has demonstrated an inhibitory role of high Cl^- in glutamate uptake (Bellocchio et al 2000; Carlson et al 1989; Cidon & Sihra 1989; Tabb et al 1992), yet changes in presynaptic Cl^- at the calyx of Held have no effect on quantal size (Price & Trussell 2006). The discrepancy between *in vitro* and *in vivo* studies likely reflect a role for Cl^- in the kinetics of transport, which are easier to detect in radiotracer flux assays, rather than in thermodynamics, which may be more important for quantal size. Indeed, Cl^- was found to have more effect on the initial rate of glutamate uptake but less on the maximal filling at steady-state, especially at higher glutamate concentrations (Wolosker et al 1996). Presynaptic K^+ affects both transport activity *in vitro* and quantal size *in vivo* presumably because the mechanism involved affects equilibrium. Despite the novelty of the mechanism described here, cation/H^+ exchange thus has greater significance for glutamatergic neurotransmission than the very well described effects of Cl^-.

As mentioned previously, a recent paper describes a role for intralumenal chloride in glutamate uptake by VGLUT1, which the authors suggest to be important during fast vesicle recycling when the lumen is likely to contain high concentrations of chloride (Schenck et al 2009). We now discover a role for cations in the modulation of Δψ that is independent of vesicle recycling since it relies on cytoplasmic K^+, and can therefore be utilized by all pools of synaptic vesicles and indeed possibly other organelles. In fact, since the stimulatory effect of K^+ intensifies with time, our mechanism may be more important for slower-recycling vesicles that have more time to equilibrate. It should also

be noted that the liposomes used in Schenck et al. have an average diameter of over 100 nm, more than double that of synaptic vesicles. This translates to a difference in surface area and volume of over 4- and 8-fold, respectively, or a halving of surface area to volume ratio. Because native vesicles are used in our experiments, the dimensions of the vesicles and hence their ΔpH and Δψ dynamics are preserved, likely representing the relevant context *in vivo*.

The results implicate an intracellular NHE in transmitter release. The dependence of cation-stimulated glutamate uptake on ΔpH, of H^+ flux on a cation gradient and of cation movement on ΔpH all support a H^+ exchange mechanism. The recognition of K^+ as well as Na^+ is also consistent with the activity of an intracellular NHE. The ability to stimulate vesicular glutamate transport despite the activity of the H^+ pump and the presence of Δψ suggest an electroneutral mechanism. The independence from Δψ of cation-driven H^+ flux and H^+-driven cation flux further support electroneutrality. Finally, the sensitivity of synaptic vesicle cation/H^+ exchange and cation-stimulated glutamate uptake to low micromolar concentrations of EIPA indicates the activity of an intracellular NHE. Interestingly, the endosomal isoforms NHE6 and 9 have recently been implicated in brain development and human disease. Mutations in NHE6 cause an X-linked recessive form of mental retardation with seizures (Gilfillan et al 2008), and polymorphisms in NHE9 have been associated with autism (Morrow et al 2008). Genetic association studies have also implicated NHE9 in attention-deficit/hyperactivity (Franke et al 2009) and addiction-related disorders (Uhl et al 2008). These phenotypes point to the importance of these isoforms in the brain, especially given that NHE5, 6 and 7 are enriched in the brain, and NHE8 and NHE9 are ubiquitously found in tissues (Nakamura et al 2005; Numata & Orlowski 2001; Numata et al 1998). The role of NHE activity in filling synaptic vesicles with glutamate now raises the possibility that these mutations may interfere with behavior by disrupting neurotransmitter release. Remarkably, recent work in *C. elegans* has demonstrated the role for an NHE homologue in chemical signaling from intestinal epithelial cells to muscle (Beg et al 2008). In this case, protons are the signal, and their release does not require vesicle fusion, but cation/H^+ exchange by synaptic vesicles may have evolved from this mechanism.

A general role for NHE in modulating pH in intracellular compartments

Finally, the results indicate a mechanism to control the expression of $\Delta\mu_{H+}$ as either ΔpH or Δψ, suggesting a novel intracellular role for NHEs. Although different ClC isoforms localize to different compartments of the endocytic pathway, their apparently fixed ionic coupling of 2 Cl^- : 1 H^+ (Accardi & Miller 2004; De Angeli et al 2006; Graves et al 2008; Zifarelli & Pusch 2009) makes it unlikely that differences in their expression or intrinsic activity can alone account for the observed variation in organelle pH, from ~6 in early endosomes, to ~4.5 in lysosomes. Similarly, changes in the expression of a Cl^- channel alone are unlikely to confer variation in ΔpH. On the other hand, the combination of a ClC (or Cl^- channel) with opposing NHE activity that converts ΔpH back into Δψ

could provide an explanation for the wide range of ΔpH: dominance of NHE over ClC activity should confer the relatively small ΔpH of early endosomes, and dominance of ClC over NHE the larger ΔpH of late endosomes and lysosomes. Consistent with this hypothesis, none of the intracellular NHEs have been localized to lysosomes—NHE6 and 9 reside earlier in the endocytic pathway, and NHE7 and 8 in the Golgi complex (Nakamura et al 2005; Numata & Orlowski 2001). The regulation of NHE and ClC trafficking may thus contribute to the variation in compartmental ΔpH.

Most work on $\Delta\mu_{H+}$ in the secretory pathway has thus far focused on the control of ΔpH rather than Δψ, which reflects the well-documented role of ΔpH in processes such as ligand dissociation from receptors and proteolysis in the lysosome. However, the importance of Δψ for vesicular glutamate transport and the identification of cation/H^+ exchange as a mechanism that promotes formation of Δψ suggest that the control of Δψ may not simply be a mechanism to regulate ΔpH. Rather, Δψ may serve as the primary driving force for transport and other novel processes which as yet remain poorly understood.

2.5 ACKNOWLEDGMENTS

The work presented in this chapter has been submitted for publication in *Nature Neuroscience*, 2009: Goh, G.Y., Huang, H., Borre, L., Trussell, L.O., and Edwards, R.H. The Presynaptic Regulation of Quantal Size: Potassium/Proton Exchange Stimulates Vesicular Glutamate Transport by Increasing Membrane Potential. The dissertation author was the primary investigator and author of this paper. Hai Huang, working in the lab of Larry Trussell, contributed Figure 2-13. Lars Borre developed the $^{22}Na^+$ uptake assay. This work was supported in part by a fellowship from the Agency for Science, Technology and Research, Singapore to G.Y.G. and the American Heart Association to L.B., and by grants from NIDCD and NINDS to L.O.T. and from NIMH and NIDA to R.H.E.

2.6 REFERENCES

Accardi A, Miller C. 2004. Secondary active transport mediated by a prokaryotic homologue of ClC Cl- channels. *Nature* 427:803-7

Beg AA, Ernstrom GG, Nix P, Davis MW, Jorgensen EM. 2008. Protons act as a transmitter for muscle contraction in C. elegans. *Cell* 132:149-60

Bellocchio EE, Reimer RJ, Fremeau RT, Jr., Edwards RH. 2000. Uptake of glutamate into synaptic vesicles by an inorganic phosphate transporter. *Science* 289:957-60

Borst JG, Helmchen F, Sakmann B. 1995. Pre- and postsynaptic whole-cell recordings in the medial nucleus of the trapezoid body of the rat. *J Physiol* 489 (Pt 3):825-40

Brauchi S, Krapivinsky G, Krapivinsky L, Clapham DE. 2008. TRPM7 facilitates cholinergic vesicle fusion with the plasma membrane. *Proc Natl Acad Sci U S A* 105:8304-8

Carlson MD, Kish PE, Ueda T. 1989. Characterization of the solubilized and reconstituted ATP-dependent vesicular glutamate uptake system. *J Biol Chem* 264:7369-76

Chambrey R, Achard JM, Warnock DG. 1997. Heterologous expression of rat NHE4: a highly amiloride-resistant Na+/H+ exchanger isoform. *Am J Physiol* 272:C90-8

Chaudhry FA, Boulland JL, Jenstad M, Bredahl MK, Edwards RH. 2008. Pharmacology of neurotransmitter transport into secretory vesicles. *Handb Exp Pharmacol*:77-106

Chow CW, Khurana S, Woodside M, Grinstein S, Orlowski J. 1999. The epithelial Na(+)/H(+) exchanger, NHE3, is internalized through a clathrin-mediated pathway. *J Biol Chem* 274:37551-8

Cidon S, Sihra TS. 1989. Characterization of a H+-ATPase in rat brain synaptic vesicles. Coupling to L-glutamate transport. *J Biol Chem* 264:8281-8

Cools AA, Janssen LH. 1986. Fluorescence response of acridine orange to changes in pH gradients across liposome membranes. *Experientia* 42:954-6

Craige B, Salazar G, Faundez V. 2004. Isolation of synaptic vesicles. *Curr Protoc Cell Biol* Chapter 3:Unit 3 12

De Angeli A, Monachello D, Ephritikhine G, Frachisse JM, Thomine S, et al. 2006. The nitrate/proton antiporter AtCLCa mediates nitrate accumulation in plant vacuoles. *Nature* 442:939-42

Diering GH, Church J, Numata M. 2009. Secretory Carrier Membrane Protein 2 Regulates Cell-surface Targeting of Brain-enriched Na+/H+ Exchanger NHE5. *J Biol Chem* 284:13892-903

Franke B, Neale BM, Faraone SV. 2009. Genome-wide association studies in ADHD. *Hum Genet*

Gilfillan GD, Selmer KK, Roxrud I, Smith R, Kyllerman M, et al. 2008. SLC9A6 mutations cause X-linked mental retardation, microcephaly, epilepsy, and ataxia, a phenotype mimicking Angelman syndrome. *Am J Hum Genet* 82:1003-10

Graves AR, Curran PK, Smith CL, Mindell JA. 2008. The Cl-/H+ antiporter ClC-7 is the primary chloride permeation pathway in lysosomes. *Nature* 453:788-92

Hartinger J, Jahn R. 1993. An anion binding site that regulates the glutamate transporter of synaptic vesicles. *J Biol Chem* 268:23122-7

Hell JW, Jahn R, eds. 1994. *Preparation of synaptic vesicles from mammalian brain*., Vols. 1. San Diego: Academic Press. 567-74 pp.

Hell JW, Maycox PR, Jahn R. 1990. Energy dependence and functional reconstitution of the gamma-aminobutyric acid carrier from synaptic vesicles. *J Biol Chem* 265:2111-7

Hill JK, Brett CL, Chyou A, Kallay LM, Sakaguchi M, et al. 2006. Vestibular hair bundles control pH with (Na+, K+)/H+ exchangers NHE6 and NHE9. *J Neurosci* 26:9944-55

Ishikawa T, Sahara Y, Takahashi T. 2002. A single packet of transmitter does not saturate postsynaptic glutamate receptors. *Neuron* 34:613-21

Johnson RG, Carty S, Scarpa A. 1982. A model of biogenic amine accumulation into chromaffin granules and ghosts based on coupling to the electrochemical proton gradient. *Fed Proc* 41:2746-54

Johnson RG, Scarpa A. 1979. Protonmotive force and catecholamine transport in isolated chromaffin granules. *J Biol Chem* 254:3750-60

Juge N, Yoshida Y, Yatsushiro S, Omote H, Moriyama Y. 2006. Vesicular glutamate transporter contains two independent transport machineries. *J Biol Chem* 281:39499-506

Krapivinsky G, Mochida S, Krapivinsky L, Cibulsky SM, Clapham DE. 2006. The TRPM7 ion channel functions in cholinergic synaptic vesicles and affects transmitter release. *Neuron* 52:485-96

Lin PJ, Williams WP, Kobiljski J, Numata M. 2007. Caveolins bind to (Na+, K+)/H+ exchanger NHE7 by a novel binding module. *Cell Signal* 19:978-88

Lin PJ, Williams WP, Luu Y, Molday RS, Orlowski J, Numata M. 2005. Secretory carrier membrane proteins interact and regulate trafficking of the organellar (Na+,K+)/H+ exchanger NHE7. *J Cell Sci* 118:1885-97

Masereel B, Pochet L, Laeckmann D. 2003. An overview of inhibitors of Na(+)/H(+) exchanger. *Eur J Med Chem* 38:547-54

Maycox PR, Deckwerth T, Hell JW, Jahn R. 1988. Glutamate uptake by brain synaptic vesicles. Energy dependence of transport and functional reconstitution in proteoliposomes. *J Biol Chem* 263:15423-8

Miesenbock G, De Angelis DA, Rothman JE. 1998. Visualizing secretion and synaptic transmission with pH-sensitive green fluorescent proteins. *Nature* 394:192-5

Moriyama Y, Maeda M, Futai M. 1990. Energy coupling of L-glutamate transport and vacuolar H(+)-ATPase in brain synaptic vesicles. *J Biochem* 108:689-93

Moriyama Y, Yamamoto A. 1995. Vesicular L-glutamate transporter in microvesicles from bovine pineal glands. Driving force, mechanism of chloride anion activation, and substrate specificity. *J Biol Chem* 270:22314-20

Morrow EM, Yoo SY, Flavell SW, Kim TK, Lin Y, et al. 2008. Identifying autism loci and genes by tracing recent shared ancestry. *Science* 321:218-23

Nagy A, Baker RR, Morris SJ, Whittaker VP. 1976. The preparation and characterization of synaptic vesicles of high purity. *Brain Res* 109:285-309

Nakamura N, Tanaka S, Teko Y, Mitsui K, Kanazawa H. 2005. Four Na+/H+ exchanger isoforms are distributed to Golgi and post-Golgi compartments and are involved in organelle pH regulation. *J Biol Chem* 280:1561-72

Numata M, Orlowski J. 2001. Molecular cloning and characterization of a novel (Na+,K+)/H+ exchanger localized to the trans-Golgi network. *J Biol Chem* 276:17387-94

Numata M, Petrecca K, Lake N, Orlowski J. 1998. Identification of a mitochondrial Na+/H+ exchanger. *J Biol Chem* 273:6951-9

Ohgaki R, Fukura N, Matsushita M, Mitsui K, Kanazawa H. 2008. Cell surface levels of organellar Na+/H+ exchanger isoform 6 are regulated by interaction with RACK1. *J Biol Chem* 283:4417-29

Onishi I, Lin PJ, Diering GH, Williams WP, Numata M. 2007. RACK1 associates with NHE5 in focal adhesions and positively regulates the transporter activity. *Cell Signal* 19:194-203

Orlowski J. 1993. Heterologous expression and functional properties of amiloride high affinity (NHE-1) and low affinity (NHE-3) isoforms of the rat Na/H exchanger. *J Biol Chem* 268:16369-77

Orlowski J, Grinstein S. 2004. Diversity of the mammalian sodium/proton exchanger SLC9 gene family. *Pflugers Arch* 447:549-65

Orlowski J, Grinstein S. 2007. Emerging roles of alkali cation/proton exchangers in organellar homeostasis. *Curr Opin Cell Biol* 19:483-92

Price GD, Trussell LO. 2006. Estimate of the chloride concentration in a central glutamatergic terminal: a gramicidin perforated-patch study on the calyx of Held. *J Neurosci* 26:11432-6

Reis M, Farage M, Wolosker H. 2000. Chloride-dependent inhibition of vesicular glutamate uptake by alpha-keto acids accumulated in maple syrup urine disease. *Biochim Biophys Acta* 1475:114-8

Roxrud I, Raiborg C, Gilfillan GD, Stromme P, Stenmark H. 2009. Dual degradation mechanisms ensure disposal of NHE6 mutant protein associated with neurological disease. *Exp Cell Res* 315:3014-27

Schenck S, Wojcik SM, Brose N, Takamori S. 2009. A chloride conductance in VGLUT1 underlies maximal glutamate loading into synaptic vesicles. *Nat Neurosci* 12:156-62

Schuldiner S, Rottenberg H, Avron M. 1972. Determination of pH in chloroplasts. 2. Fluorescent amines as a probe for the determination of pH in chloroplasts. *Eur J Biochem* 25:64-70

Shioi J, Ueda T. 1990. Artificially imposed electrical potentials drive L-glutamate uptake into synaptic vesicles of bovine cerebral cortex. *Biochem J* 267:63-8

Szabo EZ, Numata M, Lukashova V, Iannuzzi P, Orlowski J. 2005. beta-Arrestins bind and decrease cell-surface abundance of the Na+/H+ exchanger NHE5 isoform. *Proc Natl Acad Sci U S A* 102:2790-5

Szabo EZ, Numata M, Shull GE, Orlowski J. 2000. Kinetic and pharmacological properties of human brain Na(+)/H(+) exchanger isoform 5 stably expressed in Chinese hamster ovary cells. *J Biol Chem* 275:6302-7

Szaszi K, Paulsen A, Szabo EZ, Numata M, Grinstein S, Orlowski J. 2002. Clathrin-mediated endocytosis and recycling of the neuron-specific Na+/H+ exchanger NHE5 isoform. Regulation by phosphatidylinositol 3'-kinase and the actin cytoskeleton. *J Biol Chem* 277:42623-32

Tabb JS, Kish PE, Van Dyke R, Ueda T. 1992. Glutamate transport into synaptic vesicles. Roles of membrane potential, pH gradient, and intravesicular pH. *J Biol Chem* 267:15412-8

Uhl GR, Drgon T, Johnson C, Li CY, Contoreggi C, et al. 2008. Molecular genetics of addiction and related heritable phenotypes: genome-wide association approaches identify "connectivity constellation" and drug target genes with pleiotropic effects. *Ann N Y Acad Sci* 1141:318-81

Wolosker H, de Souza DO, de Meis L. 1996. Regulation of glutamate transport into synaptic vesicles by chloride and proton gradient. *J Biol Chem* 271:11726-31

Wu XS, Xue L, Mohan R, Paradiso K, Gillis KD, Wu LG. 2007. The origin of quantal size variation: vesicular glutamate concentration plays a significant role. *J Neurosci* 27:3046-56

Yu FH, Shull GE, Orlowski J. 1993. Functional properties of the rat Na/H exchanger NHE-2 isoform expressed in Na/H exchanger-deficient Chinese hamster ovary cells. *J Biol Chem* 268:25536-41

Zachos NC, Tse M, Donowitz M. 2005. Molecular physiology of intestinal Na+/H+ exchange. *Annu Rev Physiol* 67:411-43

Zifarelli G, Pusch M. 2009. Conversion of the 2 Cl(-)/1 H+ antiporter ClC-5 in a NO3(-)/H+ antiporter by a single point mutation. *EMBO J* 28:175-82

Chapter 3. Investigation of the Molecular Entity Responsible for Cation/Proton Exchange

3.1 INTRODUCTION

The results described in Chapter 2 implicate the action of an NHE in the observed cation/proton exchange in synaptic vesicles. The intracellular NHE isoforms, which are likely candidates, were relatively recently identified, and their characterization is at best limited in terms of cation sensitivities and pharmacology.

From the available data, the cation affinities from our studies (K_m of 4.1 and 140 mM for Na^+ and K^+, respectively) do not quite match the profile of any isoform (**Table 1**). K^+ does compete with Na^+ for binding to NHE1, but is not actually transported (Orlowski 1993). NHE4 does recognize K^+, but with greater affinity than for Na^+ or Li^+ (Chambrey et al 1997), in contrast to our data. Its preferential expression in the epithelia of the gastrointestinal tract and kidney (Orlowski et al 1992) and restricted localization to the hippocampal pyramidal layer in the rat brain (Bookstein et al 1996) renders it an unlikely isoform responsible for the activity we observe. Furthermore, it is uniquely activated by hyperosmotic conditions (Bookstein et al 1994) and by DIDS (Chambrey et al 1997). Neither of these isoforms are likely to be responsible for the cation/proton exchange in synaptic vesicles. The recognition of K^+ in our assays thus supports an intracellular NHE rather than a plasma membrane isoform, although the higher affinity for K^+ than Na^+ of NHE8 (Nakamura et al 2005) also renders it an unlikely candidate. It is important to note, however, that these known values refer to extracellular cations, which is equivalent to the lumenal side of our vesicles. Thus, the cation affinities obtained in our assay apply to the intracellular side of the NHE rather than the extracellular side.

Pharmacologically, the greater sensitivity of our observed cation/proton exchange to EIPA than amiloride is consistent with the general characteristic of all members of the NHE family (**Table 2**). However, the inhibitory potencies we obtained in the ^{22}Na uptake assay again do not match the known K_i values of any particular isoform except, perhaps, NHE3, which however does not recognize K^+. We are thus left with NHE6, NHE7 and NHE9 as our most likely candidates. Again, it should be noted that these inhibitors were applied to the extracellular side in the published references, rather than to the cytoplasmic side as in our studies.

Experimental Strategies and Goals

Good isoform-specific antibodies for these intracellular NHEs were not easily available at the time of study, if at all. To obtain initial clues as to the molecular identity of the protein involved, we thus expressed epitope-tagged isoforms of selected members

of the NHE family in primary cultured rat hippocampal neurons and performed co-immunostaining with synaptic vesicle proteins to determine which of them, if any, display a synaptic localization.

Table 1. Apparent affinity constants of the different NHE isoforms for extracellular monovalent cations.

	Na^+_o	Li^+_o	K^+_o
rat NHE1	10.0	3.4	19.5*
rat NHE2	50.0	2.2	none
rat NHE3	4.7	2.6	none
rat NHE4	30	yes	yes
human NHE5	18.6	0.32	slight
human NHE6	yes	-	yes
human NHE7	yes	yes	yes
human NHE8	130	>200	75
human NHE9	yes	-	yes

All values are given in mM.
"none" indicates no recognition of the cation; "yes" indicates recognition.
*K^+ inhibited $^{22}Na^+$ transport but was not itself transported.
Values were obtained from the following references: (Bookstein et al 1996; Chambrey et al 1997; Hill et al 2006; Nakamura et al 2005; Numata & Orlowski 2001; Orlowski 1993; Szabo et al 2000; Yu et al 1993).

Table 2. Inhibitory potency of some NHE inhibitors towards the different isoforms.

	rat NHE1	**rat NHE2**	**rat NHE3**	**rat NHE4**	**human NHE5**	**human NHE7**
amiloride	1.6	1.4	100	*180*	21	>2000
EIPA	0.015	0.079	2.4	*490*	0.42	-
DMA	0.023	0.25	14	*24*	-	-
HMA	0.013	-	2.4	*96*	0.37	-
benzamil	120	320	100	-	-	100-1000

All values are given in μM. K_i values are in regular font; IC_{50} values are italicized.
Values were obtained from the following references: (Bookstein et al 1996; Numata & Orlowski 2001; Orlowski 1993; Szabo et al 2000; Yu et al 1993).

3.2 MATERIALS AND METHODS

3.2.1 Molecular Biology

pCMV vectors each containing one of the epitope-tagged genes rat NHE3 or human NHE5, NHE6, NHE7, NHE8, and NHE9 were generous gifts from Dr. John Orlowski (McGill University, Canada). hNHE5 contains a triple influenza virus HA epitope in the first predicted exomembranous loop as described (Szaszi et al 2002).

rNHE3, hNHE6 and hNHE8 each contains a single HA epitope at the C-terminus, immediately before the stop codon. hNHE7 and hNHE9 each contains a single myc epitope at the C-terminus, immediately before the stop codon. All genes were subcloned into the chicken actin vector pCAGGS.

The rat NHE5 gene in pCMV vector was a generous gift from Dr. James Melvin (University of Rochester, New York). To insert a HA epitope tag into the C-terminus end of the protein, we amplified rNHE5 from the plasmid by polymerase chain reaction using the following primers: 5'-GAGCC-EcoRI-19UTR-3' (sense) and 5'-CTGGC-KpnI-13UTR-stop-HA-20CDS-3' (antisense), with sequences 5'-GAGCC-GAATTC-GCCGGCGGCCGTGCAGTGC-3' and 5'-CTGGC-GGTACC-CCGAGGCCCTGGG-CTA-GGCGTAGTCAGGCACATCGTATGGGTATCCGCC-CAGCCTGCCTCCTCTGTTGA-3', respectively. EcoRI and KpnI refer to restriction enzyme digest sites, 19UTR refers to the untranslated region upstream of the rat NHE5 gene from positions -34 to -16, 13UTR refers to the untranslated region immediately downstream from the stop codon of rat NHE5, and 20CDS refers to the 20 base pairs of the rat NHE5 gene directly upstream of the stop codon. The amplified product was then subcloned into pCAGGS and the coding region verified by sequencing.

3.2.2 Primary Hippocampal Cell Culture and Immunostaining

Hippocampi from embryonic day 19 (E19) rats were dissected, dissociated, and transfected with 3.0 μg DNA by electroporation, and cultured as previously described (Li et al 2005). For co-transfections, the amount of each plasmid used for transfection was reduced such that the total DNA used was maintained at 3.0 μg. After 13–15 days in vitro (DIV), the cells were fixed with 4% paraformaldehyde for 5 min at room temperature, followed by methanol for 5 min at -20ºC. Cells were then permeabilized and blocked in phosphate-buffered saline (PBS) containing 0.02% saponin, 1% fish skin gelatin and 5% bovine serum albumin, and immunostained with primary antibodies rat anti-HA (3F10, Roche), mouse anti-HA (HA.11, Covance), mouse anti-synaptophysin (Sigma), rabbit anti-VGLUT1 (Abcam) or rabbit anti-GFP (Molecular Probes), followed by the appropriate fluorophore-conjugated secondary antibodies. Bound antibodies were then visualized by confocal microscopy on a Zeiss LSM510 Meta microscope.

3.3 RESULTS

3.3.1 Localization of Epitope-Tagged NHEs in Primary Hippocampal Neurons

To investigate the subcellular localization of the NHE isoforms potentially responsible for our observed activity, we transfected epitope-tagged NHEs 3, 5, 6, 7, 8 and 9 into primary rat hippocampal cultures. We then co-immunostained them with synaptophysin or VGLUT1, both synaptic vesicle proteins and hence markers for synapses. Because it was possible that we overlooked colocalization in some areas of the cover slip by looking at either untransfected cells with only endogenous synaptic marker

and no epitope-tagged NHE, or at regions of transfected cells where the epitope-tagged NHE appears but are not synaptic, we also co-transfected and then co-immunostained some of the NHEs with GFP-VGLUT1, to ensure that we were imaging transfected synapses that were expressing both proteins. The immunostaining results are summarized in **Table 3**.

NHE3, NHE7 and NHE8 do not localize to synapses

NHE3-HA localized mainly to the plasma membrane in the cell body, and to some puncta in dendrites (**Fig. 3-1**). It did not colocalize with co-transfected GFP-VGLUT1.

NHE7-myc mostly localized in the cell body and proximal dendrites. Some punctate staining in distal processes was observed, but which was not positive for synaptophysin or VGLUT1 (**Fig. 3-2**).

NHE8-HA was located almost exclusively in the cell body, displaying Golgi-like staining and no colocalization with GFP-VGLUT1 (**Fig. 3-3**).

NHE5 localizes to a subset of non-glutamatergic synaptic vesicles

NHE5-HA displayed punctate staining in processes, colocalizing partially with synaptophysin (**Fig. 3-4, 3-5**), and to a small extent with VGLUT1 (**Fig. 3-4**) and co-transfected GFP-VGLUT1 (**Fig. 3-6**). Strikingly, it colocalized very well with co-transfected GFP-VMAT2 (**Fig. 3-5**), raising the possibility that NHE5 preferentially traffics to large dense-core vesicles rather than synaptic vesicles, which then implicates distinct targeting sites for the different NHE isoforms.

NHE9 localizes to some synapses

NHE9-myc, like NHE5, exhibited punctate staining in processes and colocalized with synaptophysin (**Fig. 3-7**). It appeared to display no colocalization with VGLUT1 (**Fig. 3-7**), but a little colocalization when co-transfected with GFP-VGLUT1 (**Fig. 3-8, 3-9**). This may indicate that it is preferentially targeted to non-glutamatergic synapses, again implicating possibly regulated and distinct targeting sites for the different NHE isoforms.

NHE6 localizes to glutamatergic synapses

Like NHE9, NHE6-HA exhibited punctate staining in processes and also colocalized with synaptophysin (**Fig. 3-10**). Interestingly, although it appeared to colocalize only a little with endogenous VGLUT1 (**Fig. 3-10**), it colocalized extensively

with co-transfected GFP-VGLUT1 (**Fig. 3-11**). The former observation may be a result of overlooking synapses with colocalization in certain areas of the cover slips, or may reflect highly regulated trafficking in the former case, such that the endogenous NHE6 was preferentially targeted to VGLUT1 vesicles compared to the epitope-tagged NHE6-HA. In the latter case of co-transfection of both NHE6-HA and GFP-VGLUT1, the excess copy number of both proteins may have allowed targeting of both proteins to the same vesicles.

hNHE6-HA and hNHE9-myc colocalize partially in neurons

In transfected COS7 cells, NHE6 and NHE9 were found in early and late recycling endosomes, respectively, and thus displayed some overlapping localization (Nakamura et al 2005). We thus co-transfected NHE6-HA and NHE9-myc to determine if the same phenomenon was true in neurons. Indeed, we found that the two proteins also colocalized partially (**Fig. 3-12**), consistent with their targeting to dynamic, interacting populations of endosomes.

Table 3. Summary of Immunostaining Results

	Colocalization with:		
	Synaptophysin	**VGLUT1**	**GFP-VGLUT1**
rNHE3-HA	N.A.	N.A.	none
hNHE5-HA	some	little	N.A.
rNHE5-HA	much	N.A.	little
hNHE6-HA	some	little	much
hNHE7-myc	none	none	N.A.
hNHE8-HA	N.A.	N.A.	None
hNHE9-myc	much	none	little

"N.A." indicates not assessed.

3.4 DISCUSSION

To get an idea of the trafficking patterns of the different intracellular NHE isoforms in neurons, we transfected epitope-tagged NHEs into neurons and looked for colocalization with the synaptic vesicle proteins synaptophysin and VGLUT1 as an indication of synaptic localization. Our immunostaining results lead us to a few conclusions: (1) NHE3, NHE7 and NHE8 are unlikely to localize to synaptic vesicles since neither of them display colocalization with either synaptophysin or VGLUT1/GFP-VGLUT1, with NHE7 and NHE8 localized mainly to the cell body, as expected for Golgi proteins; (2) NHE5 and NHE9 may localize to synaptic vesicles, more likely to non-glutamatergic ones, displaying colocalization with synaptophysin and slight colocalization with GFP-VGLUT1; (3) NHE6 may localize to synaptic vesicles, likely glutamatergic ones, displaying extensive colocalization with GFP-VGLUT1.

NHE6 is thus the only NHE isoform studied that displayed significant colocalization with VGLUT1. Its targeting to early endosomes (Nakamura et al 2005) which derive from the plasma membrane further renders it a likely isoform to be localized to synaptic vesicles, specialized organelles that also recycle from the plasma membrane. Moreover, its expression is most enriched in the brain, followed by the heart and skeletal muscle (Numata et al 1998), making it a strong candidate for synaptic vesicle localization. Because NHE6 and NHE9 display overlapping localization in neurons, both may reside in glutamatergic vesicles, either on the same vesicles, or on different vesicles at the same synapses.

3.5 ACKNOWLEDGMENTS

I thank Dr. John Orlowski and Dr. James Melvin for their kind gifts of the NHE-expression plasmids, and Haiyan Li and Venu Nemani for preparing the transfected hippocampal cultures.

3.6 REFERENCES

Bookstein C, Musch MW, DePaoli A, Xie Y, Rabenau K, et al. 1996. Characterization of the rat Na+/H+ exchanger isoform NHE4 and localization in rat hippocampus. *Am J Physiol* 271:C1629-38

Bookstein C, Musch MW, DePaoli A, Xie Y, Villereal M, et al. 1994. A unique sodium-hydrogen exchange isoform (NHE-4) of the inner medulla of the rat kidney is induced by hyperosmolarity. *J Biol Chem* 269:29704-9

Chambrey R, Achard JM, Warnock DG. 1997. Heterologous expression of rat NHE4: a highly amiloride-resistant Na+/H+ exchanger isoform. *Am J Physiol* 272:C90-8

Hill JK, Brett CL, Chyou A, Kallay LM, Sakaguchi M, et al. 2006. Vestibular hair bundles control pH with (Na+, K+)/H+ exchangers NHE6 and NHE9. *J Neurosci* 26:9944-55

Li H, Waites CL, Staal RG, Dobryy Y, Park J, et al. 2005. Sorting of vesicular monoamine transporter 2 to the regulated secretory pathway confers the somatodendritic exocytosis of monoamines. *Neuron* 48:619-33

Nakamura N, Tanaka S, Teko Y, Mitsui K, Kanazawa H. 2005. Four Na+/H+ exchanger isoforms are distributed to Golgi and post-Golgi compartments and are involved in organelle pH regulation. *J Biol Chem* 280:1561-72

Numata M, Orlowski J. 2001. Molecular cloning and characterization of a novel (Na+,K+)/H+ exchanger localized to the trans-Golgi network. *J Biol Chem* 276:17387-94

Numata M, Petrecca K, Lake N, Orlowski J. 1998. Identification of a mitochondrial Na+/H+ exchanger. *J Biol Chem* 273:6951-9

Orlowski J. 1993. Heterologous expression and functional properties of amiloride high affinity (NHE-1) and low affinity (NHE-3) isoforms of the rat Na/H exchanger. *J Biol Chem* 268:16369-77

Orlowski J, Kandasamy RA, Shull GE. 1992. Molecular cloning of putative members of the Na/H exchanger gene family. cDNA cloning, deduced amino acid sequence, and mRNA tissue expression of the rat Na/H exchanger NHE-1 and two structurally related proteins. *J Biol Chem* 267:9331-9

Szabo EZ, Numata M, Shull GE, Orlowski J. 2000. Kinetic and pharmacological properties of human brain Na(+)/H(+) exchanger isoform 5 stably expressed in Chinese hamster ovary cells. *J Biol Chem* 275:6302-7

Szaszi K, Paulsen A, Szabo EZ, Numata M, Grinstein S, Orlowski J. 2002. Clathrin-mediated endocytosis and recycling of the neuron-specific Na+/H+ exchanger NHE5 isoform. Regulation by phosphatidylinositol 3'-kinase and the actin cytoskeleton. *J Biol Chem* 277:42623-32

Yu FH, Shull GE, Orlowski J. 1993. Functional properties of the rat Na/H exchanger NHE-2 isoform expressed in Na/H exchanger-deficient Chinese hamster ovary cells. *J Biol Chem* 268:25536-41

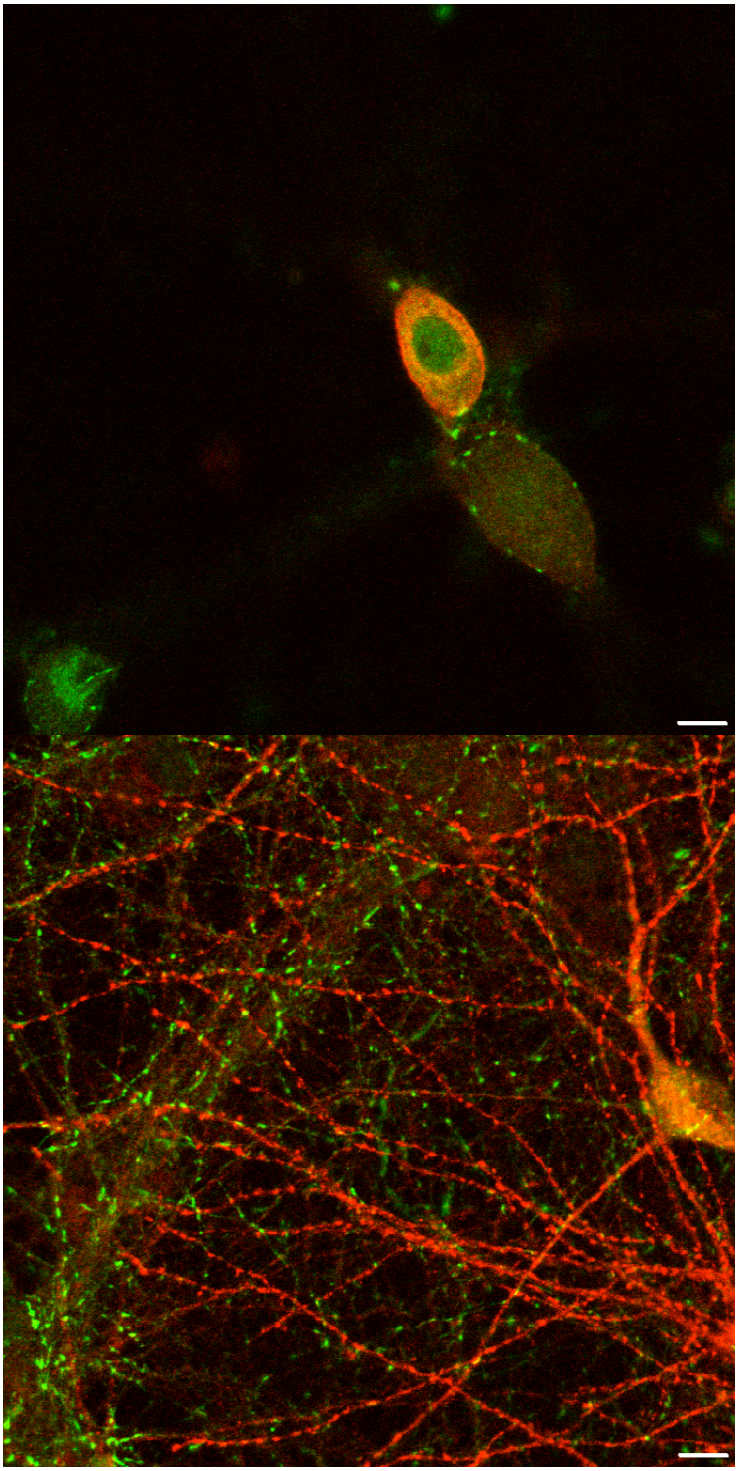

Figure 3-1. rNHE3-HA localizes to the plasma membrane and dendrites, not to synapses. rNHE3-HA is stained in red, and GFP-VGLUT1 in green. No colocalization between the two proteins is observed. rNHE3-HA localizes predominantly to the plasma membrane at the cell body (*top*), and also in punctate structures in proximal dendrites (*bottom*). GFP-VGLUT1 can be seen in puncta around the cell body, likely at the terminals of axosomatic release sites (*top*). Scale bars represent 10 μm.

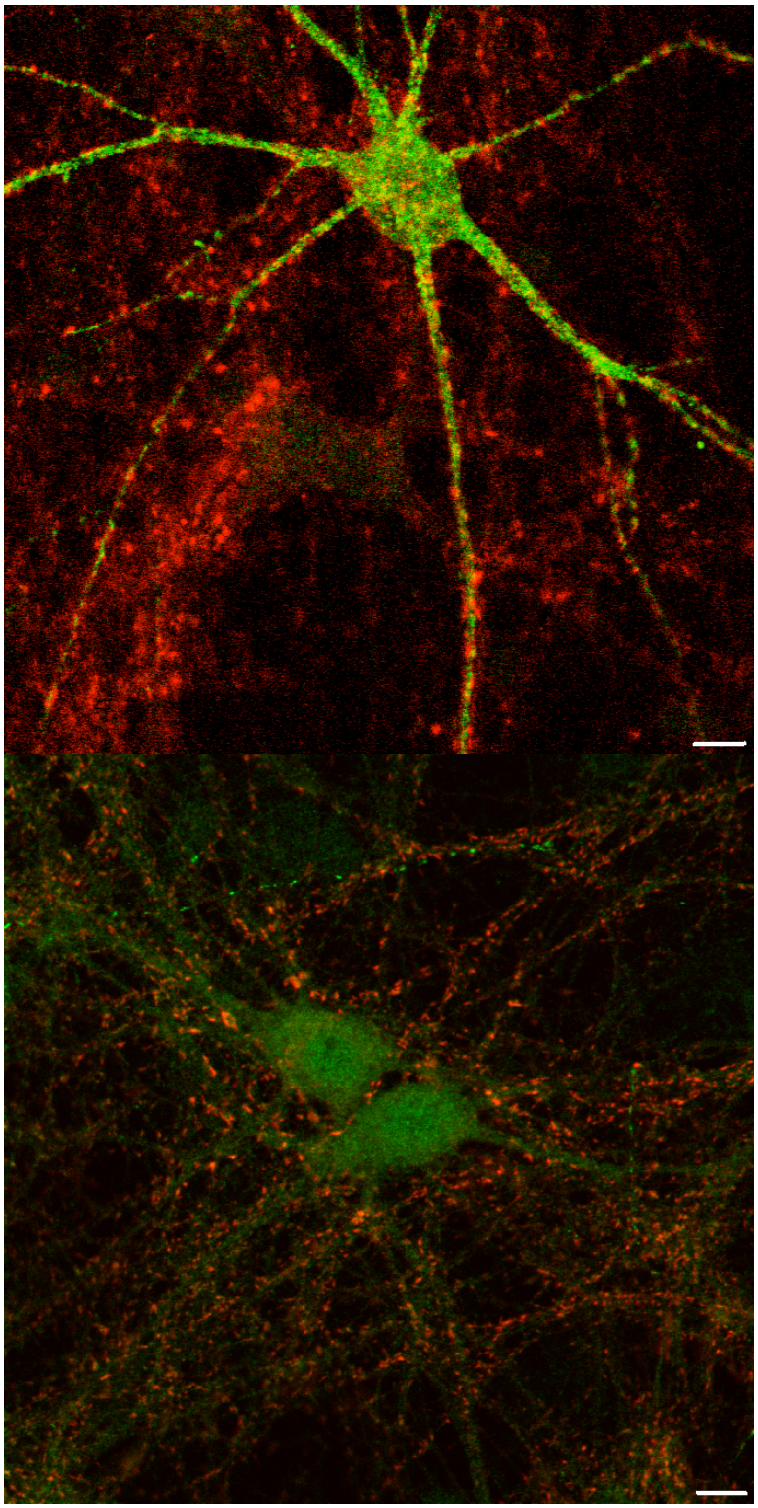

Figure 3-2. hNHE7-myc localizes mainly to the cell body, not to synapses.
hNHE7-myc is stained in green, and synaptophysin (*top* panel) and VGLUT1 (*bottom* panel) in red. No colocalization of hNHE7-myc with either protein is observed. hNHE7-myc is found mainly in intracellular structures in the cell body and proximal dendrites. Scale bars represent 10 μm.

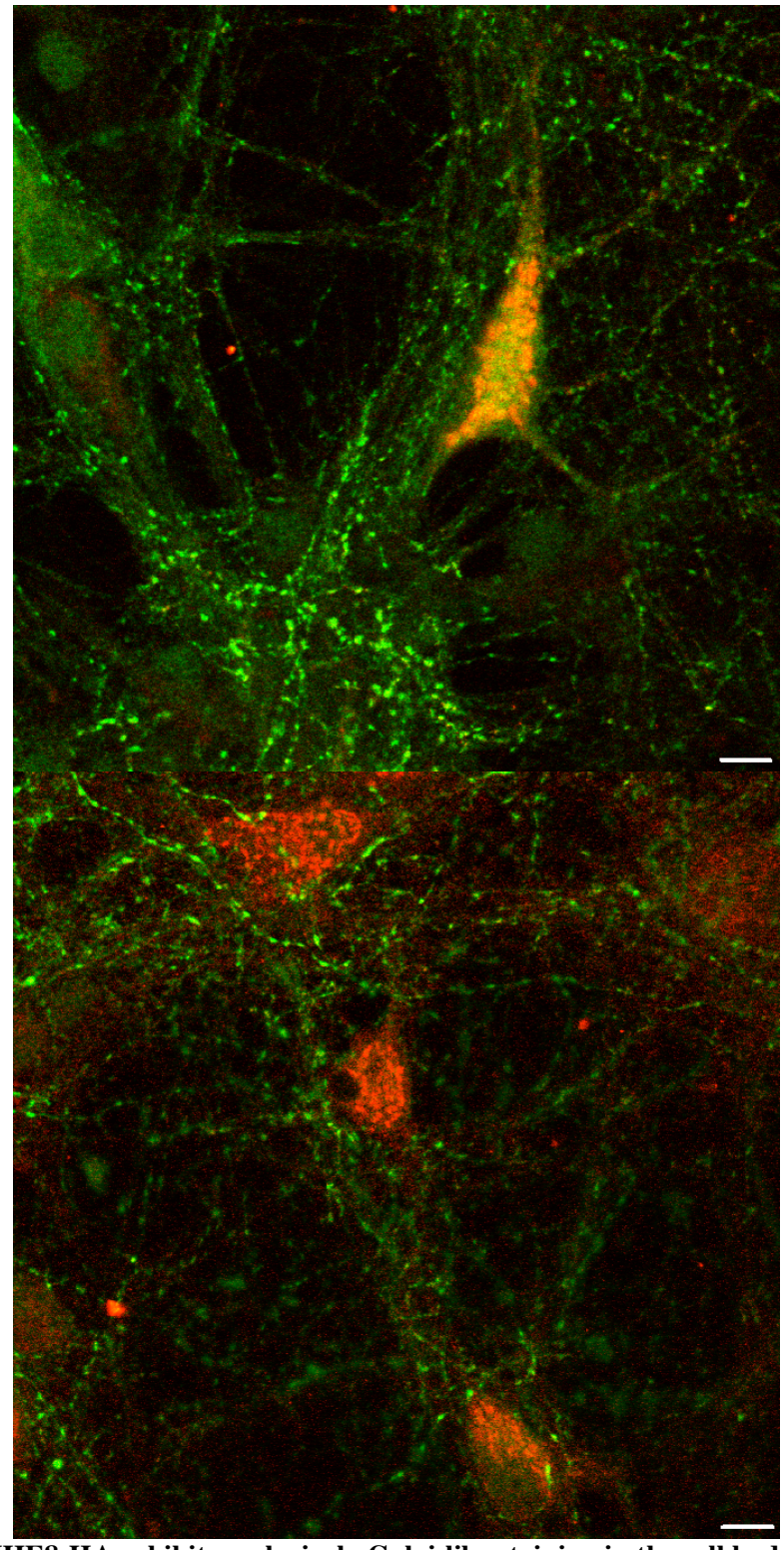

Figure 3-3. hNHE8-HA exhibits exclusively Golgi-like staining in the cell body.
hNHE8-HA is stained in red, and GFP-VGLUT1 in green. No colocalization between the two proteins is observed. hNHE8-HA localizes almost exclusively to the cell body. Scale bars represent 10 μm.

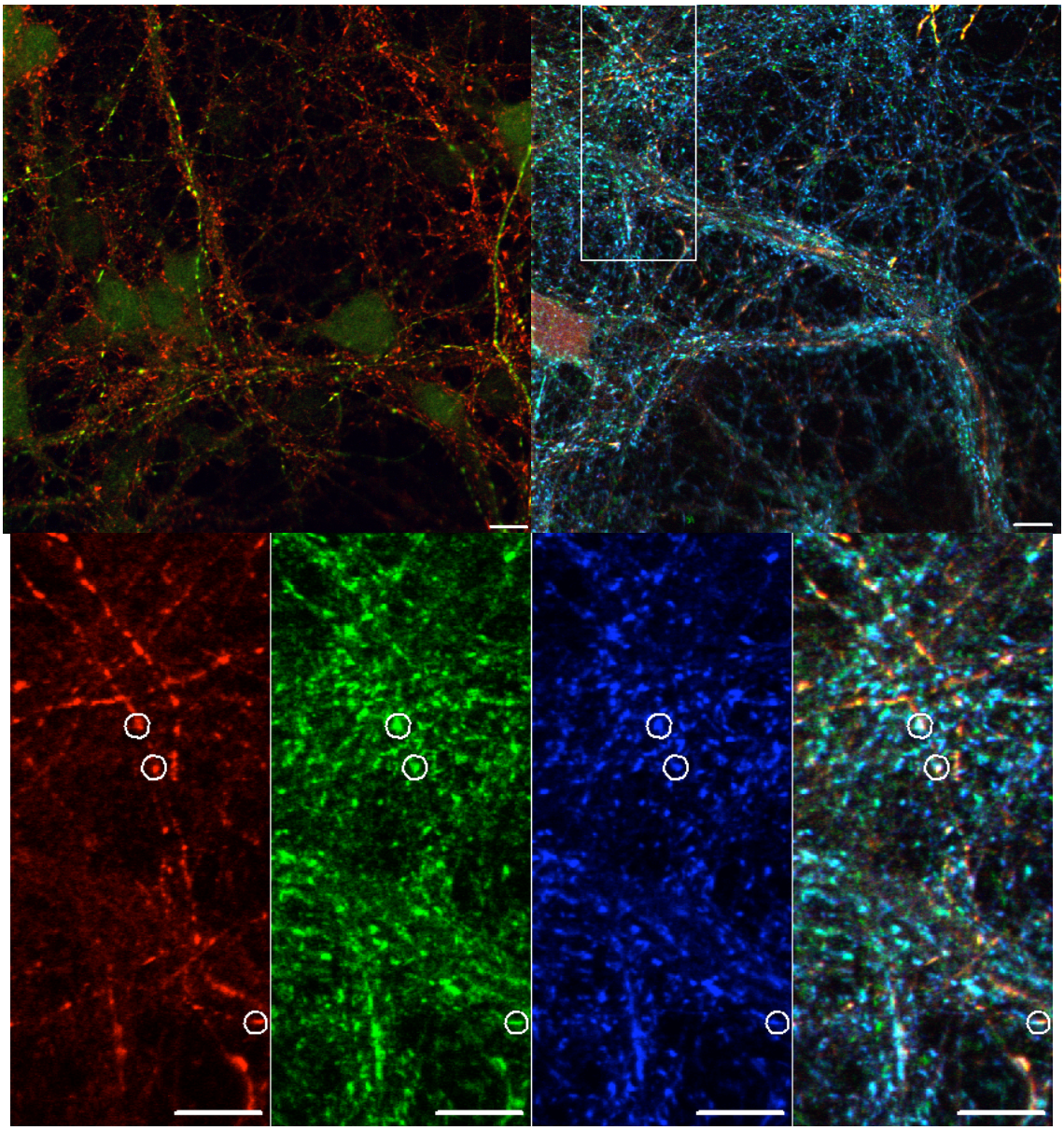

Figure 3-4. Some hNHE5-HA localizes to a subset of synapses.
hNHE5-HA is stained in red, synaptophysin in green, and VGLUT1 in blue. hNHE5-HA displays punctate localization. *Bottom* panel is a higher magnification of the boxed area in the *top right* panel, demonstrating puncta with all three proteins present, indicated by circles. hNHE5-HA colocalizes with synaptophysin, and to a slight extent with VGLUT1. Scale bars represent 10 μm.

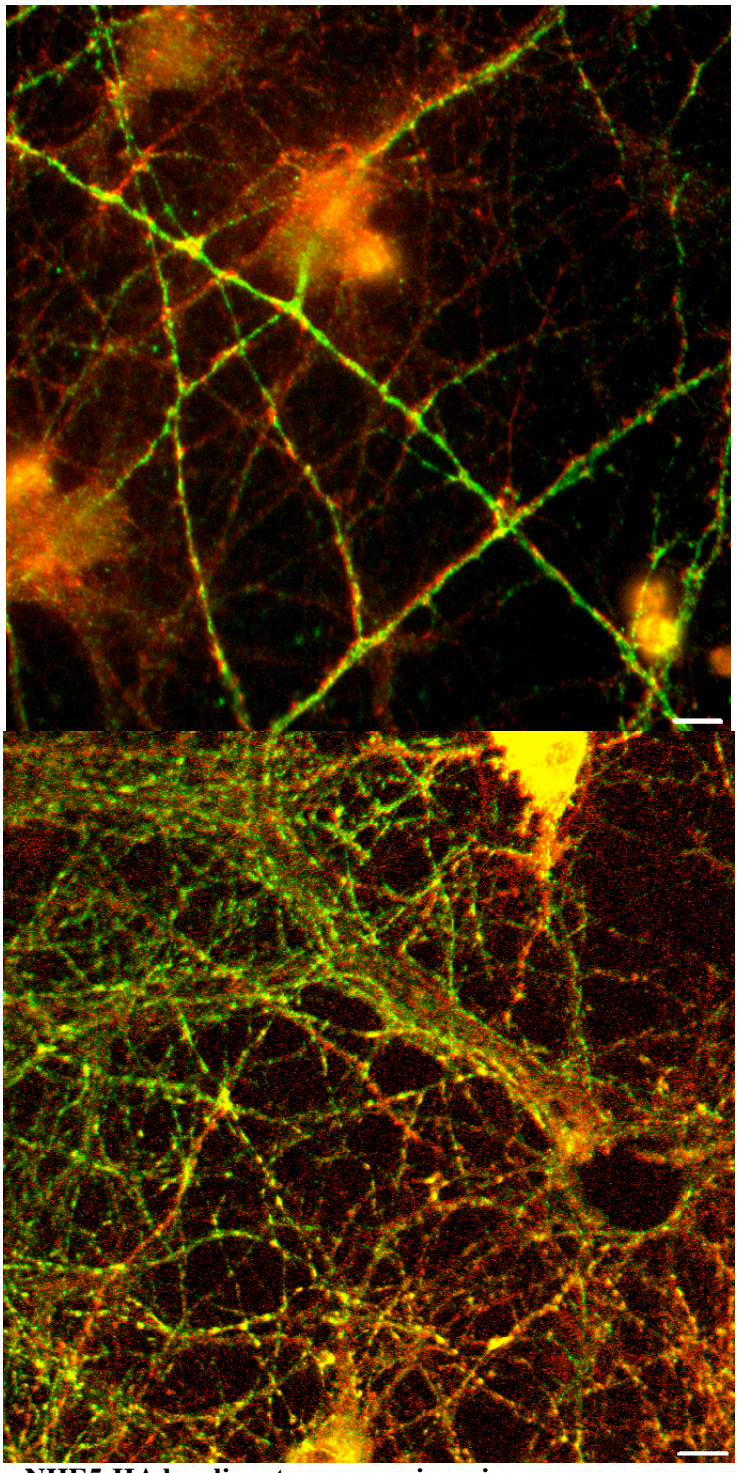

Figure 3-5. Some rNHE5-HA localizes to monoaminergic synapses.
Top: rNHE5-HA is stained in green, and synaptophysin in red. *Bottom*: rNHE5-HA is stained in red, and GFP-VMAT2 in green. rNHE5-HA displays somewhat punctate localization, colocalizing with both synaptophysin and GFP-VMAT2 to a large extent. Scale bars represent 10 μm.

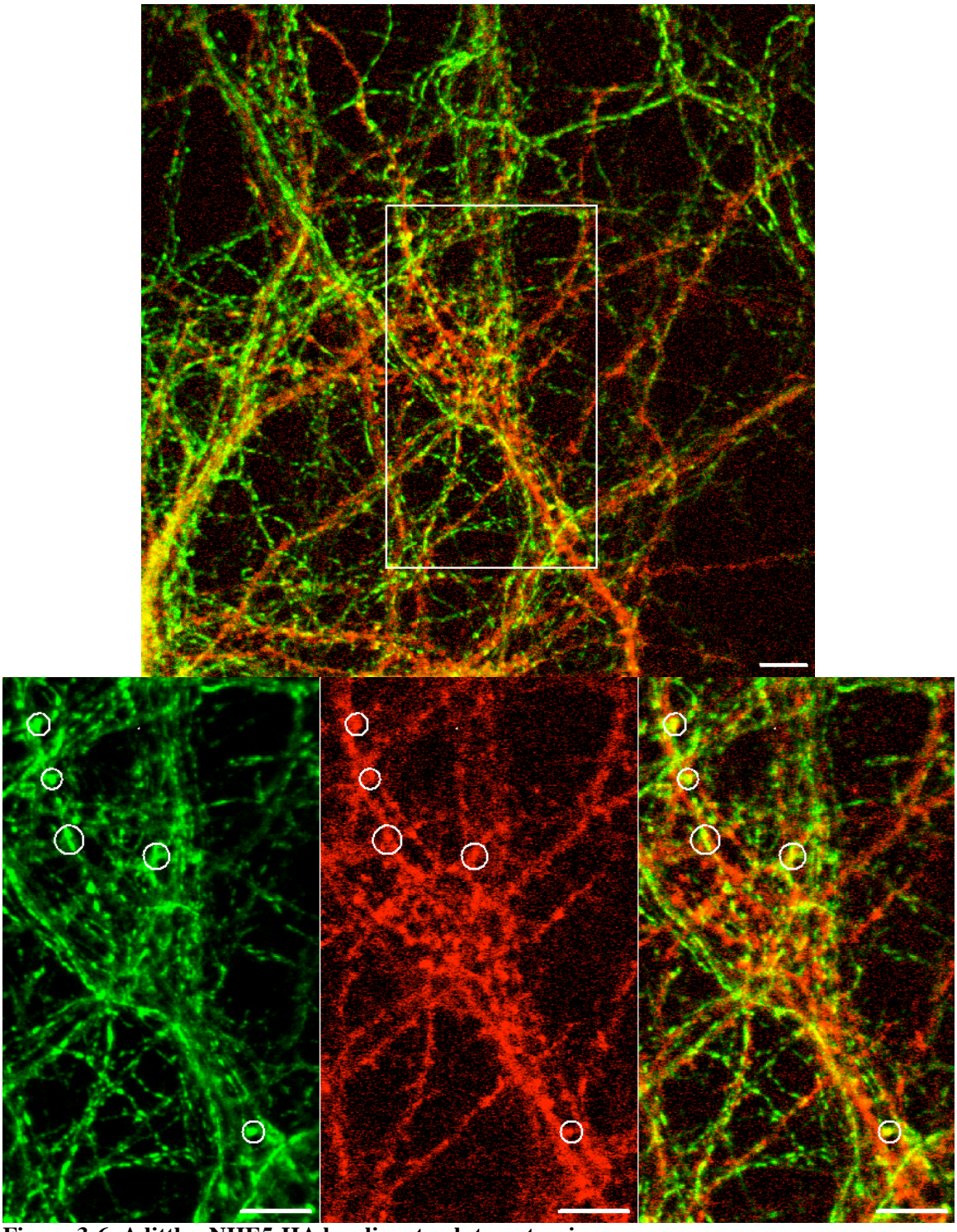

Figure 3-6. A little rNHE5-HA localizes to glutamatergic synapses.
rNHE5-HA is stained in red, and GFP-VGLUT1 in green. rNHE5-HA displays somewhat punctate localization, colocalizing with GFP-VGLUT1 only to a slight extent. *Bottom* panel is a higher magnification of the boxed area in the *top* panel, demonstrating puncta with both proteins present, indicated by circles. Scale bars represent 10 μm.

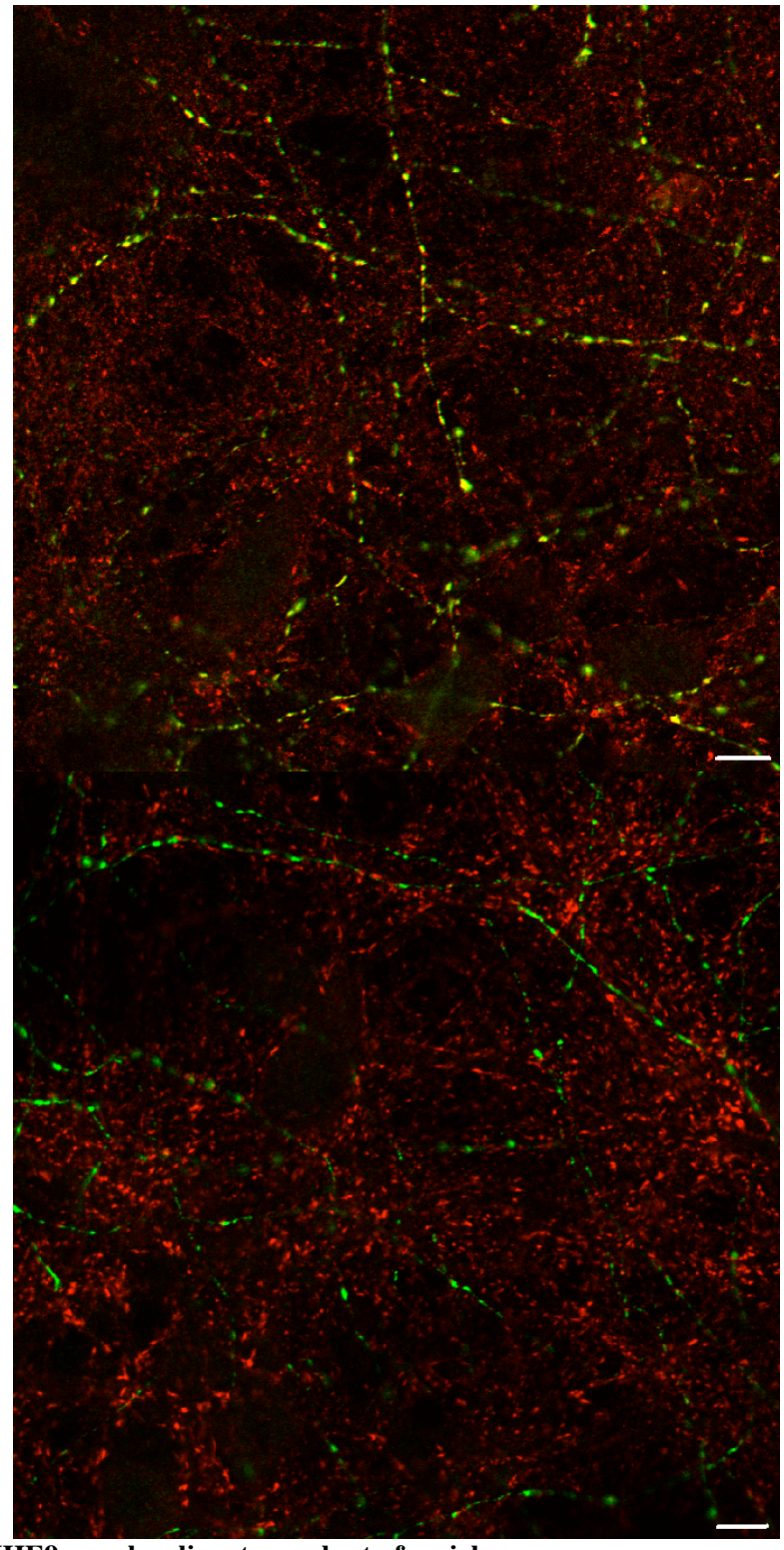

Figure 3-7. hNHE9-myc localizes to a subset of vesicles.
hNHE9-myc is stained in green, and synaptophysin (*top*) and VGLUT1 (*bottom*) in red. hNHE9-myc displays punctate localization, colocalizing with synaptophysin but not VGLUT1. Scale bars represent 10 μm.

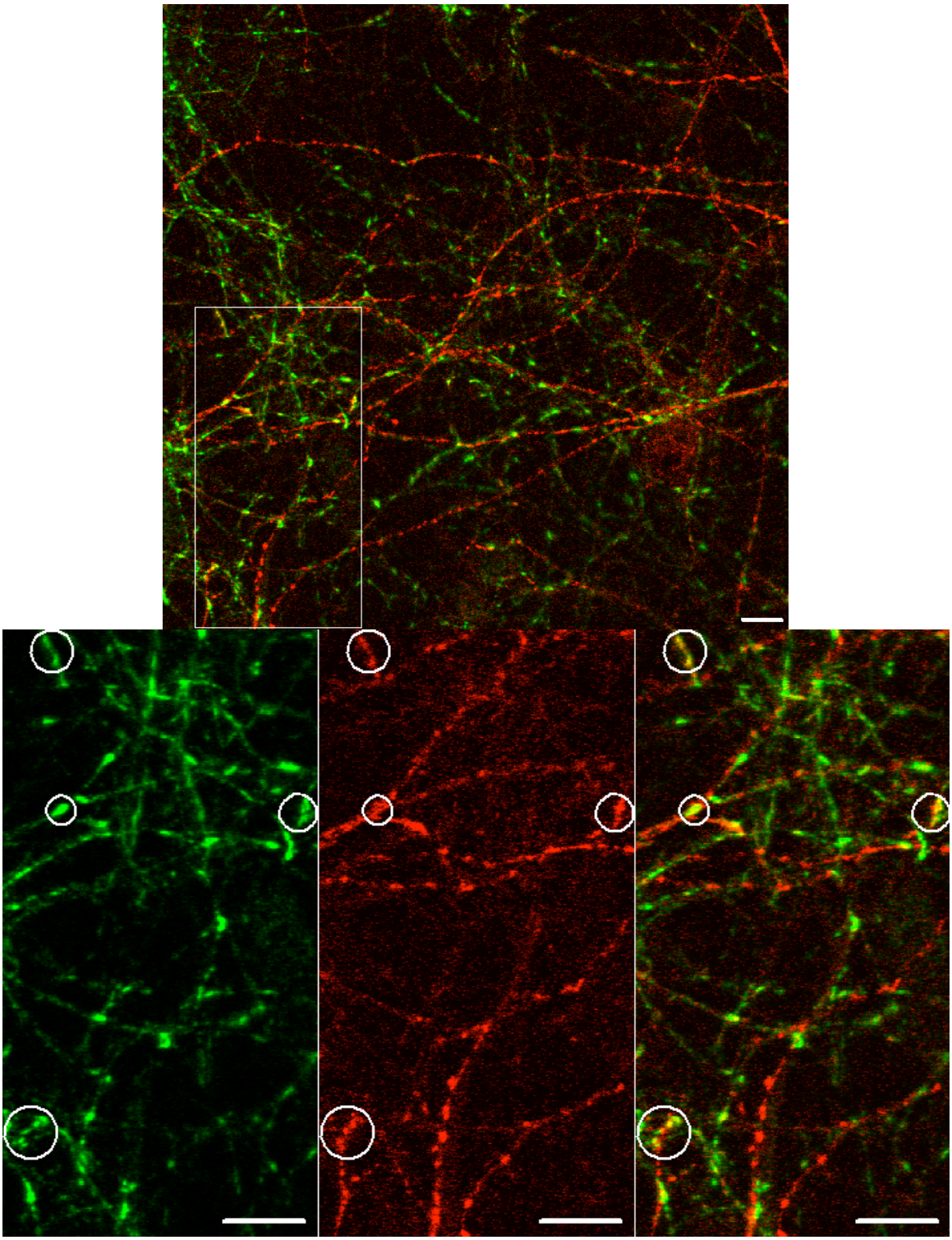

Figure 3-8. A little hNHE9-myc colocalizes with GFP-VGLUT1.
hNHE9-myc is stained in red, and GFP-VGLUT1 in green. hNHE9-myc displays punctate localization, colocalizing to a slight extent with GFP-VGLUT1. *Bottom* panel is a higher magnification of the boxed area in the *top* panel, demonstrating puncta with both proteins present, indicated by circles. Scale bars represent 10 μm.

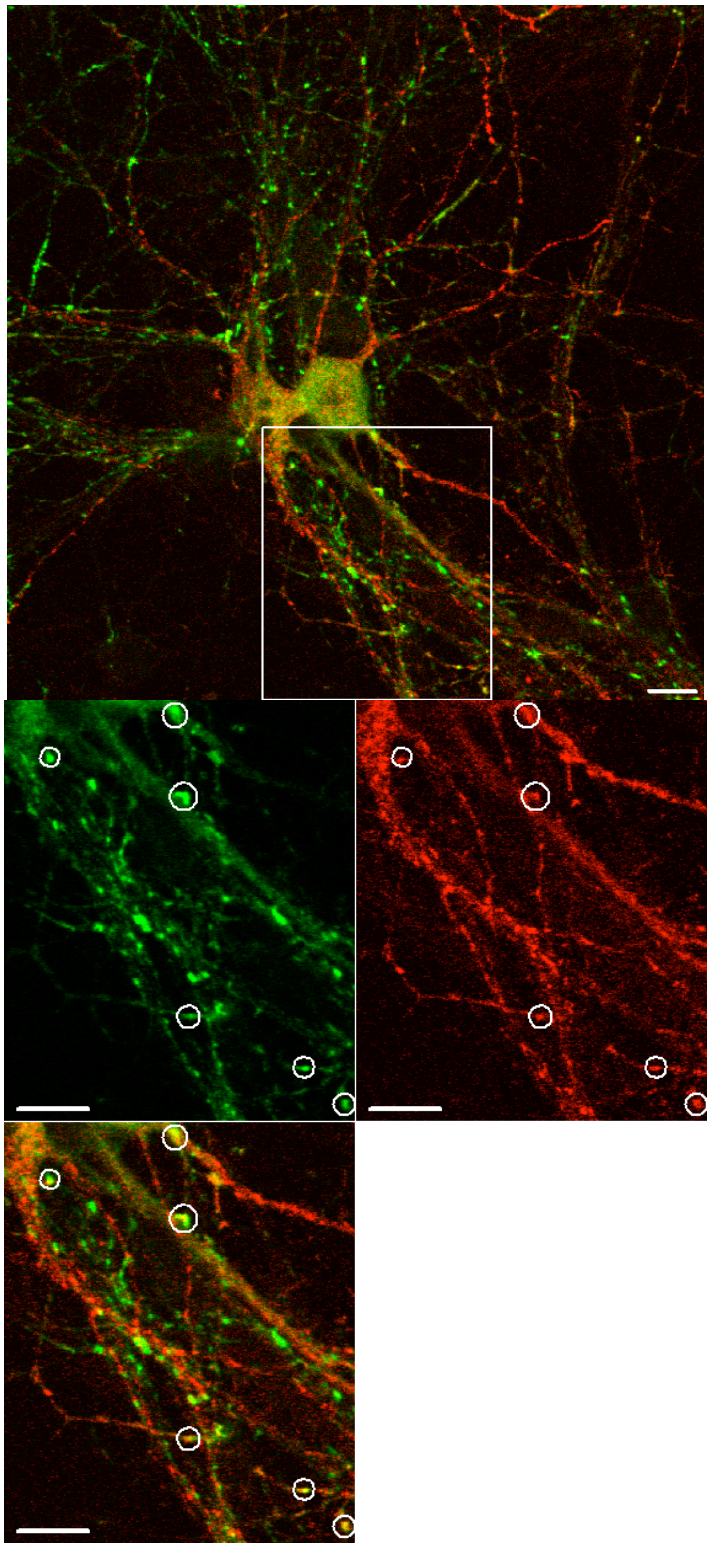

Figure 3-9. A little hNHE9-myc colocalizes with GFP-VGLUT1.
Staining of hNHE9-myc and GFP-VGLUT is as described in Figure 3-8. *Bottom* panel is a higher magnification of the boxed area in the *top* panel, demonstrating puncta with both proteins present, indicated by circles. Scale bars represent 10 μm.

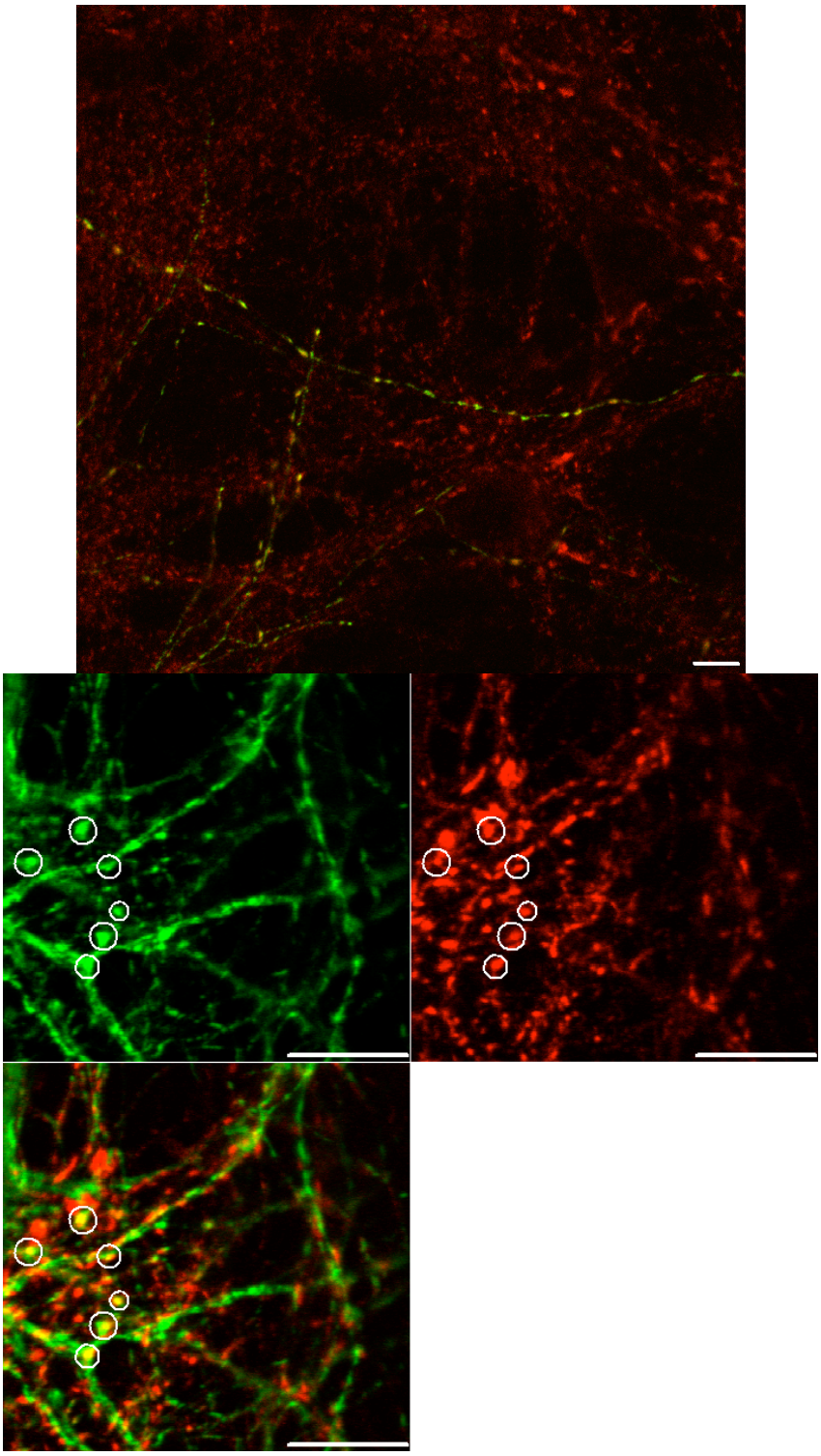

Figure 3-10. Some hNHE6-HA localizes to glutamatergic synaptic vesicles.
Top: hNHE6-HA is stained in green, and synaptophysin in red. *Bottom*: hNHE6-HA in stained in red, and GFP-VGLUT1 in green. hNHE6-HA displays punctate localization, colocalizing well with synaptophysin and to a lesser extent with VGLUT1. Scale bars represent 10 μm.

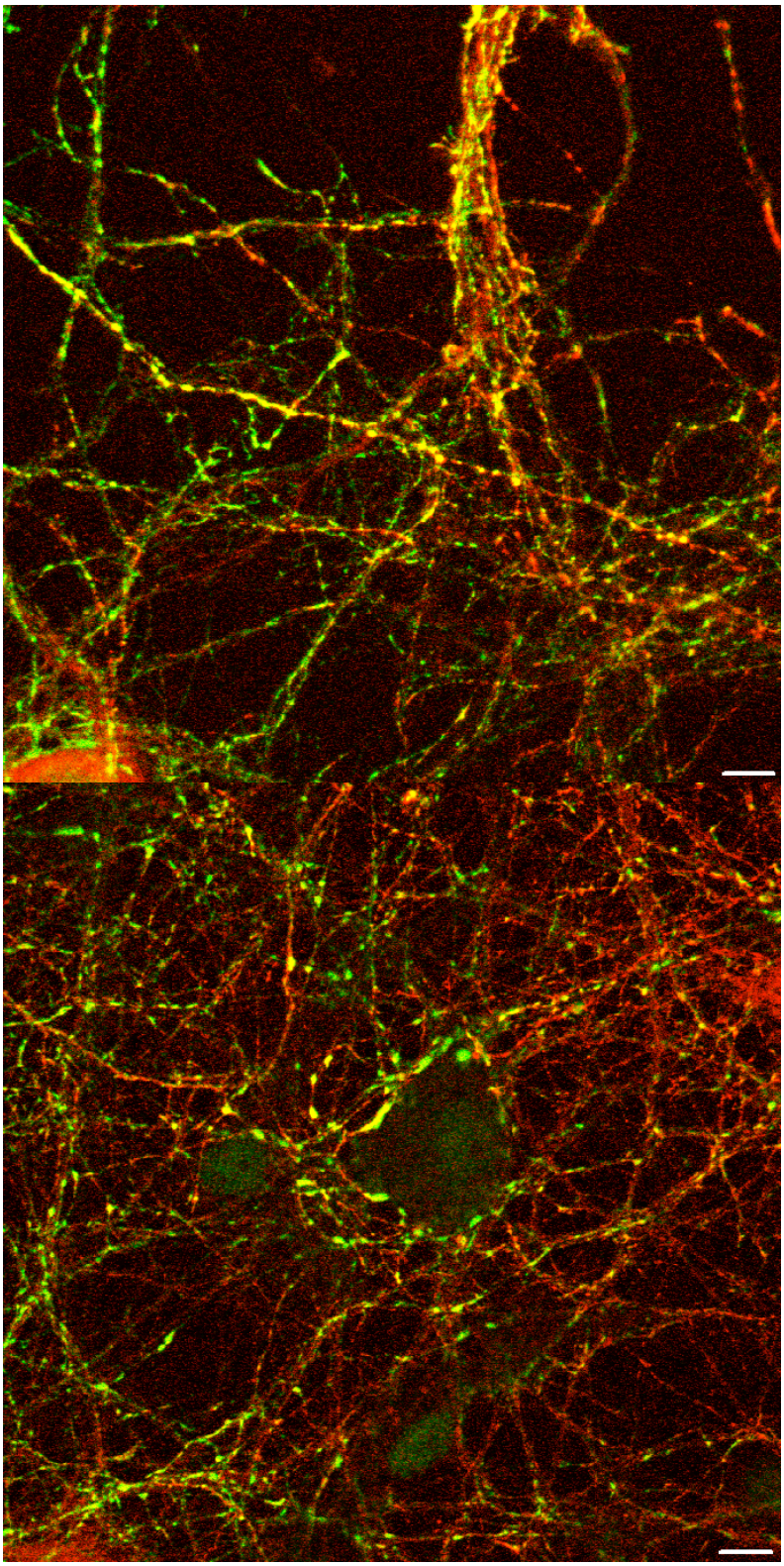

Figure 3-11. hNHE6-HA colocalizes well with GFP-VGLUT1.
hNHE6-HA is stained in red, and GFP-VGLUT1 in green. hNHE6-HA displays punctate localization, colocalizing to a large extent with GFP-VGLUT1. Scale bars represent 10 μm.

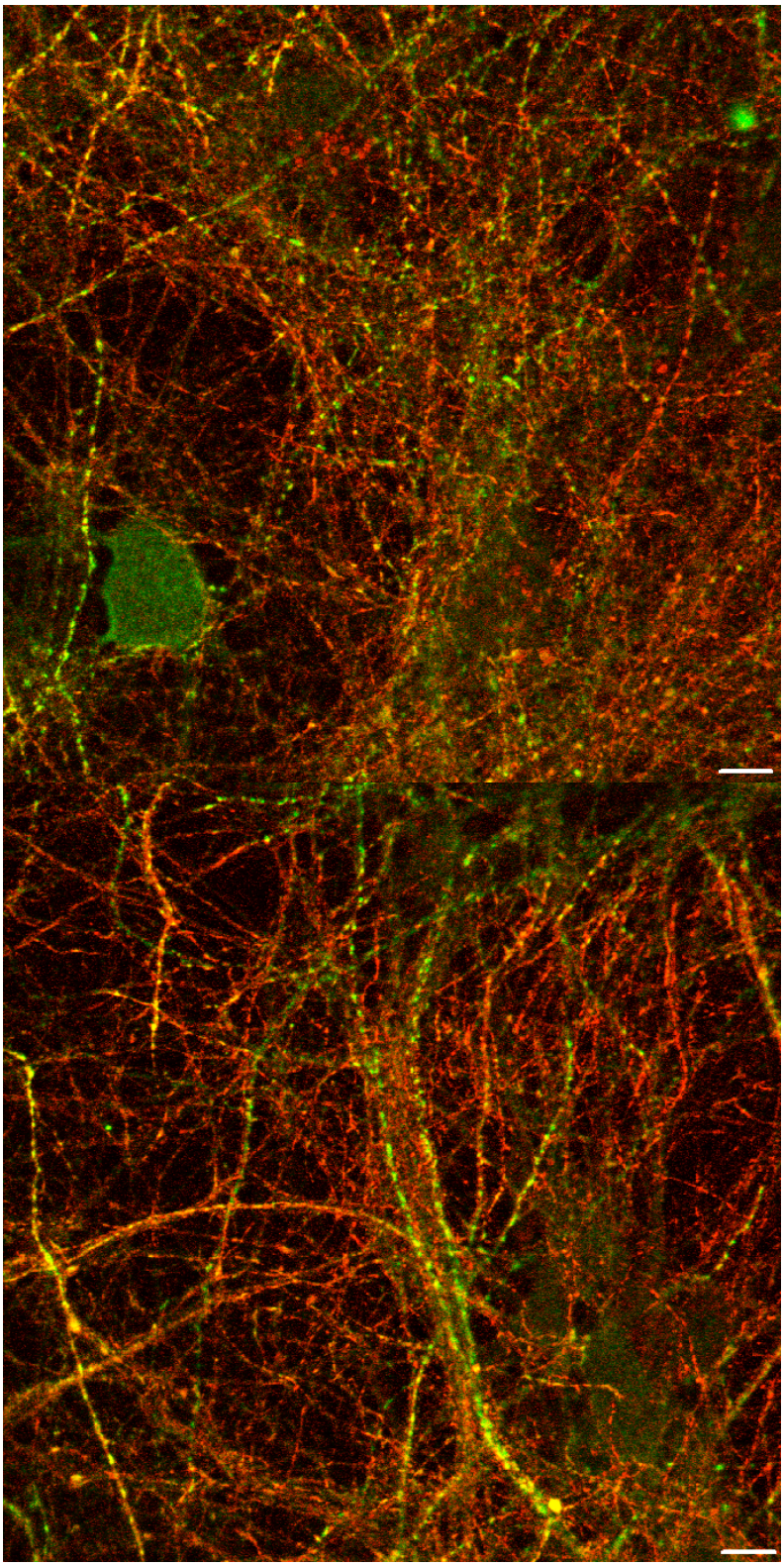

Figure 3-12. hNHE6-HA and hNHE9-myc partially colocalize in neurons.
hNHE6-HA is stained in red, and hNHE9-myc in green. Both display punctate localization, colocalizing well in some processes. Scale bars represent 10 μm.

Chapter 4. Summary, Perspectives and Future Directions

4.1 SUMMARY

The regulation of quantal size is a factor contributing to the strength of a synapse and hence to the robustness of signaling between neurons. The basic unit of synaptic transmission is thus a fundamental determinant of the function of the nervous system, which hinges on the intricately complex networks of communication between neurons. Many studies have focused on postsynaptic events that affect quantal size, such as the regulation of postsynaptic neurotransmitter receptors by phosphorylation, interactions with other proteins, and surface trafficking, but there has arisen evidence that factors in the presynaptic terminal, especially those that determine the amount of transmitter in the synaptic cleft, can also influence quantal size. These include the vesicular release mode, biosynthesis and metabolism of transmitters, vesicle size variation, and vesicular neurotransmitter transporter expression level.

The driving force for neurotransmitter transport into synaptic vesicles by their respective vesicular transporters is a major factor in determining the amount of transmitter packaged into the vesicles. In the case of monoaminergic vesicles, a chloride conductance allows the generation (and regeneration) of ΔpH to allow monoamine uptake. We wondered whether in glutamatergic vesicles, an analogous mechanism exists to promote $\Delta\psi$ for continued glutamate uptake, hence we proceeded to measure ion fluxes across synaptic vesicles, and their consequences on glutamate uptake.

Cation/H^+ Exchange Increases Glutamate Uptake into Synaptic Vesicles and hence Quantal Size

Considering a list of possible ways in which vesicles could decrease their ΔpH to promote formation of $\Delta\psi$ by the V-ATPase, we hypothesized that cation/proton exchange would be a particularly elegant mechanism to alter the $\Delta pH/\Delta\psi$ balance. We thus measured ΔpH in real time across synaptic vesicles isolated from rat brain, using the fluorescent amine acridine orange. In this assay, we found that a pre-imposed outwardly-directed Na^+-gradient across the synaptic vesicles drives the acidification of the vesicular lumen. We concluded from its insensitivity to H^+ ionophore CCCP and sensitivity to NHE inhibitor EIPA that this phenomenon is independent of $\Delta\psi$ and reflects electroneutral cation/proton exchange. Consistent with intracellular NHEs, it also recognizes Li^+, and K^+ with low affinity. We further ruled out a channel mechanism by demonstrating the probable lack of a substantial K^+ conductance in our vesicles. To better define the subpopulation of vesicles in which we were interested, we functionally selected for glutamatergic vesicles by driving acidification with ATP and glutamate, in the same acridine orange assay. We then tested again for the ability of monovalent cations to alkalinize these vesicles specifically acidified with glutamate, and found that the same exchange activity is indeed present on glutamatergic vesicles. Finally, we tested

our hypothesis that cation/proton exchange, by reducing the ΔpH in the presence of an active V-ATPase, should increase the Δψ. We measured Δψ across synaptic vesicles using the ratiometric fluorophore oxonol VI and found that indeed, the addition of K^+ increases synaptic vesicle Δψ, and its interaction with NH_4^+ supports that its effect is due to decrease of ΔpH.

Having demonstrated cation/proton exchange activity on glutamatergic vesicles, we next used radiolabeled glutamate to test the effect of potassium on glutamate uptake into synaptic vesicles. As would be predicted with an increase of Δψ, the presence of potassium stimulates glutamate uptake into synaptic vesicles, compared to a choline control. This stimulation is not due to a direct effect on VGLUT, but rather increases over time, supporting an effect on the thermodynamic driving force of uptake, which would be expected to weaken over time and hence benefit more from cation/proton exchange. Consistent with the results in the acridine orange assay, Na^+ and Li^+ also stimulate glutamate uptake, and consistent with the results in the oxonol VI assay, the stimulatory effects of K^+ and NH_4^+ on glutamate uptake are mutually occlusive. As a proof of principle, we demonstrated that glutamate uptake is stimulated in the presence of the ionophore nigericin, a K^+/H^+ exchanger, but not valinomycin, a K^+ channel, suggesting that a channel mechanism is ineffective at stimulating glutamate uptake.

To test the physiological relevance of our *in vitro* results, we performed paired electrophysiological recordings at the calyx of Held, a giant central auditory glutamatergic synapse. We dialyzed the presynaptic terminal with either K^+-rich or $NMDG^+$-rich solutions and measured the resultant miniature excitatory postsynaptic currents (mEPSCs) on the postsynaptic terminal. The mEPSCs are responses to spontaneous release of single synaptic vesicles and reflect the amount of glutamate released, which in turn reflects the amount of glutamate packaged into the synaptic vesicles. In remarkable quantitative corroboration with our *in vitro* findings, K^+ causes ~70% larger mEPSC amplitudes compared to $NMDG^+$.

We next studied $^{22}Na^+$ uptake to directly demonstrate cation/proton exchange across glutamatergic vesicles, and then used the assay and the available pharmacology to characterize the proteins responsible. We first showed that glutamate-acidified vesicles accumulate more $^{22}Na^+$ compared to aspartate control, confirming that Na^+/H^+ exchange indeed occurs on glutamatergic vesicles, and that the $^{22}Na^+$ entry is ΔpH-driven. The inhibition of $^{22}Na^+$ uptake by V-ATPase inhibitor Bafilomycin A1, VGLUT inhibitor Evans Blue, and NHE inhibitor EIPA support the hypothesis that formation of ΔpH by the V-ATPase, together with VGLUT, drives uptake through an NHE. A further dose-response to EIPA and amiloride demonstrate high sensitivity to EIPA and less to amiloride, characteristic of NHEs. On the other hand, general Na^+ and K^+ channel blockers tetrodotoxin and tetraethylamine, as well as non-selective TRP channel blockers ruthenium red and 2-APB all have no specific effect on glutamate-dependent $^{22}Na^+$ uptake, further arguing against the role of a channel in this phenomenon. With this pharmacological data, we tested the sensitivity of cation-stimulated glutamate uptake to

EIPA and found that indeed, increasing amounts of EIPA (15, 30 and 50 μM) progressively inhibit the stimulation of glutamate uptake by 20 mM Na^+, in good agreement with the other pharmacological data in the study.

We thus strongly favor the hypothesis that an NHE is present on glutamatergic synaptic vesicles and is responsible for cation/proton exchange-dependent stimulation of glutamate uptake.

Colocalization Studies and Pharmacology Implicate an NHE

There are nine mammalian isoforms of NHE, at least six of which demonstrate some intracellular localization. To obtain molecular clues to the identity of the NHE that may reside in synaptic vesicles, we studied the synaptic localization of epitope-tagged NHEs transfected into primary hippocampal cultures. Our results indicate that NHEs 5, 6, and 9 all exhibit some extent of localization to synapses, but NHE6 does so most extensively, especially with co-transfected VGLUT1, and is thus a leading candidate.

4.2 PERSPECTIVES

A Presynaptic Mechanism of Quantal Size Regulation

This study illustrates a novel mode of presynaptic regulation of quantal size – the modulation of the driving force for glutamate transport by cation/proton exchange. In many ways, the mechanism of glutamate transport into synaptic vesicles is still poorly understood. The stoichiometry of transport is still unknown, and the effects of chloride on the transport and the transporter are still debated. However, its strong dependence on $\Delta\psi$ is clear, and here we have found a mechanism that maintains $\Delta\psi$ to drive glutamate transport.

Regulation by intracellular K^+ concentration

This mechanism could potentially be leveraged *in vivo* to regulate glutamate uptake. Our data demonstrate that the stimulation of glutamate uptake by potassium increases linearly with potassium concentration, consistent with a thermodynamic effect. Kinetic characterization also indicates that the K^+ carrier is not saturated at physiological concentrations, thus possibly providing a point of regulation. The intracellular potassium concentration is not generally thought to vary *in vivo*, though some observations indicate that it may: (i) Photostimulation of leech photoreceptors induced a decrease of 10 mM in intracellular potassium (Walz 1985); (ii) Intracellular potassium content in primary astrocytes increased by 63% within 50 s when extracellular potassium was raised from 3 to 12 mM (Walz & Hinks 1985); (iii) Activation of $K_v1.3$ channels in neuronal spine-like structures formed out of CHO cell membranes by electrode suction causes rapid depletion of potassium in the restricted compartment (Wang et al 1998), providing evidence for

compartmentalized ionic transients and raising the possibility that such localized ionic fluctuations also occur in axonal boutons. Although these are non-neuronal cells, this data suggests possible similar variations in neuronal cytoplasmic potassium concentration. Admittedly, the linear dose response of glutamate uptake to K^+ concentration renders small fluctuations in K^+ concentration unlikely to have large effects on glutamate uptake, although the possibility of ultra-fine transmitter concentration tuning cannot be discounted, since glutamate receptors, especially extrasynaptic ones, can be sensitive to fluctuations in extracellular glutamate concentration.

Regulation by NHE trafficking

Perhaps a more likely system of regulation of this mechanism is the regulation of NHE trafficking to the synaptic vesicle. A possible scenario is the trafficking of NHE to specific subsets of synaptic vesicles, which can be differentiated by cell, synapse, functional pool (such as the readily releasable, recycling, or reserve pools), or neurotransmitter contained, as mentioned in Chapter 3. Indeed, NHE trafficking between intracellular compartments and the cell surface has been shown to be dependent on a variety of proteins including clathrin (Chow et al 1999), caveolin (Lin et al 2007), β-arrestin (Szabo et al 2005), phosphatidylinositol-3 kinase and F-actin (Szaszi et al 2002), receptor for activated C kinase 1 (RACK1) (Ohgaki et al 2008; Onishi et al 2007), and secretory carrier membrane proteins (SCAMPs) (Diering et al 2009; Lin et al 2005). The SCAMPs are of particular interest because SCAMP1, 3 and 5 are synaptic vesicle proteins (Takamori et al 2006), with SCAMP1 and 5 particularly enriched at synaptic vesicles (Fernandez-Chacon & Sudhof 2000), raising the likelihood that an NHE traffics to synaptic vesicles via interaction with a SCAMP.

Although little is known about the physiological functions of the intracellular NHEs, some insights can be gathered from Nhx1p, the yeast ortholog of mammalian NHEs 6, 7 and 9. Nhx1p contributes to Na^+ resistance by sequestering Na^+ into an endosomal/prevacuolar compartment (Nass et al 1997), and also sequesters K^+ (Brett et al 2005). Null or functionally-inactive mutants result in acidification and trafficking defects (Brett et al 2005), abnormal prevacuolar morphology and protein missorting (Bowers et al 2000). This suggests a possible intriguing function of Na^+/H^+ exchangers not just as regulators of endosomal pH, but as regulators of membrane trafficking. Finally, Nhx1p is negatively regulated by Gyp6, a GTPase activating protein for Ypt6 which is implicated in endosome to Golgi membrane trafficking (Ali et al 2004). The NHE on a synaptic vesicle could similarly be functionally regulated by a similar protein, such that it is active and stimulates glutamate uptake only under certain conditions. Indeed, regulation of the activity of plasma membrane NHE1 is well studied, and involves phosphorylation as well as binding to regulatory molecules including calmodulin, calcineurin homologous protein (CHP), ezrin, radixin, and moesin (ERM), and PIP_2 (Malo & Fliegel 2006; Putney et al 2002). The cytosolic C-terminus of NHE6 leaves room for similarly diverse interactions.

Modulation of ΔΨ and ΔpH in Intracellular Organelles

Although the differential pH values of organelles in the endocytic and secretory pathways are well-characterized, the mechanisms underlying the variation are still unclear. ClC proteins are important in providing an ionic shunt to allow the generation of ΔpH in some compartments (Jentsch 2008), and we wondered if there exists an analogous mechanism that promotes generation of Δψ. Our finding that cation/proton exchange increases Δψ across synaptic vesicles which in turn stimulates glutamate transport raises the possibility that the NHEs, localized throughout the endosecretory pathways, may generally be important for enhancing Δψ-dependent transport processes in their respective organelles.

More speculatively, they may also be important in creating the milieus in which other Δψ-dependent processes occur. For example, the recent discovery of a voltage-sensing phosphatase, VSP, casts open a whole new area of physiology involving electrical to chemical transduction (Okamura et al 2009), and implicates novel modes of cellular signaling as yet unknown. Δψ has also been found to influence protein translocation across the membrane (Geller & Green 1989; Schuenemann et al 1999; van Dalen et al 1999), thus it could conceivably influence protein conformation and function even in mature endosecretory vesicles.

Finally, the synaptic vesicle NHE could also function in "reverse mode" where lumenal monovalent cation is exchanged for cytoplasmic protons, as in our sodium-loading experiments. Since synaptic vesicles recycle from the plasma membrane, they are likely to contain high concentrations of Na^+ after endocytosis, which will likely exchange for protons to acidify the vesicles. This could be stimulatory to processes that rely more on ΔpH, such as VMAT-mediated monoamine uptake, and may be especially useful, for example, when an anion shunt to facilitate net proton pumping is lacking.

4.3 FUTURE DIRECTIONS

RNA interference of NHE isoforms in neuronal cells

Since good isoform-specific antibodies are not readily available for all the NHE isoforms, RNA interference (RNAi) is a viable strategy to "screen" on a small scale several isoforms of NHEs. An experimental plan would be to knock down NHE expression in neuronal cultures, and measure the resultant mEPSC amplitudes, which should reflect neurotransmitter uptake into synaptic vesicles. The advantage of this technique is that in the case of redundancy or compensatory upregulation, multiple isoforms could concurrently be knocked down with relative ease, compared to generating a double-knockout mouse. The effects on release of different neurotransmitters could also potentially be studied, by isolating neurons from different regions of the brain and further isolating the relevant neurotransmitter receptors by pharmacological inhibition of other receptors.

A disadvantage of this approach is that much optimization may be required to obtain near-100% transfection efficiencies in neurons, which is required because in dissociated cultures, it is onerous, if not practically impossible, to determine the sites that are post-synaptic to a transfected cell. Alternatively, autaptic cultures in which islands of single neurons synapse on themselves could be used. Another limitation of RNAi is that *in vitro* biochemical studies on isolated synaptic vesicles cannot be performed, because of the inhibitively limited yield of vesicles from neuronal cultures.

Knockout Mouse Models

Although not advisable as a first-pass method of screening isoforms, knockout mice for the NHE isoforms would be an ideal model in which to test the phenomenon as well as characterize any phenotypes resulting from the loss of the NHE, if the RNAi results give a good lead. Knockout mice for some intracellular isoforms are available commercially and would allow for a much larger scope of assays, biochemical as well as physiological and behavioral. For example, the direct effect of the absence of an NHE on glutamate transport can be better studied using *in vitro* assays described in this dissertation; Developmental studies characterizing any age-dependent phenomena can be performed; Any anatomical and functional deficits resulting from the loss of the NHE can also be characterized in the animal.

The drawbacks of knockout mouse models are, of course, the large expenses of time and cost, and the possibility of compensation by other members of the family. Indeed, a recent study of NHE6 in HeLa cells found that single knockdown of either NHE6 or NHE9 alone had no effect on endosomal acidification, and only double-knockdown of both isoforms resulted in enhanced acidification of early endosomes (Roxrud et al 2009). In the case of upregulation or redundancy, a combination of methods could be used, in which RNAi is performed in the background of the knockout, i.e. using cells cultured from the knockout.

Reconstitution and Characterization of NHE Characteristics

Once the molecular identity of the NHE in synaptic vesicles is determined, more detailed studies of its properties and mechanism of action would be instructive. A clean way to characterize the transport functions of a protein would be to reconstitute the purified protein in proteoliposomes. The compositions of the internal and external buffers can be well-controlled, and fluxes can be attributed to the protein with more certainty given the proper controls, the best being functionally-inactive mutants. Sequence homology of NHE members would allow such a strategy, since a transport-deficient NHE8 mutant has already been demonstrated (Nakamura et al 2005), based on studies of mutant NHE1 (Fafournoux et al 1994; Murtazina et al 2001). Taking the assay a step further, the NHE could be co-reconstituted with VGLUT, or possibly with VGLUT and a H^+-pumping ATPase, to simulate the *in vivo* situation without all other complicating factors.

Computational Modeling

Given the realistic situation of numerous transporters and thus fluxes occurring on the synaptic vesicle membrane, a useful approach might be to perform computational modeling of the relevant transport processes to consider all factors holistically in a systematic manner. This will give a more precise, controlled angle to the sometimes fuzzy processes of quantitation in biology. It should enable the comparison of predicted outcomes to known facts and help to eliminate or strengthen hypotheses, as well as furnish predictive insights.

4.4 REFERENCES

Ali R, Brett CL, Mukherjee S, Rao R. 2004. Inhibition of sodium/proton exchange by a Rab-GTPase-activating protein regulates endosomal traffic in yeast. *J Biol Chem* 279:4498-506

Bowers K, Levi BP, Patel FI, Stevens TH. 2000. The sodium/proton exchanger Nhx1p is required for endosomal protein trafficking in the yeast Saccharomyces cerevisiae. *Mol Biol Cell* 11:4277-94

Brett CL, Tukaye DN, Mukherjee S, Rao R. 2005. The yeast endosomal Na+K+/H+ exchanger Nhx1 regulates cellular pH to control vesicle trafficking. *Mol Biol Cell* 16:1396-405

Chow CW, Khurana S, Woodside M, Grinstein S, Orlowski J. 1999. The epithelial Na(+)/H(+) exchanger, NHE3, is internalized through a clathrin-mediated pathway. *J Biol Chem* 274:37551-8

Diering GH, Church J, Numata M. 2009. Secretory Carrier Membrane Protein 2 Regulates Cell-surface Targeting of Brain-enriched Na+/H+ Exchanger NHE5. *J Biol Chem* 284:13892-903

Fafournoux P, Noel J, Pouyssegur J. 1994. Evidence that Na+/H+ exchanger isoforms NHE1 and NHE3 exist as stable dimers in membranes with a high degree of specificity for homodimers. *J Biol Chem* 269:2589-96

Fernandez-Chacon R, Sudhof TC. 2000. Novel SCAMPs lacking NPF repeats: ubiquitous and synaptic vesicle-specific forms implicate SCAMPs in multiple membrane-trafficking functions. *J Neurosci* 20:7941-50

Geller BL, Green HM. 1989. Translocation of pro-OmpA across inner membrane vesicles of Escherichia coli occurs in two consecutive energetically distinct steps. *J Biol Chem* 264:16465-9

Hill JK, Brett CL, Chyou A, Kallay LM, Sakaguchi M, et al. 2006. Vestibular hair bundles control pH with (Na+, K+)/H+ exchangers NHE6 and NHE9. *J Neurosci* 26:9944-55

Jentsch TJ. 2008. CLC chloride channels and transporters: from genes to protein structure, pathology and physiology. *Crit Rev Biochem Mol Biol* 43:3-36

Lin PJ, Williams WP, Kobiljski J, Numata M. 2007. Caveolins bind to (Na+, K+)/H+ exchanger NHE7 by a novel binding module. *Cell Signal* 19:978-88

Lin PJ, Williams WP, Luu Y, Molday RS, Orlowski J, Numata M. 2005. Secretory carrier membrane proteins interact and regulate trafficking of the organellar (Na+,K+)/H+ exchanger NHE7. *J Cell Sci* 118:1885-97

Malo ME, Fliegel L. 2006. Physiological role and regulation of the Na+/H+ exchanger. *Can J Physiol Pharmacol* 84:1081-95

Murtazina R, Booth BJ, Bullis BL, Singh DN, Fliegel L. 2001. Functional analysis of polar amino-acid residues in membrane associated regions of the NHE1 isoform of the mammalian Na+/H+ exchanger. Eur J Biochem 268:4674-85

Nakamura N, Tanaka S, Teko Y, Mitsui K, Kanazawa H. 2005. Four Na+/H+ exchanger isoforms are distributed to Golgi and post-Golgi compartments and are involved in organelle pH regulation. J Biol Chem 280:1561-72

Nass R, Cunningham KW, Rao R. 1997. Intracellular sequestration of sodium by a novel Na+/H+ exchanger in yeast is enhanced by mutations in the plasma membrane H+-ATPase. Insights into mechanisms of sodium tolerance. J Biol Chem 272:26145-52

Ohgaki R, Fukura N, Matsushita M, Mitsui K, Kanazawa H. 2008. Cell surface levels of organellar Na+/H+ exchanger isoform 6 are regulated by interaction with RACK1. J Biol Chem 283:4417-29

Okamura Y, Murata Y, Iwasaki H. 2009. Voltage-sensing phosphatase: actions and potentials. J Physiol 587:513-20

Onishi I, Lin PJ, Diering GH, Williams WP, Numata M. 2007. RACK1 associates with NHE5 in focal adhesions and positively regulates the transporter activity. Cell Signal 19:194-203

Putney LK, Denker SP, Barber DL. 2002. The changing face of the Na+/H+ exchanger, NHE1: structure, regulation, and cellular actions. Annu Rev Pharmacol Toxicol 42:527-52

Roxrud I, Raiborg C, Gilfillan GD, Stromme P, Stenmark H. 2009. Dual degradation mechanisms ensure disposal of NHE6 mutant protein associated with neurological disease. Exp Cell Res 315:3014-27

Schuenemann TA, Delgado-Nixon VM, Dalbey RE. 1999. Direct evidence that the proton motive force inhibits membrane translocation of positively charged residues within membrane proteins. J Biol Chem 274:6855-64

Szabo EZ, Numata M, Lukashova V, Iannuzzi P, Orlowski J. 2005. beta-Arrestins bind and decrease cell-surface abundance of the Na+/H+ exchanger NHE5 isoform. Proc Natl Acad Sci U S A 102:2790-5

Szaszi K, Paulsen A, Szabo EZ, Numata M, Grinstein S, Orlowski J. 2002. Clathrin-mediated endocytosis and recycling of the neuron-specific Na+/H+ exchanger NHE5 isoform. Regulation by phosphatidylinositol 3'-kinase and the actin cytoskeleton. J Biol Chem 277:42623-32

Takamori S, Holt M, Stenius K, Lemke EA, Gronborg M, et al. 2006. Molecular anatomy of a trafficking organelle. Cell 127:831-46

van Dalen A, Killian A, de Kruijff B. 1999. Delta psi stimulates membrane translocation of the C-terminal part of a signal sequence. J Biol Chem 274:19913-8

Walz B. 1985. Light-Induced-Changes of Extracellular and Intracellular Potassium Concentration in Photoreceptors of the Leech, Hirudo-Medicinalis. Journal of

Comparative Physiology a-Sensory Neural and Behavioral Physiology 157:199-210
Walz W, Hinks EC. 1985. Carrier-mediated KCl accumulation accompanied by water movements is involved in the control of physiological K+ levels by astrocytes. Brain Res 343:44-51
Wang LY, Gan L, Perney TM, Schwartz I, Kaczmarek LK. 1998. Activation of Kv3.1 channels in neuronal spine-like structures may induce local potassium ion depletion. Proc Natl Acad Sci U S A 95:1882-7